Technical Report

OSUBMI-TR-2010-n01/ BU-CE-1016

Hypergraph Partitioning through
Vertex Separators on Graphs

Enver Kayaaslan, Ali Pınar, Ümit V. Çatalyürek
and Cevdet Aykanat

Sep 2010

The Ohio State University
Department of Biomedical Informatics
3190 Graves Hall, 333 W. 10th Avenue
Columbus, OH 43210
http://bmi.osu.edu

Bilkent University
Computer Engineering Department
Faculty of Engineering
06800 Ankara, Turkey
http://cs.bilkent.edu.tr

HYPERGRAPH PARTITIONING THROUGH VERTEX SEPARATORS ON GRAPHS

ENVER KAYAASLAN*, ALI PINAR†, ÜMIT ÇATALYÜREK‡, AND CEVDET AYKANAT§

Abstract. The modeling flexibility provided by hypergraphs has drawn a lot of interest from the combinatorial scientific community, leading to novel models and algorithms, their applications, and development of associated tools. Hypergraphs are now a standard tool in combinatorial scientific computing. The modeling flexibility of hypergraphs however, comes at a cost: algorithms on hypergraphs are inherently more complicated than those on graphs, which sometimes translate to nontrivial increases in processing times. Neither the modeling flexibility of hypergraphs, nor the runtime efficiency of graph algorithms can be overlooked. Therefore, the new research thrust should be how to cleverly trade-off between the two. This work addresses one method for this trade-off by solving the hypergraph partitioning problem by finding vertex separators on graphs. Specifically, we investigate how to solve the hypergraph partitioning problem by seeking a vertex separator on its net intersection graph **(NIG)**, where each net of the hypergraph is represented by a vertex, and two vertices share an edge if their nets have a common vertex. We propose a vertex-weighting scheme to attain good node-balanced hypergraphs, since NIG model cannot preserve node balancing information. Vertex-removal and vertex-splitting techniques are described to optimize cutnet and connectivity metrics, respectively, under the recursive bipartitioning paradigm. We also developed an implementation for our GPVS-based HP formulations by adopting and modifying a state-of-the-art GPVS tool onmetis. Experiments conducted on a large collection of sparse matrices confirmed the validity of our proposed techniques.

Key words. hypergraph partitioning; combinatorial scientific computing; graph partitioning by vertex separator; sparse matrices.

AMS subject classifications.

1. Introduction. A hypergraph is a generalization of a graph, since it replaces edges that connect only two vertices, with hyperedges (nets) that can connect multiple vertices. This generalization provides a critical modeling flexibility that allows accurate formulation of many important problems in combinatorial scientific computing. Our initial motivations for hypergraph models were accurate modeling of the nonzero structure of unsymmetric and rectangular sparse matrices to minimize communication volume for iterative solvers [8, 9, 11, 12, 13, 23, 5, 54, 55, 56, 57, 58] and permutation to block-angular form for coarse-grain parallelism [3]. The real impact of these works turned out to be the introduction of hypergraph models to the combinatorial scientific computing community. Since then, the modeling power of hypergraphs appealed to many researchers and was applied to a wide variety of parallel and distributed computing applications such as data aggregation [15], image-space parallel direct volume rendering [7], parallel mixed integer linear programming [52], data declustering for multi-disk databases [37, 41], scheduling file-sharing tasks in heterogeneous master-slave computing environments [33, 34, 36], and work-stealing scheduling [59]. Hy-

pergraphs were also applied to applications outside the parallel computing domain such as road network clustering for efficient query processing [19, 20, 21], pattern-based data clustering [42], reducing software development and maintenance costs [4], processing spatial join operations [50], and improving locality in memory or cache performance [1, 51, 60]. Hypergraphs and hypergraph partitioning are now standard tools of combinatorial scientific computing.

Increasing popularity of hypergraphs has been going hand in hand with the development of effective hypergraph partitioning (HP) tools: wide applicability of hypergraphs motivated development of fast HP tools, and availability of effective HP tools motivated further applications. This virtuous cycle produced sequential HP tools such as hMeTiS [32], PaToH [10] and Mondriaan [58], and parallel HP tools such as Parkway [53] and Zoltan [22], all of which adopt the multilevel framework successfully. While these tools provide good performances both in terms of solution quality and processing times, they are hindered by the inherent complexity of dealing with hypergraphs. Algorithms on hypergraphs are more difficult both in terms of computational complexity and runtime performance, since operations on nets are performed on sets of vertices as opposed to pairs of vertices as in graphs. The wide interest over the last decade has proven the modeling flexibility of hypergraphs to be essential, but the runtime efficiency of graph algorithms cannot be overlooked, either. Therefore, we believe that the new research thrust should be how to cleverly trade-off between the modeling flexibility of hypergraphs and the practicality of graphs.

How can we solve problems that are most accurately modeled with hypergraphs using graph algorithms without sacrificing too much from what is really important for the application? This question has been asked before, and the motivation was either theoretical [29] or practical [14, 28] when the absence of HP tools behested these attempts. This earlier body of work investigated the relation between HP and graph partitioning by edge separator (GPES), and achieved little success. Today, we are facing a more difficult task, as effectiveness of available HP tools sets high standards for novel approaches. On the other hand, we can draw upon the progress on related problems, in particular the advances in tools for graph partitioning by vertex separator (GPVS), which is the main theme of this work.

We investigate solving the HP problem by finding vertex separator on the *net intersection graph* (NIG) of the hypergraph. In the NIGof a hypergraph, each net is represented by a vertex and and each vertex of the hypergraph is replaced with a clique of the nets connecting that vertex. A vertex separator on this graph defines a net separator for the hypergraph. This model has been initially studied for circuit partitioning [2]. While faster algorithms can be designed to find vertex separators on graphs, the NIG model has the drawback of attaining balanced partitions. Once vertices of the hypergraphs are replaced with cliques, it will be impossible to preserve the vertex weight information accurately. Therefore, we can view the NIG model as a way to trade off computational efficiency with exact modeling power.

What motivates us to investigate NIGs to solve HP problems arising in scientific computing applications is that in many applications, definition of balance cannot be very precise [3, 43, 44] or there are additional constraints that cannot be easily incorporated into partitioning algorithms and tools [46]; or partitioning is used as part of a divide-and-conquer algorithm [45]. For instance, hypergraph models can be used to permute a linear program (LP) constraint matrix to a block angular form for parallel solution with decomposition methods. Load balance can be achieved by balancing subproblems during partitioning. However, it is not possible to accurately predict

solution time of an LP, and equal sized subproblems only increase the likelihood of computational balance. Hypergraph models have recently been used to find null-space bases that have a sparse inverse [45]. This application requires finding a column-space basis B as a submatrix of a sparse matrix A, so that B^{-1} is sparse. Choosing B to have a block angular form limits the fill in B^{-1}, but merely a block angular form for B will not be sufficient, since B has to be nonsingular to be a column-space basis for A. Enforcing numerical or even structural nonsingularity of subblocks during partitioning is a nontrivial task, if possible, and thus partitioning is used as part of a divide-and-conquer paradigm, where the partitioning phase is followed by a correction phase, if subblocks are non-singular. Both of these cases present examples of applications, where hypergraphs provide effective models, but balance among parts is only weakly defined. As we will show in the experiments, the NIG model can effectively be employed for these applications to achieve high quality solutions in a shorter time. We show that it is easy to enforce a balance criteria on the internal nets of hypergraph partitioning by enforcing vertex balancing during the partitioning of the NIG. However, the NIG model cannot completely preserve the node balancing information in the hypergraph. We propose a weighting scheme for the vertices of NIG, which is quite effective in attaining fairly node balanced partitions of the hypergraph. The proposed vertex balancing scheme for NIG partitioning can be easily enhanced to improve the balancing quality of the hypergraph partitions in a simple post processing phase.

The recursive bipartitioning (RB) paradigm is widely used for multiway HP and known to produce good solution qualities [10, 32]. At each RB step, cutnet removal and cutnet splitting techniques [9] are adopted to optimize the cutsize according to the *cutnet* and *connectivity* metrics, respectively, which are the most commonly used cutsize metrics in scientific and parallel computing [3, 9] as well as VLSI layout design [2, 40]. In this paper, we propose separator-vertex removal and separator-vertex splitting techniques for RB-based partitioning of the NIG, which exactly correspond to the cutnet removal and cutnet splitting techniques, respectively. We also propose an implementation for our GPVS-based HP formulations by adopting and modifying a state-of-the-art GPVS tool used in fill-reducing sparse matrix ordering.

2. Preliminaries. In this section, we will provide the basic definitions and techniques that will be adopted in the remainder of this paper.

2.1. Graph Partitioning. An undirected graph $\mathcal{G} = (\mathcal{V}, \mathcal{E})$ is defined as a set $\mathcal{V}$ of vertices and a set $\mathcal{E}$ of edges. Every edge $e_{ij} \in \mathcal{E}$ connects a pair of distinct vertices v_i and v_j. We use the notation $Adj(v_i)$ to denote the set of vertices adjacent to vertex v_i. We extend this operator to include the adjacency set of a vertex subset $\mathcal{V}' \subset \mathcal{V}$, i.e., $Adj(\mathcal{V}') = \{v_j \in \mathcal{V} - \mathcal{V}' : v_j \in Adj(v_i) \text{ for some } v_i \in \mathcal{V}'\}$. Two disjoint vertex subsets $\mathcal{V}_k$ and $\mathcal{V}_\ell$ are said to be adjacent if $Adj(\mathcal{V}_k) \cap \mathcal{V}_\ell \neq \emptyset$ (equivalently $Adj(\mathcal{V}_\ell) \cap \mathcal{V}_k \neq \emptyset$) and non-adjacent otherwise. The degree $d(v_i)$ of a vertex v_i is equal to the number of edges incident to v_i, i.e., $d(v_i) = |Adj(v_i)|$. A weight $w(v_i) \geq 0$ is associated with each vertex v_i.

An edge subset $\mathcal{E}_S$ is a K-way *edge separator* if its removal disconnects the graph into at least K connected components. That is, $\Pi_{ES}(\mathcal{G}) = \{\mathcal{V}_1, \mathcal{V}_2, \ldots, \mathcal{V}_K\}$ is a K-way vertex partition of $\mathcal{G}$ by edge separator $\mathcal{E}_S \subset \mathcal{E}$ if each part $\mathcal{V}_k$ is non-empty; parts are pairwise disjoint; and the union of parts gives $\mathcal{V}$. Edges between the vertices of different parts belong to $\mathcal{E}_S$, and are called *cut (external)* edges and all other edges are called *uncut (internal)* edges.

A vertex subset $\mathcal{V}_S$ is a K-way *vertex separator* if the subgraph induced by

the vertices in $\mathcal{V} - \mathcal{V}_S$ has at least K connected components. That is, $\Pi_{VS}(\mathcal{G}) = \{\mathcal{V}_1, \mathcal{V}_2, \ldots, \mathcal{V}_K; \mathcal{V}_S\}$ is a K-way vertex partition of $\mathcal{G}$ by vertex separator $\mathcal{V}_S \subset \mathcal{V}$ if each part $\mathcal{V}_k$ is non-empty; all parts and the separator are pairwise disjoint; parts are pairwise non-adjacent; and the union of parts and the separator gives $\mathcal{V}$. The non-adjacency of the parts implies that $Adj(\mathcal{V}_k) \subseteq \mathcal{V}_S$ for each $\mathcal{V}_k$. A vertex $v_i \in \mathcal{V}_k$ is said to be a boundary vertex of part $\mathcal{V}_k$ if it is adjacent to any vertex in $\mathcal{V}_S$. A vertex separator is said to be *narrow* if no subset of it forms a separator, and *wide* otherwise.

The objective of graph partitioning is finding a separator of smallest size subject to a given balance criteria on the weights of the K parts. The weight $W(\mathcal{V}_k)$ of a part V_k is defined as the sum of the weights of the vertices in $\mathcal{V}_k$, i.e.,

$$W(\mathcal{V}_k) = \sum_{v_i \in \mathcal{V}_k} w(v_i) \tag{2.1}$$

and the balance criteria is defined as

$$\max_{1 \le k \le K} W(\mathcal{V}_k) \le (1 + \epsilon) W_{avg}, \quad \text{where} \tag{2.2}$$

$$W_{avg} = \frac{\sum_{k=1}^{K} W(\mathcal{V}_k)}{K}$$

Here, W_{avg} is the weight each part must have in the case of perfect balance, and ϵ is the maximum imbalance ratio allowed. We proceed with formal definitions for the GPES and GPVS problems, both of which are known to be NP-hard [6].

DEFINITION 2.1 (Problem GPES). *Given a graph* $\mathcal{G} = (\mathcal{V}, \mathcal{E})$, *an integer* K, *and a maximum allowable imbalance ratio* ϵ. *The GPES problem is finding a K-way vertex partition* $\Pi_{ES}(\mathcal{G}) = \{\mathcal{V}_1, \mathcal{V}_2, \ldots, \mathcal{V}_K\}$ *of* $\mathcal{G}$ *by edge separator* $\mathcal{E}_S$ *that satisfies the balance criterion given in* (2.2) *while minimizing the cutsize, which is defined as*

$$cutsize(\Pi_{ES}) = \sum_{e_{ij} \in \mathcal{E}_S} c(e_{ij}), \tag{2.3}$$

where $c(e_{ij}) \ge 0$ *is the cost of edge* $e_{ij} = (v_i, v_j)$.

DEFINITION 2.2 (Problem GPVS). *Given a graph* $\mathcal{G} = (\mathcal{V}, \mathcal{E})$, *an integer* K, *and a maximum allowable imbalance ratio* ϵ. *The GPVS problem is finding a K-way vertex partition* $\Pi_{VS}(\mathcal{G}) = \{\mathcal{V}_1, \mathcal{V}_2, \ldots, \mathcal{V}_K; \mathcal{V}_S\}$ *of* $\mathcal{G}$ *by vertex separator* $\mathcal{V}_S$ *that satisfies the balance criterion given in* (2.2) *while minimizing the cutsize, which is defined as one of*

$$a)\ cutsize(\Pi_{VS}) = \sum_{v_i \in \mathcal{V}_S} c(v_i) \tag{2.4}$$

$$b)\ cutsize(\Pi_{VS}) = \sum_{v_i \in \mathcal{V}_S} c(v_i)(\lambda(v_i) - 1) \tag{2.5}$$

where $c(v_i) \ge 0$ *is the cost of vertex* v_i.

In the general GPVS definition given above, both a weight and a cost are associated with each vertex. The weights are used in computing loads of parts for balancing, whereas the costs are utilized in computing the cutsize. In the standard GPVS definitions in the literature, the weights and costs of the vertices are taken as identical. The reason for our general GPVS definition will become clear in Section 3.

In the cutsize definition given in (2.4), each separator vertex incurs its cost to the cutsize, whereas in (2.5), the connectivity of a vertex is considered while incurring its cost to the cutsize. The *connectivity* $\lambda(v_i)$ of a vertex v_i denotes the number of parts connected by v_i, where a vertex that is adjacent to any vertex in a part is said to *connect* that part.

The techniques for solving GPES and GPVS problems are closely related. An *indirect* approach to solve the GPVS problem is to first find an edge separator through GPES, and then translate it to any vertex separator. After finding an edge separator, this approach takes vertices adjacent to separator edges as a wide separator to be refined to a narrow separator, with the assumption that a small edge separator is likely to yield a small vertex separator. The wide-to-narrow refinement problem [48] is described as a minimum vertex cover problem on the bipartite graph induced by the cut edges. A minimum vertex cover can be taken as a narrow separator for the whole graph, because each cut edge will be adjacent to any vertex in the vertex cover.

2.2. Hypergraph Partitioning. A hypergraph $\mathcal{H} = (\mathcal{U}, \mathcal{N})$ is defined as a set $\mathcal{U}$ of nodes (vertices) and a set $\mathcal{N}$ of nets among those vertices. We refer to the vertices of $\mathcal{H}$ as nodes, to avoid the confusion between graphs and hypergraphs. Every net $n_i \in \mathcal{N}$ connects a subset of nodes, i.e., $n_i \subseteq \mathcal{U}$. The nodes connected by a net n_i are called *pins* of n_i and denoted as $Pins(n_i)$. We extend this operator to include the pin list of a net subset $\mathcal{N}' \subset \mathcal{N}$, i.e., $Pins(\mathcal{N}') = \bigcup_{n_i \in \mathcal{N}'} Pins(n_i)$. The size $s(n_i)$ of a net n_i is equal to the number of its pins, i.e., $s(n_i) = |Pins(n_i)|$. The set of nets that connect a node u_j is denoted as $Nets(u_j)$. We also extend this operator to include the net list of a node subset $\mathcal{U}' \subset \mathcal{U}$, i.e., $Nets(\mathcal{U}') = \bigcup_{u_j \in \mathcal{U}'} Nets(u_j)$. The degree $d(u_j)$ of a node u_j is equal to the number of nets that connect u_j, i.e., $d(u_j) = |Nets(u_j)|$. The total number p of pins denote the size of $\mathcal{H}$ where $p = \sum_{n_i \in \mathcal{N}} s(n_i) = \sum_{u_j \in \mathcal{U}} d(u_j)$. A graph is a special hypergraph such that each net has exactly two pins. A weight $w(u_j)$ is associated with each node u_j, whereas a cost $c(n_i)$ is associated with each net n_i. A weight $w(n_i)$ can also be associated with each net n_i as we will discuss later in this section.

A net subset $\mathcal{N}_S$ is a K-way *net separator* if its removal disconnects the hypergraph into at least K connected components. That is, $\Pi_{\mathcal{U}}(\mathcal{H}) = \{\mathcal{U}_1, \mathcal{U}_2, \ldots, \mathcal{U}_K\}$ is a K-way node partition of $\mathcal{H}$ by net separator $\mathcal{N}_S \subset \mathcal{N}$ if each part $\mathcal{U}_k$ is non-empty; parts are pairwise disjoint; and the union of parts gives $\mathcal{U}$. In a partition $\Pi_{\mathcal{U}}(\mathcal{H})$, a net that connects any node in a part is said to *connect* that part. The *connectivity* $\lambda(n_i)$ of a net n_i denotes the number of parts connected by n_i. Nets connecting multiple parts belong to $\mathcal{N}_S$, and are called *cut (external)* (i.e., $\lambda(n_i) > 1$), and *uncut (internal)* otherwise (i.e., $\lambda(n_i) = 1$). The set of internal nets of a part $\mathcal{U}_k$ is denoted as $\mathcal{N}_k$, for $k = 1, \ldots, K$. So, although $\Pi_{\mathcal{U}}(\mathcal{H})$ is defined as a K-way partition on the node set of $\mathcal{H}$, it can also be considered as inducing a $(K+1)$-way partition $\Pi_{\mathcal{N}}(\mathcal{H}) = \{\mathcal{N}_1, \ldots, \mathcal{N}_K; \mathcal{N}_S\}$ on the net set.

As in the GPES and GPVS problems, the objective of HP problem is finding a net separator of smallest size subject to a given balance criteria on the weights of the K parts. The weight $W(\mathcal{U}_k)$ of a part $\mathcal{U}_k$ is defined either as the sum of the weights of nodes in $\mathcal{U}_k$, i.e.,

$$W(\mathcal{U}_k) = \sum_{u_j \in \mathcal{U}_k} w(u_j) \tag{2.6}$$

or as the sum of weights of internal nets of part $\mathcal{U}_k$, i.e.,

$$W(\mathcal{U}_k) = \sum_{n_i \in \mathcal{N}_k} w(n_i) \tag{2.7}$$

The former and latter part weight computation schemes together with the load balancing criteria given in (2.2) will be referred to here as node and net balancing, respectively. We proceed with formal definition for the HP problem, which is also known to be NP-hard [40].

DEFINITION 2.3 (Problem HP). *Given a hypergraph $\mathcal{H} = (\mathcal{U}, \mathcal{N})$, an integer K, and a maximum allowable imbalance ratio ϵ. The HP problem is finding a K-way node partition $\Pi_{\mathcal{U}}(\mathcal{H}) = \{\mathcal{U}_1, \mathcal{U}_2, \ldots, \mathcal{U}_K\}$ of $\mathcal{H}$ that satisfies the balance criterion given in (2.2) while minimizing the cutsize, which is defined as one of*

$$a)\ cutsize(\Pi_{\mathcal{U}}) = \sum_{n_i \in \mathcal{N}_S} c(n_i) \tag{2.8}$$

$$b)\ cutsize(\Pi_{\mathcal{U}}) = \sum_{n_i \in \mathcal{N}_S} c(n_i)(\lambda(n_i) - 1) \tag{2.9}$$

The cutsize metrics given in (2.8) and (2.9) are referred to as the *cut-net* and *connectivity* metrics, respectively, [9, 13, 40].

3. Formulating the HP Problem as a GPVS Problem. In this section, we first review the previous work on alternative models for solving the HP problem. Then, we describe our novel and accurate GPVS-based formulations and present the relation between HP and GPVS problems from a matrix theoretical view. Finally, we present our implementation based on adapting a state-of-the-art GPVS tool.

3.1. Alternative Models for Solving the HP Problem. As indicated in the survey by Alpert and Kahng [2], hypergraphs are commonly used to represent circuit netlist connections in solving the circuit partitioning and placement problems in VLSI layout design. The circuit partitioning problem is to divide a system specification into clusters to minimize inter-cluster connections. Other circuit representation models were also proposed and used in the VLSI literature including dual hypergraph, clique-net graph (CNG) and net-intersection graph (NIG) [2]. Hypergraphs represent circuits in a natural way so that the circuit partitioning problem is directly described as an HP problem. Thus, these alternative models can be considered as alternative approaches for solving the HP problem.

The dual of a hypergraph $\mathcal{H} = (\mathcal{U}, \mathcal{N})$ is defined as a hypergraph $\mathcal{H}'$, where the nodes and nets of $\mathcal{H}$ become, respectively, the nets and nodes of $\mathcal{H}'$. That is, $\mathcal{H}' = (\mathcal{U}', \mathcal{N}')$ with $Nets(u_i') = Pins(n_i)$ for each $u_i' \in \mathcal{U}'$ and $n_i \in \mathcal{N}$, and $Pins(n_j') = Nets(u_j)$ for each $n_j' \in \mathcal{N}'$ and $u_j \in \mathcal{U}$.

In the CNG model, the vertex set of the target graph is equal to the node set of the given hypergraph. Each net of the given hypergraph is represented by a clique of vertices corresponding to its pins. The multiple edges between two vertices are contracted into a single edge, the cost of which is set equal to the sum of the cost of the edges it represents. If an edge is in the cut set of a GPES then all nets represented by this edge are in the cut set of HP. Ideally, no matter how nodes of a net are partitioned, the contribution of a cut net to the cutsize should always be one in a bipartition when unit net costs are assumed. However, the deficiency of the CNG
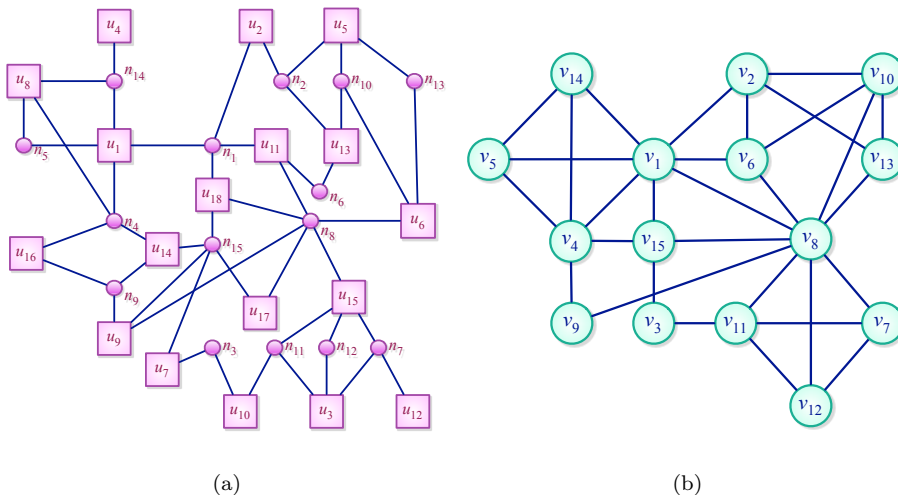
FIG. 3.1. (a) A sample hypergraph $\mathcal{H}$ and (b) the corresponding NIG representation $\mathcal{G}$.

representation is that it is impossible to achieve such a *perfect* edge-cost assignment of the edges as proved by Ihler et al. [29].

In the NIG representation $\mathcal{G} = (\mathcal{V}, \mathcal{E})$ of a given hypergraph $\mathcal{H} = (\mathcal{U}, \mathcal{N})$, each vertex v_i of $\mathcal{G}$ corresponds to net n_i of $\mathcal{H}$. Two vertices $v_i, v_j \in \mathcal{V}$ of $\mathcal{G}$ are adjacent if and only if respective nets $n_i, n_j \in \mathcal{N}$ of $\mathcal{H}$ share at least one pin, i.e., $e_{ij} \in \mathcal{E}$ if and only if $Pins(n_i) \cap Pins(n_j) \neq \emptyset$. So,

$$Adj(v_i) = \{v_j \ : \ n_j \in \mathcal{N} \ni Pins(n_i) \cap Pins(n_j) \neq \emptyset\}. \tag{3.1}$$

Note that for a given hypergraph $\mathcal{H}$, NIG $\mathcal{G}$ is well-defined, however there is no unique reverse construction [2]. Figures 3.1(a) and 3.1(b), respectively, display a sample hypergraph $\mathcal{H}$ and the corresponding NIG representation $\mathcal{G}$. In the figure, the sample hypergraph $\mathcal{H}$ contains 18 nodes and 15 nets, whereas the corresponding NIG $\mathcal{G}$ contains 15 vertices and 30 edges.

Both dual hypergraph and NIG models view the HP problem in terms of partitioning nets instead of nodes. Kahng [30] and Cong, Hagen, and Kahng [16] exploited this perspective of the NIG model to formulate the hypergraph bipartitioning problem as a two-stage process. In the first stage, nets of $\mathcal{H}$ are bipartitioned through 2-way GPES of its NIG $\mathcal{G}$. The resulting net bipartition induces a partial node bipartition on $\mathcal{H}$. Because, the nodes (pins) that are connected only by the nets on one side of the bipartition can be unambigiuosly assigned to that side. However, other nodes may be connected by the nets on both sides of the bipartition. Thus, the second stage involves finding the best completion of the partial node bipartition; i.e., a part assignment for the shared nodes such that the cutsize is minimized. This problem is known as the module (node) contention problem in the VLSI community. Kahng [30] used a winner-loser heuristic [27], whereas Cong et al. [16] used a matching-based (IG-match) algorithm for solving the 2-way module contention problem optimally. Cong, Labio, and Shivakumar [17] extended this approach to K-way HP through using the dual hypergraph model. In the first stage, a K-way net partition is obtained through partitioning the dual hypergraph. For the second stage, they formulated the

K-way module contention problem as a min-cost max-flow problem through defining binding factors between nodes and nets, and a preference function between parts and nodes.

Here, we reveal the fact that the module contention problem encountered in the second stage of the NIG-based hypergraph bipartitioning approaches [16, 30] is similar to the wide-to-narrow separator refinement problem encountered in the second stage of the indirect GPVS approaches widely used in nested-dissection based low-fill orderings for sparse matrix factorization. The module contention and separator refinement algorithms effectively work on the bipartite graph induced by the cut edges of a two-way GPES of the NIG representation of hypergraphs and the standard graph representation of sparse matrices, respectively. The winner-loser assignment heuristic [27, 30] used by Kahng [30] is very similar to the minimum-recovery heuristic proposed by Leiserson and Lewis [39] for separator refinement. Similarly, the IG-match algorithm proposed by Cong et al. [16] is similar to the maximum-matching based minimum vertex-cover algorithm [38, 47] used by Pothen, Simon, and Liou [48] for separator refinement. While not explicitly stated in the literature, these net-bipartitioning-based HP algorithms using the NIG model can be viewed as trying to solve the HP problem through an indirect GPVS of the NIG representation.

More recently, Trifunovic and Knottenbelt [53] proposed a coloring-based graph model for partitioning special type of hypergraphs which arise in fine-grain (nonzero-based) partitioning of sparse matrices [13, 11] for parallel matrix vector multiply. In such hypergraphs, each vertex is connected by exactly two nets and their dual hypergraphs are bipartite graphs. A K-way edge coloring on this bipartite graph is decoded as a K-way partitioning of the nodes (nonzeros) of the original hypergraph. The coloring objective, which is defined in terms of the number of distinct colors incident to the vertices, correctly models the total interprocessor communication volume. Since connectivity cutsize metric (2.9) also correctly models total interprocessor communication volume, the coloring objective exactly models the connectivity cutsize metric (2.9). Although this model is proposed for special type of hypergraphs in which each node is connected by exactly two nets, the model easily extends to more general hypergraphs where nodes are connected by arbitrary number of nets.

3.2. An Accurate Formulation of HP as GPVS on NIG Model. We propose a net-partitioning based K-way HP algorithm that avoids the module contention problem by describing the HP problem as a GPVS problem through the NIG model. The following theorem lays down the basis for our GPVS-based HP formulation. Let $\mathcal{G} = (\mathcal{V}, \mathcal{E})$ denote the NIG of a given hypergraph $\mathcal{H} = (\mathcal{U}, \mathcal{N})$. The cost of each net n_i of $\mathcal{H}$ is assigned as the cost of the respective vertex v_i of $\mathcal{G}$, i.e., $c(v_i) = c(n_i)$. For brevity of the presentation we assume unit net costs here, but all proposed models and methods generalize to hypergraphs with non-unit net costs.

THEOREM 1. *A K-way vertex partition $\Pi_{VS}(\mathcal{G}) = \{\mathcal{V}_1, \ldots, \mathcal{V}_K; \mathcal{V}_S\}$ of $\mathcal{G}$ by a narrow vertex separator $\mathcal{V}_S$ induces a K-way contention-free net partition $\Pi_{\mathcal{N}}(\mathcal{H}) = \{\mathcal{N}_1 \equiv \mathcal{V}_1, \mathcal{N}_2 \equiv \mathcal{V}_2, \ldots, \mathcal{N}_K \equiv \mathcal{V}_K; \mathcal{N}_S \equiv \mathcal{V}_S\}$ of $\mathcal{H}$ by a net separator $\mathcal{N}_S$.*

Proof. By definition of GPVS, we have $Adj(\mathcal{V}_k) \cap \mathcal{V}_\ell = \emptyset$ for $1 \leq k < \ell \leq K$. This implies that $Pins(\mathcal{N}_k) \cap Pins(\mathcal{N}_\ell) = \emptyset$ for $1 \leq k < \ell \leq K$. Because, if any two nets $n_i \in \mathcal{N}_k$ and $n_j \in \mathcal{N}_\ell$ shared at least one pin, then there would be an edge e_{ij} between vertices $v_i \in \mathcal{V}_k$ and $v_j \in \mathcal{V}_\ell$ of $\mathcal{G}$, which would correspond to an edge between parts $\mathcal{V}_k$ and $\mathcal{V}_\ell$ of $\Pi_{VS}(\mathcal{G})$ contradicting the definition of GPVS. Therefore, any two nets belonging to two different net parts don't share any pin, thus ensuring the contention-free property of the net partition $\Pi_{\mathcal{N}}(\mathcal{H})$. □
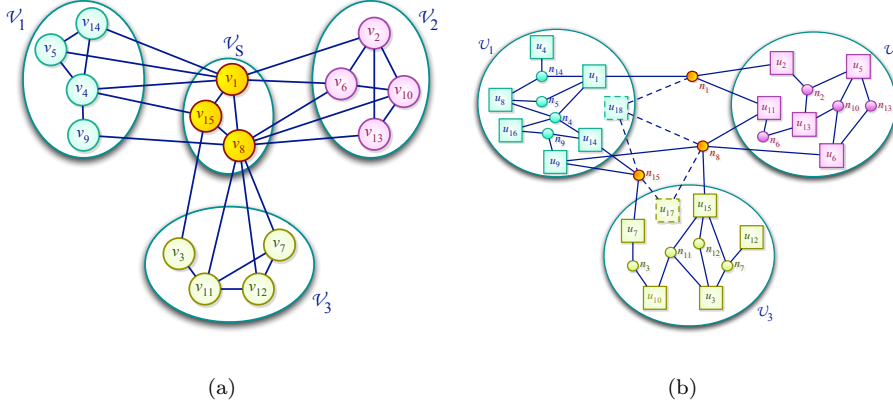
FIG. 3.2. *(a) A 3-way GPVS of the sample NIG given in Figure 3.1(b) and (b)corresponding partitioning of the hypergraph.*

COROLLARY 1. *A K-way contention-free net partition of $\mathcal{H}$ by a net separator $\mathcal{N}_S$*

$$\Pi_{\mathcal{N}}(\mathcal{H}) = \{\mathcal{N}_1 \equiv \mathcal{V}_1, \ldots, \mathcal{N}_K \equiv \mathcal{V}_K; \mathcal{N}_S \equiv \mathcal{V}_S\} \tag{3.2}$$

induces a K-way partial node partition

$$\Pi'_{\mathcal{U}}(\mathcal{H}) = \{\mathcal{U}'_1 = Pins(\mathcal{N}_1), \ldots, \mathcal{U}'_K = Pins(\mathcal{N}_K)\} \tag{3.3}$$

Let $\mathcal{U}_F$ denote the set of remaining nodes. Note that $\mathcal{U}_F$ also corresponds to the set of nodes that are only connected by the nets of the separator $\mathcal{N}_S$. That is,

$$\mathcal{U}_F = \mathcal{U} - \bigcup_{k=1}^{K} \mathcal{U}'_k = \{u_i \in \mathcal{U} : Nets(u_i) \subseteq \mathcal{N}_S \equiv \mathcal{V}_S\} \tag{3.4}$$

The nodes in $\mathcal{U}_F$ will be referred to here as *free* nodes.

Figure 3.2(a) shows a 3-way GPVS $\Pi_{VS}(\mathcal{G})$ of the sample NIG $\mathcal{G}$ given in Figure 3.1(b). Figure 3.2(b) shows the 3-way partial and complete node partition $\Pi'_{\mathcal{U}}(\mathcal{H})$ of the sample $\mathcal{H}$, which is induced by $\Pi_{VS}(\mathcal{G})$. Partitial node partition is displayed with nodes drawn with solid lines, and complete node partition is achieved by adding 2 free nodes (drawn with dashed lines). The sample $\mathcal{H}$ given in Figure 3.1(a) contains only 2 free nodes, which are u_{17} and u_{18}. Comparison of Figures 3.2(a) and 3.2(b) illustrates that the separator vertices v_1, v_8 and v_{15} of $\Pi_{VS}(\mathcal{G})$ induce the cut nets n_1, n_8, and n_{15} of $\Pi'_{\mathcal{U}}(\mathcal{H})$, respectively.

For any arbitrary assignment of free nodes, we can construct a complete node partition in the following form,

$$\Pi_{\mathcal{U}}(\mathcal{H}) = \{\mathcal{U}_1 \supseteq \mathcal{U}'_1, \mathcal{U}_2 \supseteq \mathcal{U}'_2, \ldots, \mathcal{U}_K \supseteq \mathcal{U}'_K\} \tag{3.5}$$

Note that any K-way node partition of $\mathcal{H}$ inducing the $(K+1)$-way net partition $\Pi_{\mathcal{N}}(\mathcal{H})$ has to be in the form above.

THEOREM 2. *Given a K-way vertex partition $\Pi_{VS}(\mathcal{G})$ of $\mathcal{G}$ by a narrow vertex separator $\mathcal{V}_S$, any node partition $\Pi_{\mathcal{U}}(\mathcal{H})$ of $\mathcal{H}$ as constructed according to (3.5) induces the $(K+1)$-way net partition $\Pi_{\mathcal{N}}(\mathcal{H}) = \{\mathcal{N}_1 \equiv \mathcal{V}_1, \ldots, \mathcal{N}_K \equiv \mathcal{V}_K; \mathcal{N}_S \equiv \mathcal{V}_S\}$ such that the connectivity of each cut net in $\mathcal{N}_S$ is greater than or equal to the connectivity of the corresponding separator vertex in $\mathcal{V}_S$.*

Proof. Let $\Pi_{\mathcal{U}}(\mathcal{H})$ be a node partition of $\mathcal{H}$ as constructed according to (3.5). Consider the net $n_i \in \mathcal{N}_k$ corresponding to a vertex $v_i \in \mathcal{V}_k$ of $\Pi_{VS}(\mathcal{G})$. Since $Pins(n_i) \subseteq \mathcal{U}_k$, n_i will be an internal net of node part $\mathcal{U}_k$ for node partition $\Pi_{\mathcal{U}}(\mathcal{H})$. Consider any net $n_s \in \mathcal{N}_S$ corresponding to separator vertex $v_s \in \mathcal{V}_S$ of $\Pi_{VS}(\mathcal{G})$. Since $\mathcal{V}_S$ is narrow, there exists at least two vertices $v_{j_1} \in \mathcal{V}_{k_1}$ and $v_{j_2} \in \mathcal{V}_{k_2}$ adjacent to v_s such that $k_1 \neq k_2$. Then, corresponding nets n_{j_1} and n_{j_2} are internal nets of $\mathcal{U}_{k_1}$ and $\mathcal{U}_{k_2}$, respectively by Theorem 1. Since the vertices v_{j_1} and v_{j_2} are adjacent to v_s in $\mathcal{G}$, there exists two nodes u_{h_1} and u_{h_2} such that $u_{h_1} \in Pins(n_{j_1}) \cap Pins(n_i)$ and $u_{h_2} \in Pins(n_{j_2}) \cap Pins(n_i)$ by the NIG definition. By the construction of $\Pi_{\mathcal{U}}(\mathcal{H})$, since $Pins(n_{j_1}) \subseteq \mathcal{U}_{k_1}$ and $Pins(n_{j_2}) \subseteq \mathcal{U}_{k_2}$, we have $u_{h_1} \in \mathcal{U}_{k_1}$ and $u_{h_2} \in \mathcal{U}_{k_2}$, which in turn implies that n_s is a cut net for the node partition $\Pi_{\mathcal{U}}(\mathcal{H})$. Therefore $\Pi_{\mathcal{U}}(\mathcal{H})$ induces the net partition $\Pi_{\mathcal{N}}(\mathcal{H}) = \{\mathcal{N}_1 \equiv \mathcal{V}_1, \ldots, \mathcal{N}_K \equiv \mathcal{V}_K; \mathcal{N}_S \equiv \mathcal{V}_S\}$.

Consider the connectivity of the net $n_s \in \mathcal{N}_S$ corresponding to a separator vertex $v_s \in \mathcal{V}_S$ of $\Pi_{VS}(\mathcal{G})$. Since $Pins(\mathcal{N}_k) \subseteq \mathcal{U}_k$, for $1 \leq k \leq K$, if vertex-part $\mathcal{V}_k$ of $\Pi_{VS}(\mathcal{G})$ contains a vertex $v_j \in \mathcal{V}_k$ that is adjacent to v_s then node-part $\mathcal{U}_k$ of $\Pi_{\mathcal{U}}(HP)$ contains a node u_h such that $u_h \in Pins(n_s) \cap Pins(n_j)$. Thus, if a separator vertex $v_s \in \mathcal{V}_S$ connects vertex part $\mathcal{V}_k$, the net $n_s \in \mathcal{N}_S$ also connects node part $\mathcal{U}_k$. The connectivity of net n_s may become strictly greater than that of vertex v_s if n_s connects a free node u_f assigned to a part $\mathcal{U}_\ell$ that is not connected by n_s in partial node partition $\Pi'_{\mathcal{U}}(\mathcal{H})$, i.e., $\mathcal{U}'_\ell \cap Pins(n_s) = \emptyset$. $\square$

COROLLARY 2. *Given a K-way vertex partition $\Pi_{VS}(\mathcal{G})$ of $\mathcal{G}$ by a narrow vertex separator $\mathcal{V}_S$, the separator size of $\Pi_{VS}(\mathcal{G})$ is equal to the cutsize of node partition $\Pi_{\mathcal{U}}(\mathcal{H})$ induced by $\Pi_{VS}(\mathcal{G})$ according to cutnet metric, whereas the separator size of $\Pi_{VS}(\mathcal{G})$ approximates the cutsize of node partition $\Pi_{\mathcal{U}}(\mathcal{H})$ induced by $\Pi_{VS}(\mathcal{G})$ according to the connectivity metric.*

Comparison of Figures 3.2(a) and 3.2(b) illustrates that the connectivities of separator vertices in Π_{VS} are exactly equal to those of the cut nets of induced partial node partition $\Pi'_{\mathcal{U}}(\mathcal{H})$. Figure 3.2(b) shows a 3-way complete node partition $\Pi_{\mathcal{U}}(\mathcal{H})$ obtained by assigning the free nodes (shown with dashed lines) u_{17} and u_{18} to parts $\mathcal{U}_3$ and $\mathcal{U}_1$, respectively. This free node assignment does not increase the connecvitivities of the cut nets. However a different free node assignment might increase the connectivities of the cut nets. For example, assigning free node u_{17} to part $\mathcal{U}_2$ instead of $\mathcal{U}_3$ will increase the connectivity of net n_{15} by 1.

3.2.1. Recursive-bipartitioning-based partitioning. In the recursive bipartitioning (RB) paradigm, a hypergraph is first partitioned into 2 parts. Then, each part of the bipartition is further bipartitioned recursively until the desired number of parts, K is achieved. The following corollary forms the basis for the use of RB-based GPVS for RB-based HP according to the connectivity and the cut-net metrics.

COROLLARY 3. *Let $\Pi_{VS}(\mathcal{G}) = \{\mathcal{V}_1, \mathcal{V}_2; \mathcal{V}_S\}$ be a partition of $\mathcal{G}$ by a vertex separator $\mathcal{V}_S$, and let $\Pi_{\mathcal{U}}(\mathcal{H}) = \{\mathcal{U}_1, \mathcal{U}_2\}$ be a node partition of $\mathcal{H}$ that induces the net partition $\Pi_{\mathcal{N}}(\mathcal{H}) = \{\mathcal{N}_1 \equiv \mathcal{V}_1, \mathcal{N}_2 \equiv \mathcal{V}_2; \mathcal{N}_S \equiv \mathcal{V}_S\}$. The connectivity of a net n_i in $\Pi_{\mathcal{U}}(\mathcal{H})$ is equal to the connectivity of the corresponding vertex v_i in $\Pi_{VS}(\mathcal{G})$.*

Separator-vertex removal: In RB-based multiway HP, the cut-net metric is formu-

lated by cut-net removal after each RB step. In this method, after each hypergraph bipartitioning step, each cut net is discarded from further RB steps. That is, a node bipartition $\Pi_{\mathcal{U}}(\mathcal{H}) = \{\mathcal{U}_1, \mathcal{U}_2\}$ of the current hypergraph $\mathcal{H}$, which induces the net bipartition $\Pi_{\mathcal{N}}(\mathcal{H}) = \{\mathcal{N}_1, \mathcal{N}_2; \mathcal{N}_S\}$, is decoded as generating two sub-hypergraphs $\mathcal{H}_1 = (\mathcal{U}_1, \mathcal{N}_1)$ and $\mathcal{H}_2 = (\mathcal{U}_2, \mathcal{N}_2)$ for further RB steps. Hence, the total cutsize of the resulting multiway partition of $\mathcal{H}$ according to the cut-net metric will be equal to the sum of the number of cut nets of the bipartition obtained at each RB step.

The cut-net metric can be formulated in the RB-GPVS-based multiway HP by separator-vertex removal so that each separator vertex is discarded from further RB steps. That is, at each RB step, a 2-way vertex separator $\Pi_{VS}(\mathcal{G}) = \{\mathcal{V}_1, \mathcal{V}_2; \mathcal{V}_S\}$ of $\mathcal{G}$ is decoded as generating two sub-graphs $\mathcal{G}_1 = (\mathcal{V}_1, \mathcal{E}_1)$ and $\mathcal{G}_2 = (\mathcal{V}_2, \mathcal{E}_2)$, where $\mathcal{E}_1$ and $\mathcal{E}_2$ denote the internal edges of vertex parts $\mathcal{V}_1$ and $\mathcal{V}_2$, respectively. In other words, $\mathcal{G}_1$ and $\mathcal{G}_2$ are the sub-graphs of $\mathcal{G}$ induced by the vertex parts $\mathcal{V}_1$ and $\mathcal{V}_2$, respectively. $\mathcal{G}_1$ and $\mathcal{G}_2$ constructed in this way become the NIG representations of hypergraphs $\mathcal{H}_1$ and $\mathcal{H}_2$, respectively. Hence, the sum of the number of separator vertices of the 2-way GPVS obtained at each RB step will be equal to the total cutsize of the resulting multiway partition of $\mathcal{H}$ according to the cut-net metric.

Separator-vertex splitting: In RB-based multiway HP, the connectivity metric is formulated by adopting the cut-net splitting method after each RB step. In this method, each RB step, $\Pi_{\mathcal{U}}(\mathcal{H}) = \{\mathcal{U}_1, \mathcal{U}_2\}$ is decoded as generating two sub-hypergraphs $\mathcal{H}_1 = (\mathcal{U}_1, \mathcal{N}_1)$ and $\mathcal{H}_2 = (\mathcal{U}_2, \mathcal{N}_2)$ as in the cut-net removal method. Then, each cut net n_s of $\Pi_{\mathcal{U}}(\mathcal{H})$ is split into two pin-wise disjoint nets n_s^1 and n_s^2 with $Pins(n_s^1) = Pins(n_s) \cap \mathcal{U}_1$ and $Pins(n_s^2) = Pins(n_s) \cap \mathcal{U}_2$, where n_s^1 and n_s^2 are added to the net lists of $\mathcal{H}_1$ and $\mathcal{H}_2$, respectively. In this way, the total cutsize of the resulting multiway partition according to the connectivity metric will be equal to the sum of the number of cut nets of the bipartition obtained at each RB step [9].

The connectivity metric can be formulated in the RB-GPVS-based multiway HP by separator-vertex splitting, which is not as easy as the separator-vertex removal method and it needs special attention. In a straightforward implementation of this method, a 2-way vertex separator $\Pi_{VS}(\mathcal{G}) = \{\mathcal{V}_1, \mathcal{V}_2; \mathcal{V}_S\}$ is decoded as generating two subgraphs $\mathcal{G}_1$ and $\mathcal{G}_2$ which are the sub-graphs of $\mathcal{G}$ induced by the vertex sets $\mathcal{V}_1 \cup \mathcal{V}_S$ and $\mathcal{V}_2 \cup \mathcal{V}_S$, respectively. That is, each separator vertex $v_s \in \mathcal{V}_S$ is split into two vertices v_s^1 and v_s^2 with $Adj(v_s^1) = Adj(v_s) \cap (\mathcal{V}_1 \cup \mathcal{V}_S)$ and $Adj(v_s^2) = Adj(v_s) \cap (\mathcal{V}_2 \cup \mathcal{V}_S)$. Then, the split vertices v_s^1 and v_s^2 are added to the subgraphs $(\mathcal{V}_1, \mathcal{E}_1)$ and $(\mathcal{V}_2, \mathcal{E}_2)$ to form $\mathcal{G}_1$ and $\mathcal{G}_2$, respectively.

This straightforward implementation of separator-vertex splitting method can be overcautious because of the unnecessary replication of separator edges in both subgraphs $\mathcal{G}_1$ and $\mathcal{G}_2$. Here an edge is said to be a separator edge if two vertices connected by the edge are both in the separator $\mathcal{V}_S$. Consider a separator edge $(v_{s_1}, v_{s_2}) \in \mathcal{E}$ in a given bipartition $\Pi_{VS}(\mathcal{G}) = \{\mathcal{V}_1, \mathcal{V}_2; \mathcal{V}_S\}$ of $\mathcal{G}$, where $\Pi_{\mathcal{U}}(\mathcal{H}) = \{\mathcal{U}_1, \mathcal{U}_2\}$ is a bipartition of $\mathcal{H}$ induced by $\Pi_{VS}(\mathcal{G})$ according to construction given in (3.5). If both $\mathcal{U}_1$ and $\mathcal{U}_2$ contain at least one node that induces the separator edge (v_{s_1}, v_{s_2}) of $\mathcal{G}$ then the replication of (v_{s_1}, v_{s_2}) in both subgraphs $\mathcal{G}_1$ and $\mathcal{G}_2$ is necessary. If, however, all hypergraph nodes that induce the edge (v_{s_1}, v_{s_2}) of $\mathcal{G}$ remain in only one part of $\Pi_{\mathcal{U}}(\mathcal{H})$ then the replication of (v_{s_1}, v_{s_2}) on the graph corresponding to the other part is unnecessary. For example, if all nodes connected by both nets n_{s_1} and n_{s_2} of $\mathcal{H}$ remain in $\mathcal{U}_1$ of $\Pi_{\mathcal{U}}(\mathcal{H})$ then the edge (v_{s_1}, v_{s_2}) should be replicated in only $\mathcal{G}_1$. $\mathcal{G}_1$ and $\mathcal{G}_2$ constructed in this way become the
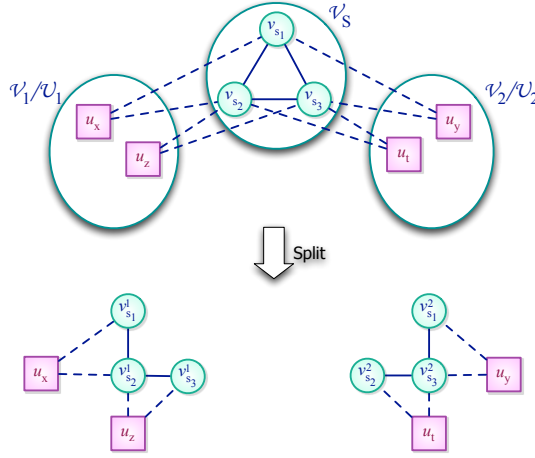
FIG. 3.3. *Separator-vertex splitting.*

NIG representations of hypergraphs $\mathcal{H}_1$ and $\mathcal{H}_2$, respectively. Hence, the sum of the number of separator vertices of the 2-way GPVS obtained at each RB step will be equal to the total cutsize of the resulting multiway partition of $\mathcal{H}$ according to the connectivity metric.

Figure 3.3 illustrates three separator vertices v_{s_1}, v_{s_2} and v_{s_3} in a 2-way vertex separator and their splits into vertices $v_{s_1}^1, v_{s_2}^1, v_{s_3}^1$ and $v_{s_1}^2, v_{s_2}^2, v_{s_3}^2$. The three separator vertices v_{s_1}, v_{s_2} and v_{s_3} are connected with each other by three separator edges (v_{s_1}, v_{s_2}), (v_{s_1}, v_{s_3}) and (v_{s_2}, v_{s_3}) in order to show three distinct cases of separator edge replication in the accurate implementation. The figure also shows four hypergraph nodes u_x, u_y, u_z and u_t which induce the three separator edges, where u_x, u_z are assigned to part $\mathcal{U}_1$ and u_y, u_t are assigned to part $\mathcal{U}_2$. Since only u_x induces the separator edge (v_{s_1}, v_{s_2}) and u_x is assigned to $\mathcal{U}_1$, it is sufficient to replicate the separator edge (v_{s_1}, v_{s_2}) in only $\mathcal{V}_1$. Symmetrically, since only u_y induces the separator edge (v_{s_1}, v_{s_3}) and u_y is assigned to $\mathcal{U}_2$, it is sufficient to replicate the separator edge (v_{s_1}, v_{s_3}) in only $\mathcal{V}_2$. However, since u_z and u_t both induce the separator edge (v_{s_2}, v_{s_3}) and u_z and u_t are respectively assigned to $\mathcal{U}_1$ and $\mathcal{U}_2$, it is necessary to replicate the separator edge (v_{s_2}, v_{s_3}) in both $\mathcal{V}_1$ and $\mathcal{V}_2$.

This accurate implementation of the separator-vertex splitting method depends on the availability of both $\mathcal{H}$ and its NIG representation $\mathcal{G}$ at the beginning of each RB step. Hence, after each RB step, the sub-hypergraphs $\mathcal{H}_1$ and $\mathcal{H}_2$ should be constructed as well as the subgraphs $\mathcal{G}_1$ and $\mathcal{G}_2$. We briefly summarize the details of the proposed implementation method performed at each RB step. A 2-way GPVS is performed on $\mathcal{G}$ to obtain a vertex separator $\Pi_{VS}(\mathcal{G})$. Then, a node bipartition $\Pi_{\mathcal{U}}(\mathcal{H})$ of $\mathcal{H}$ is constructed according to (3.5) by decoding the vertex separator $\Pi_{VS}(\mathcal{G})$ of $\mathcal{G}$. Then, the 2-way vertex separator $\Pi_{VS}(\mathcal{G})$ is used together with the node bipartition $\Pi_{\mathcal{U}}(\mathcal{H})$ to generate subgraphs $\mathcal{G}_1$ and $\mathcal{G}_2$ as described above. The sub-hypergraphs $\mathcal{H}_1$ and $\mathcal{H}_2$ are also constructed for the use in subsequent RB steps. An alternative implementation could be first generating sub-hypergraphs $\mathcal{H}_1$ and $\mathcal{H}_2$ from $\Pi_{\mathcal{U}}(\mathcal{H})$ and then constructing subgraphs $\mathcal{G}_1$ and $\mathcal{G}_2$ from $\mathcal{H}_1$ and $\mathcal{H}_2$, respectively, using NIG construction. However, this alternative implementation method is significantly inefficient compared to the proposed implementation, since construction of the NIG representation from a given hypergraph is computationally expensive.

3.2.2. Balancing constraint. Consider a node partition $\Pi_{\mathcal{U}}(\mathcal{H}) = \{\mathcal{U}_1, \mathcal{U}_2, \ldots, \mathcal{U}_K\}$ of $\mathcal{H}$ constructed from the vertex separator $\Pi_{VS}(\mathcal{G}) = \{\mathcal{V}_1, \mathcal{V}_2, \ldots, \mathcal{V}_K\}$ of NIG $\mathcal{G}$ according to (3.5). Since the vertices of $\mathcal{G}$ correspond to the nets of the given hypergraph $\mathcal{H}$, it is easy to enforce a balance criterion on the nets of $\mathcal{H}$ by setting $w(v_i) = w(n_i)$. For example, assuming unit net weights, the partitioning constraint of balancing on the vertex counts of parts of $\Pi_{VS}(\mathcal{G})$ infers balance among the internal net counts of node parts of $\Pi_{\mathcal{U}}(\mathcal{H})$.

However, balance on the nodes of $\mathcal{H}$ can not be directly enforced during the GPVS of $\mathcal{G}$, because the NIG model suffers from information loss on hypergraph nodes. Here, we propose a vertex-weighting model for estimating the cumulative weight of hypergraph nodes in each vertex part $\mathcal{V}_k$ of the vertex separator $\Pi_{VS}(\mathcal{G})$. In this model, the objective is to find appropriate weights for the vertices of $\mathcal{G}$ so that vertex-part weight $W(\mathcal{V}_k)$ computed according to (2.1) approximates the node-part weight $W(\mathcal{U}_k)$ computed according to (2.6).

The NIG model can also be viewed as a clique-node model since each node u_h of the hypergraph induces an edge between each pair of vertices corresponding to the nets that connect u_h. So, the edges of $\mathcal{G}$ implicitly represent the nodes of $\mathcal{H}$. Each hypergraph node u_h of degree d_h induces $\binom{d_h}{2}$ clique edges among which the weight $w(u_h)$ is distributed evenly. That is, every clique edge induced by node u_h can be considered as having a uniform weight of $w(u_h)/\binom{d_h}{2}$. Multiple edges between the same pair of vertices is collapsed into a single edge whose weight is equal to the sum of the weights of its constituent edges. Hence, the weight $w(e_{ij})$ of each edge e_{ij} of $\mathcal{G}$ becomes,

$$w(e_{ij}) = \sum_{u_h \in Pins(n_i) \cap Pins(n_j)} \frac{w(u_h)}{\binom{d_h}{2}} \tag{3.6}$$

Then, the weight of each edge is uniformly distributed between the pair of vertices connected by that edge. That is, edge e_{ij} contributes $w(e_{ij})/2$ to both v_i and v_j. Hence, in the proposed model, the weight $w(v_i)$ of vertex v_i becomes,

$$w(v_i) = \frac{1}{2} \sum_{v_j \in Adj(v_i)} w(e_{ij})$$

$$= \sum_{u_h \in Pins(n_i)} \frac{w(u_h)}{d_h} \tag{3.7}$$

Consider an internal hypergraph node u_h of part $\mathcal{U}_k$ of $\Pi_{\mathcal{U}}(\mathcal{H})$. Since all graph vertices corresponding to the nets that connect u_h are in part $\mathcal{V}_k$ of $\Pi_{VS}(\mathcal{G})$, u_h will contribute $w(u_h)$ to $W(\mathcal{V}_k)$. Consider a boundary hypergraph node u_h of part $\mathcal{U}_k$ with an external degree $\delta_h < d_h$, i.e., u_h is connected by δ_h cut nets. Thus, u_h will contribute by an amount of $(1 - \delta_h/d_h)w(u_h)$ to $W(\mathcal{V}_k)$ instead of $w(u_h)$. So, vertex-part weight $W(\mathcal{V}_k)$ of $\mathcal{V}_k$ in $\Pi_{VS}(\mathcal{G})$ will be less than the actual node-part weight $W(\mathcal{U}_k)$ of $\mathcal{U}_k$ in $\Pi_{\mathcal{U}}(\mathcal{H})$. As the vertex-part weights of different parts of $\Pi_{VS}(\mathcal{G})$ will involve similar errors, the proposed method can be expected to produce a sufficiently good balance on the node-part weights of $\Pi_{\mathcal{U}}(\mathcal{H})$.

The free nodes can easily be exploited to improve the balance during the completion of partial node partition. For the cut-net metric in (2.8), we perform free-node-to-part assignment after obtaining K-way GPVS, since arbitrary assignments of free nodes do not disturb the cutsize by Corollary 2. However, for the connectivity
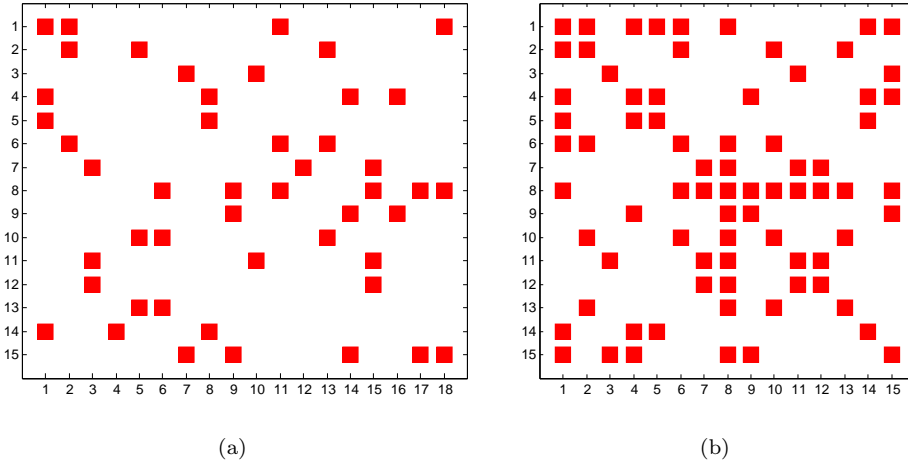
FIG. 3.4. *(a) A sample matrix A whose row-net hypergraph representation $\mathcal{H}_A$ is equal to the sample hypergraph $\mathcal{H}$ given in Figure 3.1(a) and (b) the matrix $Z = AA^T$.*

metric in (2.9), free-node-to-part assignment needs special attention if it is performed after obtaining a K-way GPVS. According to Theorem 2, arbitrary assignments of free nodes may increase the connectivity of cut nets. So, for the connectivity cutsize metric, we perform free-node-to-part assignment after each RB step to improve the balance. Note that free-node-to-part assignment performed in this way does not increase the connectivity of cut nets in the RB-GPVS-based by Corollary 3. For both cutsize metrics, the best-fit-decreasing heuristic [49] used in solving the bin-packing problem is adapted to obtain a complete node partition/bipartition. Free nodes are assigned to parts in decreasing weight, where the best-fit criterion corresponds to assigning a free node to a part that currently has the minimum weight. Initial part weights are taken as the weights of the two parts in partial node bipartition.

3.3. Matrix Theoretical View of the Relation Between HP and GPVS. We will first briefly discuss the row-net and column-net models we proposed for representing rectangular as well as symmetric and nonsymmetric square matrices in our earlier work [8, 9, 44, 43]. These two models are duals: the row-net representation of a matrix is equal to the column-net representation of its transpose. Here, we only discuss the row-net model for permuting a matrix A into a primal singly-bordered block-diagonal (SB) form, whereas the column-net model can be used for permuting A into a dual SB form. In the row-net hypergraph model, an $M \times N$ matrix $A = (a_{ij})$ is represented as a hypergraph $\mathcal{H}_A = (\mathcal{U}, \mathcal{N})$ on N nodes and M nets with the number of pins equal to the number of nonzeros in matrix A. Node and net sets $\mathcal{U}$ and $\mathcal{N}$ correspond, respectively, to the columns and rows of A. There exist one net n_i and one node u_j for each row i and column j, respectively. Net $n_i \subseteq \mathcal{U}$ contains the nodes corresponding to the columns that have a nonzero entry in row i, i.e., $u_j \in n_i$ if and only if $a_{ij} \neq 0$. That is, $Pins(n_i)$ represents the set of columns that have a nonzero in row i of A, and in a dual manner $Nets(u_j)$ represents the set of rows that have a nonzero in column j of A. Figure 3.4(a) shows an 15×18 matrix A whose row-net hypergraph representation $\mathcal{H}_A$ is equal to the sample hypergraph $\mathcal{H}$ given in Figure 3.1(a).

(a)   (b)
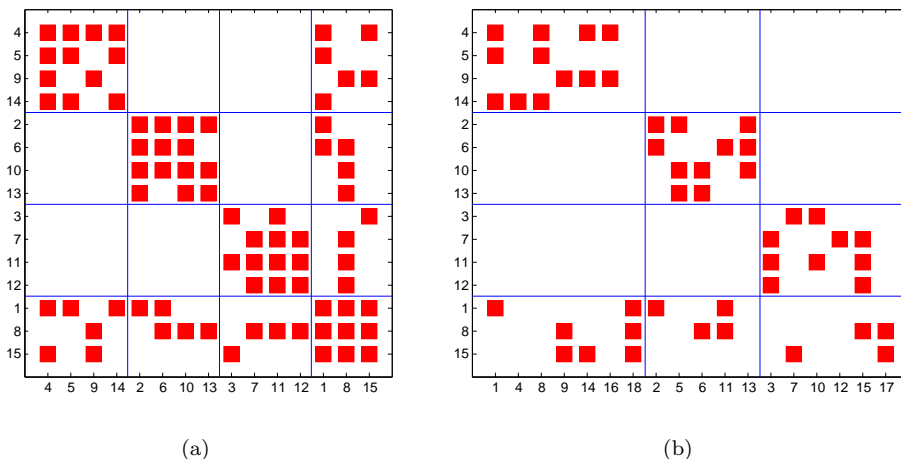
FIG. 3.5. *A 3-way DB from of the AA^T matrix (a) SB form A_{SB} of A shown in Figure 3.4(a).*

Let $\mathcal{G}_{NIG}(\mathcal{H}_A) = (\mathcal{V}, \mathcal{E})$ denote the NIG model for the row-net hypergraph representation $\mathcal{H}_A = (\mathcal{U}, \mathcal{N})$ of matrix A. By definition of the NIG model, the vertices of $\mathcal{G}_{NIG}$ will represent the rows of A, and $e_{ij} \in \mathcal{E}$ if and only if $Pins(n_i) \cap Pins(n_j) \neq \emptyset$. Since $Pins(n_i)$ represents the set of columns that have a nonzero in row i of A, $Pins(n_i) \cap Pins(n_j) \neq \emptyset$ corresponds to the condition that rows i and j of A have a nonzero in at least one common column. Let $Z = (z_{ij})$ denote the $M \times M$ matrix $Z = AA^T$, an $\langle . \rangle$ denote inner-product operator. Since $z_{ij} = \langle r_i, r_j^T \rangle$, z_{ij} will be nonzero if and only if $e_{ij} \in \mathcal{E}$. Hence, the sparsity pattern of symmetric matrix Z will correspond to the adjacency matrix representation of $\mathcal{G}_{NIG}$. In other words, $\mathcal{G}_{NIG}$ will be equivalent to the standard graph representation of symmetric matrix Z, i.e., $\mathcal{G}_{NIG}(\mathcal{H}_A) \equiv \mathcal{G}_{AA^T}$. Note that although vertex v_i of $\mathcal{G}_{NIG}$ represents only row i of A, it represents both row i and column i of AA^T in $\mathcal{G}_{AA^T}$.

Figure 3.4(b) shows the 15×15 matrix $Z = AA^T$. Note that the standard graph representation of Z is equivalent to the NIG representation $\mathcal{G}_{NIG}(\mathcal{H}_A)$ of $\mathcal{H}_A$. As has long been used for nested dissection ordering for sparsity preserving factorizations, the problem of transforming a symmetric matrix into a DB form through symmetric row/column permutation can be modeled as a GPVS problem on its standard graph representation. So, Figure 3.5(a) shows a 3-way DB form of the AA^T matrix induced by the 3-way GPVS $\Pi_{VS}(\mathcal{G})$ of $\mathcal{G}_{NIG}(\mathcal{H}_A)$ shown in Figure 3.4(b). Recall that the 3-way partition $\Pi_{\mathcal{U}}(\mathcal{H}_A)$ shown in Figure 3.1(b) is induced by $\Pi_{VS}(\mathcal{G})$. Hence, $\Pi_{VS}(\mathcal{G})$ induces the same SB form A_{SB} of A as shown in Figure 3.5(b).

3.4. Multilevel implementation of GPVS-based HP formulation. The state-of-the-art graph and hypergraph partitioning tools that adopt the multilevel framework, consist of three phases: *coarsening*, *initial partitioning*, and *uncoarsening*. In the first phase, a multilevel clustering is applied starting from the original graph/hypergraph by adopting various matching heuristics until the number of vertices in the coarsened graph/hypergraph reduces below a predetermined threshold value. Clustering corresponds to coalescing highly interacting vertices to supernodes. In the second phase, a partition is obtained on the coarsest graph/hypergraph using various heuristics including FM, which is an iterative refinement heuristic proposed

for graph/hypergraph partitioning by Fiduccia and Mattheyses [24] as a faster implementation of the KL algorithm proposed by Kernighan and Lin [35]. In the third phase, the partition found in the second phase is successively projected back towards the original graph/hypergraph by refining the projected partitions on the intermediate level uncoarser graphs/hypergraphs using various heuristics including FM.

One of the most important applications of GPVS is George's *nested–dissection* algorithm [25, 26], which has been widely used for reordering of the rows/columns of a symmetric, sparse, and positive definite matrix to reduce *fill* in the factor matrices. Here, GPVS is defined on the standard graph model of the given symmetric matrix. The basic idea in the nested dissection algorithm is to reorder symmetric matrix into a 2-way DB form so that no fill can occur in the off-diagonal blocks. The DB form of the given matrix is obtained through a symmetric row/column permutation induced by a 2-way GPVS. Then, both diagonal blocks are reordered by applying the dissection strategy recursively. The performance of the nested-dissection reordering algorithm depends on finding small vertex separators at each dissection step.

In this work, we adapted and modified the *onmetis* ordering code of *MeTiS* [31] for implementing our GPVS-based HP formulation. *onmetis* utilizes RB paradigm for obtaining multiway GPVS. Since K is not known in advance for ordering applications, recursive bipartitioning operations continue until the weight of a part becomes sufficiently small. In our implementation, we terminate the recursive bipartitioning process whenever the number of parts become K.

The separator refinement scheme used in the uncoarsening phase of *onmetis* considers vertex moves from vertex separator $\Pi_{VS}(\mathcal{G})$ to both $\mathcal{V}_1$ and $\mathcal{V}_2$ in $\Pi_{VS} = \{\mathcal{V}_1, \mathcal{V}_2; \mathcal{V}_S\}$. During these moves, *onmetis* uses the following feasibility constraint, which incorporates the size of the separator in balancing, i.e.,

$$\max\{W(\mathcal{V}_1), W(\mathcal{V}_2)\} \leq (1 + \epsilon)\frac{W(\mathcal{V}_1) + W(\mathcal{V}_2) + W(\mathcal{V}_S)}{2} = W_{max} \qquad (3.8)$$

However, this may become a loose balancing constraint compared to (2.2) for relatively large separator sizes which is typical during refinements of coarser graphs. This loose balancing constraint is not an important concern in *onmetis*, because it is targeted for fill-reducing sparse matrix ordering which is not very sensitive to the imbalance between part sizes. Nevertheless, this scheme degrades the load balancing quality of our GPVS-based HP implementation, where load balancing is more important in the applications for which HP is utilized. We modified *onmetis* by computing the maximum part weight constraint as

$$W_{max} = (1 + \epsilon)(W(\mathcal{V}_1) + W(\mathcal{V}_2))/2 \qquad (3.9)$$

at the beginning of each FM pass, whereas *onmetis* computes W_{max} according to (3.8) once for all FM passes, in a level. Furthermore, *onmetis* maintains only one value for each vertex which denotes both the weight and the cost of the vertex. We added a second field for each vertex to hold the weight and the cost of the vertex separately. The weights and the costs of vertices are accumulated independently during vertex coalescings performed by matchings at the coarsening phases. Recall that weight values are used for maintaining the load balancing criteria, whereas cost values are used for computing the size of the separator. That is, FM gains of the separator vertices are computed using the cost values of those vertices.

The GPVS-based HP implementation obtained by adapting *onmetis* as described in this subsection will be referred to as *onmetisHP*.

4. Experimental Results. We test the performance of our GPVS-based HP formulation by partitioning matrices from the linear-programming (LP) and the positive definite (PD) matrix collections of the University of Florida matrix collection [18]. Matrices in the latter collection are square and symmetric, whereas the matrices in the former collection are rectangular. The row-net hypergraph models [9, 13] of the test matrices constitute our test set. In these hypergraphs, nets are associated with unit cost. To show the validity of our GPVS-based HP formulation, test hypergraphs are partitioned by both $PaToH$ and $onmetisHP$ and default parameters are utilized in both tools. In general, the maximum imbalance ratio ϵ was set to be 10%.

We excluded small matrices that have less than 1000 rows or 1000 columns. In the LP matrix collection, there were 190 large matrices out of 342 matrices. Out of these 190 large matrices, 5 duplicates, 1 extremely large matrix and 5 matrices, for which NIG representations are extremely large were excluded. We also excluded 26 outlier matrices which yield large separators[1] to avoid skewing the results. Thus, 153 test hypergraphs are used from the LP matrix collection. In the PD matrix collection, there were 170 such large matrices out of 223 matrices. Out of these 170 large matrices, 2 duplicates, 2 matrices, for which NIG representations are extremely large and 7 matrices with large separators were excluded. Thus, 159 test hypergraphs are used from the PD matrix collection. We experimented with K-way partitioning of test hypergraphs for $K = 2, 4, 8, 16, 32, 64$, and 128. For a specific K value, K-way partitioning of a test hypergraph constitutes a partitioning instance. For the LP collection, instances in which $min\{|\mathcal{U}|, |\mathcal{N}|\} < 50K$ are discarded as the parts would become too small. So, $153, 153, 153, 153, 135, 100$, and 65 hypergraphs are partitioned for $K = 2, 4, 8, 16, 32, 64$, and 128, respectively, for the LP collection. Similarly for the PD collection, instances in which $|\mathcal{U}| < 50K$ are discarded. So, $159, 159, 159, 159, 145, 131$, and 109 hypergraphs are partitioned for $K = 2, 4, 8, 16, 32, 64$, and 128, respectively for the PD collection. In this section, we summarize our findings in these experiments. Please refer to the Appendix for detailed experimental results for each partitioning instance.

The hypergraphs obtained from the LP matrix collection are used for permuting the matrices into singly-bordered (SB) block-angular-form for coarse-grain parallelization of linear-programming applications [3]. Here, minimizing the cutsize according to the cut-net metric (2.4) corresponds to minimizing the size of the row border in the induced SB form. In these applications, nets are either associated with unit weights or weights that are equal to the nonzeros in the respective rows. In the former case, net balancing corresponds to balancing the row counts of the diagonal blocks, whereas in the latter case, net balancing corresponds to balancing the nonzero counts of the diagonal blocks. Experimental comparisons are provided only for the former case, because $PaToH$ does not support different cost and weight associations to nets.

The hypergraphs obtained from the PD matrix collection are used for minimizing communication overhead in column-parallel matrix-vector multiply algorithm in iterative solvers. Here, minimizing the cutsize according to the connectivity metric (2.5) corresponds to minimizing the total communication volume when the point-to-point inter-processor communication scheme is used [9]. Minimizing the cutsize according to the cut-net metric (2.4) corresponds to minimizing the total communication volume when the collective communication scheme is used [13]. In these applications, nodes associated with weights that are equal to the nonzeros in the respective columns. So, balancing part weights corresponds to computational load balancing.

---

[1]Here, a separator is said to be large if it includes more than 33% of all nets.

In the following tables, the performance figures are computed and displayed as follows. Since both $PaToH$ and $onmetisHP$ tools involve randomized heuristics, 10 different partitions are obtained for each partitioning instance and the geometric average of the 10 resultant partitions are computed as the representative results for both HP tools on the particular partitioning instance. For each partitioning instance, the cutsize value is normalized with respect to the total number of nets in the respective hypergraph. Recall that all test hypergraphs have unit-cost nets. So, for the cut-net metric, these normalized cutsize values show the fraction of the cut nets. For the connectivity metric, these normalized cutsize values show the average net connectivity. For each partitioning instance, the running time of $PaToH$ is normalized with respect to that of $onmetisHP$, thus showing the speedup obtained by $onmetisHP$ for that partitioning instance. These normalized cutsize values and speedup values as well as percent load imbalance values are summarized in the tables by taking the geometric averages for each K value.

TABLE 4.1
Performance averages on the LP matrix collection for cut-net metric with net balancing.

	$PaToH$		$onmetisHP$		
K	cutsize	$\%LI$	cutsize	$\%LI$	speedup
2	0.02	1.2%	0.03	0.3%	2.04
4	0.02	1.9%	0.05	2.6%	2.45
8	0.07	3.1%	0.09	6.9%	2.64
16	0.09	5.2%	0.14	13.0%	2.78
32	0.13	8.8%	0.18	23.1%	2.83
64	0.15	11.5%	0.21	27.8%	2.83
128	0.16	13.5%	0.21	31.3%	2.76

Table 4.1 displays overall performance averages of $onmetisHP$ compared to those of $PaToH$ for the cut-net metric in (see (2.8)) with net balancing on the LP matrix collection. As seen in Table 4.1, $onmetisHP$ obtains hypergraph partitions of comparable cutsize quality with those of $PaToH$. However, load balancing quality of partitions produced by $onmetisHP$ is worse than those of $PaToH$, especially with increasing K. As seen in the table, $onmetisHP$ runs significantly faster than $PaToH$ for each K. For example, $onmetisHP$ runs 2.83 times faster than $PaToH$ for 32-way partitionings on the average.

TABLE 4.2
Performance averages on the PD matrix collection for cut-net metric with node balancing.

	$PaToH$		$onmetisHP$				
K	cutsize	$\%LI$	cutsize	$exp\%LI_p$	$act\%LI_p$	$act\%LI_c$	speedup
2	0.01	0.1%	0.01	0.2%	0.2%	0.1%	1.40
4	0.03	0.3%	0.03	0.9%	1.5%	1.1%	1.75
8	0.05	0.4%	0.05	2.8%	3.7%	2.7%	1.96
16	0.08	0.6%	0.08	6.7%	7.4%	5.4%	1.98
32	0.12	0.9%	0.12	13.4%	12.8%	9.2%	2.17
64	0.17	1.2%	0.16	22.1%	19.8%	13.5%	2.27
128	0.25	1.6%	0.24	32.5%	28.8%	17.9%	2.25

Table 4.2 displays overall performance averages of $onmetisHP$ compared to those of $PaToH$ for the cut-net metric with node balancing on the PD matrix collection. In the table, $exp\%LI_p$ and $act\%LI_p$ respectively denote the expected and actual percent load imbalance values for the partial node partitions of the hypergraphs induced by K-way GPVS. $act\%LI_c$ denotes the actual load imbalance values for the complete

node partitions obtained after free-node-to-part assignment. The small discrepancies between the $exp\%LI_p$ and $act\%LI_p$ values show the validity of the approximate weighting scheme proposed in Section 3.2 for the vertices of the NIG. As seen in the table, for each K, the $act\%LI_c$ value is considerably smaller than the $act\%LI_p$ value. This experimental finding confirms the effectiveness of the free-node-to-part assignment scheme mentioned in Section 3.2. As seen in Table 4.2, $onmetisHP$ obtains hypergraph partitions of comparable cutsize quality with those of $PaToH$. However, load balancing quality of partitions produced by $onmetisHP$ is considerably worse than those of $PaToH$. As seen in the table, $onmetisHP$ runs considerably faster than $PaToH$ for each K.

TABLE 4.3
Comparison of accurate and overcautious separator-vertex splitting implementations with averages on the PD matrix collection for connectivity metric with node balancing.

| K | *overcautous / accurate* | | |
	cutsize	$\%LI$	*speedup*
2	1.00	0.63	1.29
4	1.02	0.79	1.50
8	1.10	0.79	1.61
16	1.29	0.70	1.63
32	1.56	0.64	1.61
64	1.84	0.69	1.60
128	2.09	0.60	1.54

Table 4.3 is constructed based on the PD matrix collection to show the validity of the accurate vertex splitting formulation proposed in Section 3.2.1 for the connectivity cutsize metric (see (2.9)). In this table, speedup, cutsize and load imbalance values of $onmetisHP$ that uses the straightforward (overcautious) separator-vertex splitting implementation are normalized with respect to those of $onmetisHP$ that uses the accurate implementation. In the straightforward implementation, free-node-to-part assignment is performed after obtaining a K-way GPVS, since hypergraphs are not carried through the RB process. Free nodes are assigned to parts in decreasing weight, where the best-fit criterion corresponds to assigning a free node to a part which increases connectivity cutsize by the smallest amount with ties are broken in favor of the part with minimum weight. As seen in the table, the overcautious implementation leads to slightly better load balance than accurate implementation, because overcautious implementation performs free-node-to-part assignment on the K-way partial node partition induced by the K-way GPVS. As also seen in the table, the overcautious implementation, as expected, leads to slightly better speedup than the accurate implementation. However, the accurate implementation leads to significantly less cutsize values.

Table 4.4 displays overall performance averages of $onmetisHP$ compared to those of $PaToH$ for the connectivity metric with node balancing on the PD matrix collection. In contrast to Table 4.2, load imbalance values are not displayed for partial node partitions in Table 4.4, because free-node-to-part assignments are performed after each 2-way GPVS operation for the sake of accurate implementation of the separator-vertex splitting method as mentioned in Section 3.2. So, $\%LI$ values displayed in Table 4.4 show the actual percent imbalance values for the K-way node partitions obtained. As seen in Table 4.4, similar to results of Table 4.2, $onmetisHP$ obtains hypergraph partitions of comparable cutsize quality with those of $PaToH$, whereas load balancing quality of partitions produced by $onmetisHP$ is considerably

TABLE 4.4
Performance averages on the PD matrix collection for connectivity metric with node balancing.

	PaToH		onmetisHP		
K	cutsize	%LI	cutsize	%LI	speedup
2	1.03	0.1%	1.03	0.2%	1.29
4	1.08	0.3%	1.08	0.8%	1.50
8	1.15	0.5%	1.15	1.7%	1.61
16	1.26	0.7%	1.25	4.1%	1.63
32	1.37	1.0%	1.36	7.9%	1.61
64	1.49	1.5%	1.47	11.8%	1.60
128	1.63	1.9%	1.60	16.5%	1.54

worse than those of $PaToH$. As seen in Table 4, $onmetisHP$ still runs considerably faster than $PaToH$ for each K for the connectivity metric. However, the speedup values in Table 4.4 , are considerable smaller compared to those displayed in Table 2, which is due to the fact that $onmetisHP$ carries hypergraphs during the RB process for the sake of accurate implementation of the separator-vertex splitting method as mentioned in Section 3.2.

A common property of Tables 4.1, 4.2, and 4.4, is the increasing speedup of $onmetisHP$ compared to $PaToH$ with increasing K values. This experimental finding stems from the fact that the initial NIG construction overhead amortizes with increasing K. Another common property of Tables 4.1, 4.2, and 4.4, is that $onmetisHP$ runs significantly faster than $PaToH$, while producing partitions of comparable cutsize quality with, however, worse load balancing quality. These experimental findings justify our GPVS-based hypergraph partitioning formulation for effective parallelization of applications in which computational balance definition is not very precise and preprocessing overhead due to partitioning overhead is important.

5. Conclusions. We have presented how the hypergraph partitioning problem can be efficiently and effectively solved through finding vertex separators on the net intersection graph representation of a hypergraph. Our empirical study on a wide set of test matrices showed that runtimes can be as much as 4.17 times faster, with the cutsize quality is preserved on average (and improved in many cases), while balance was achieved for small number of parts and remained acceptable for large number of parts. Moreover, we proposed techniques that can trade off cutsize and runtime against balance, showing that balance can be achieved even for high number of parts. Overall results prove that, the proposed hypergraph partitioning through vertex separators on graphs is ideal for applications where balance is not well-defined, which is the main motivation for our work, and competitive for application where balance is important.

We believe that the success of the proposed methods point to several future research directions. First, better vertex weighting schemes to approximate the node balance is an area that can make a significant impact. We believe exploiting domain specific information or devising techniques that can apply to certain classes of graphs, as opposed to constructing generic approximations that can work for all graphs, is a promising avenue to explore. Secondly, the algorithms we have used in this paper, were only slightly adjusted for the particular problem we were solving. There is a lot of room for improvements in algorithms for finding vertex separators with balanced hypergraph partitions, and we believe these algorithms can be designed and implemented on the existing partitioning graph partitioning frameworks, which means strong algorithmic ideas can be translated into effective software tools with rel-

atively little effort. Finally, this paper is only an example of the growing importance of graph partitioning and the need for more flexible models for graph partitioning. Graph partitioning now is an internal step for divide-and-conquer based methods, whose popularity will only increase with the growing problems sizes. As such, requirements for graph partitioning will keep growing and broadening. While, the state of the art for graph partitioning has drastically improved from the days of merely minimizing the number of cut edges, while keeping the number of vertices balanced between the *two* parts, we believe there is still a lot of room for growth for more general models for graph partitioning.

REFERENCES

[1] K. Akbudak, E. Kayaaslan, and C. Aykanat, *Cache locality exploiting methods and models for sparse matrix-vector multiplication*, Technical Report, (2010).

[2] C. J. Alpert and A. B. Kahng, *Recent directions in netlist partitioning: A survey*, VLSI Journal, 19 (1995), pp. 1–81.

[3] C. Aykanat, A. Pinar, and U. V. Çatalyürek, *Permuting sparse rectangular matrices into block-diagonal form*, SIAM Journal on Scientific Computing, 26 (2004), pp. 1860–1879.

[4] R. H. Bisseling, J. Byrka, S. Cerav-Erbas, N. Gvozdenović, M. Lorenz, R. Pendavingh, C. Reeves, M. Röger, and A. Verhoeven, *Partitioning a call graph*, in Proceedings Study Group Mathematics with Industry 2005, Amsterdam, CWI, Amsterdam, 2005.

[5] R. H. Bisseling and I. Flesch, *Mondriaan sparse matrix partitioning for attacking cryptosystems by a parallel block lanczos algorithm: a case study*, Parallel Comput., 32 (2006), pp. 551–567.

[6] T. N. Bui and C. Jones, *Finding good approximate vertex and edge partitions is NP-hard*, Infomation Processing Letters, 42 (1992), pp. 153–159.

[7] B. B. Cambazoglu and C. Aykanat, *Hypergraph-partitioning-based remapping models for image-space-parallel direct volume rendering of unstructured grids*, IEEE Transactions on Parallel and Distributed Systems, 18 (2007), pp. 3–16.

[8] U. V. Çatalyürek and C. Aykanat, *Decomposing irregularly sparse matrices for parallel matrix-vector multiplications*, in Proceedings of 3rd International Symposium on Solving Irregularly Structured Problems in Parallel, Irregular'96, vol. 1117 of Lecture Notes in Computer Science, Springer-Verlag, 1996, pp. 75–86.

[9] ———, *Hypergraph-partitioning based decomposition for parallel sparse-matrix vector multiplication*, IEEE Transactions on Parallel and Distributed Systems, 10 (1999), pp. 673–693.

[10] ———, *PaToH: A Multilevel Hypergraph Partitioning Tool, Version 3.0*, Bilkent University, Department of Computer Engineering, Ankara, 06533 Turkey. PaToH is available at `http://bmi.osu.edu/~umit/software.htm`, 1999.

[11] ———, *A fine-grain hypergraph model for 2D decomposition of sparse matrices*, in Proceedings of 15th International Parallel and Distributed Processing Symposium (IPDPS), San Francisco, CA, April 2001.

[12] ———, *A hypergraph-partitioning approach for coarse-grain decomposition*, in ACM/IEEE SC2001, Denver, CO, November 2001.

[13] U. V. Çatalyürek, C. Aykanat, and B. Ucar, *On two-dimensional sparse matrix partitioning: Models, methods, and a recipe*, SIAM Journal on Scientific Computing, 32 (2010), pp. 656–683.

[14] P. K. Chan, D. F. Schlag, and J. Y. Zien, *Spectral K-way ratio-cut partitioning and clustering*, in Proceedings of the 30th Design Automation Conference, ACM/IEEE, 1993, pp. 749–754.

[15] C. Chang, T. Kurc, A. Sussman, U. V. Çatalyürek, and J. Saltz, *A hypergraph-based workload partitioning strategy for parallel data aggregation*, in Proceedings of the Eleventh SIAM Conference on Parallel Processing for Scientific Computing, SIAM, Mar. 2001.

[16] J. Cong, L. Hagen, and A. B. Kahng, *Net partitions yield better module partitions*, in Proceedings of 29th ACM/IEEE Design Automation Conference, 1992, pp. 47–52.

[17] J. Cong, W. Labio, and N. Shivakumar, *Multi-way VLSI circuit partitioning based on dual net representation*, in Proceedings of IEEE International Conference on Computer-Aided Design, 1994, pp. 56–62.

[18] T. Davis, *The University of Florida sparse matrix collection*, Tech. Report REP-2007-298, CISE Department, University of Florida, Gainesville, FL, USA, 2007.

[19] E. Demir and C. Aykanat, *Efficient successor retrieval operations for aggregate query processing on clustered road networks*, Inf. Sci., 180 (2010), pp. 2743–2762.

[20] E. Demir, C. Aykanat, and B. Barla Cambazoglu, *Clustering spatial networks for aggregate query processing: A hypergraph approach*, Inf. Syst., 33 (2008), pp. 1–17.

[21] E. Demir, C. Aykanat, and B. B. Cambazoglu, *A link-based storage scheme for efficient aggregate query processing on clustered road networks*, Inf. Syst., 35 (2010), pp. 75–93.

[22] K. Devine, E. Boman, R. Heaphy, R. Bisseling, and U. Catalyurek, *Parallel hypergraph partitioning for scientific computing*, in Proceedings of 20th International Parallel and Distributed Processing Symposium (IPDPS), IEEE, 2006.

[23] N. Dingle, P. Harrison, and W. Knottenbelt, *Uniformization and Hypergraph Partitioning for the Distributed Computation of Response Time Densities in Very Large Markov Models*, Journal of Parallel and Distributed Computing, 64 (2004), pp. 908–920.

[24] C. M. Fiduccia and R. M. Mattheyses, *A linear-time heuristic for improving network partitions*, in Proceedings of the 19th ACM/IEEE Design Automation Conference, 1982, pp. 175–181.

[25] A. George and J. W. H. Liu, *Computer solution of large sparse positive definite systems*, Prentice-Hall, 1981.

[26] J. A. George, *Nested dissection of a regular finite element mesh*, SIAM Journal on Numerical Analysis, 10 (1973), pp. 345–363.

[27] G. Hachtel, A. Newton, and A. Sangiovanni-Vincentelli, *An algorithm for optimal pla folding*, IEEE Transactions on Computer-Aided Design of Integrated Circuits and Systems, 1 (1982), pp. 63–77.

[28] S. W. Hadley, B. L. Mark, and A. Vanelli, *An efficient eigenvector approach for finding netlist partitions*, IEEE Transactions on Computer-Aided Design, 11 (1992), pp. 885–892.

[29] E. Ihler, D. Wagner, and F. Wagner, *Modeling hypergraphs by graphs with the same mincut properties*, Information Processing Letters, 45 (1993), pp. 171–175.

[30] A. B. Kahng, *Fast hypergraph partition*, in Proceedings of the 26th ACM/IEEE Design Automation Conference, 1989, pp. 762–766.

[31] G. Karypis and V. Kumar, *MeTiS A Software Package for Partitioning Unstructured Graphs, Partitioning Meshes, and Computing Fill-Reducing Orderings of Sparse Matrices Version 4.0*, University of Minnesota, Department of Comp. Sci. and Eng., Army HPC Research Center, Minneapolis, 1998.

[32] G. Karypis, V. Kumar, R. Aggarwal, and S. Shekhar, *hMeTiS A Hypergraph Partitioning Package Version 1.0.1*, University of Minnesota, Department of Comp. Sci. and Eng., Army HPC Research Center, Minneapolis, 1998.

[33] K. Kaya and C. Aykanat, *Iterative-improvement-based heuristics for adaptive scheduling of tasks sharing files on heterogeneous master-slave environments*, IEEE Trans. Parallel Distrib. Syst., 17 (2006), pp. 883–896.

[34] K. Kaya, B. Uçar, and C. Aykanat, *Heuristics for scheduling file-sharing tasks on heterogeneous systems with distributed repositories*, J. Parallel Distrib. Comput., 67 (2007), pp. 271–285.

[35] B. W. Kernighan and S. Lin, *An efficient heuristic procedure for partitioning graphs*, The Bell System Technical Journal, 49 (1970), pp. 291–307.

[36] G. Khanna, N. Vydyanathan, T. Kurc, U. Catalyurek, P. Wyckoff, J. Saltz, and P. Sadayappan, *A hypergraph partitioning based approach for scheduling of tasks with batch-shared I/O*, in Proceedings of the 5th IEEE/ACM International Symposium on Cluster Computing and the Grid (CCGrid 2005), May 2005.

[37] M. Koyutürk and C. Aykanat, *Iterative-improvement-based declustering heuristics for multi-disk databases*, Inf. Syst., 30 (2005), pp. 47–70.

[38] E. Lawler, *Combinatorial Optimization: Networks and Matroids*, Holt, Rinehart, and Winston, 1976.

[39] C. E. Leiserson and J. G. Lewis, *Orderings for parallel sparse symmetric matrix factorization*, in Third SIAM Conference on Parallel Processing for Scientific Computing, 1987, pp. 27–31.

[40] T. Lengauer, *Combinatorial Algorithms for Integrated Circuit Layout*, Willey–Teubner, Chichester, U.K., 1990.

[41] D.-R. Liu and M.-Y. Wu, *A hypergraph based approach to declustering problems*, Distrib. Parallel Databases, 10 (2001), pp. 269–288.

[42] M. M. Ozdal and C. Aykanat, *Hypergraph models and algorithms for data-pattern-based clustering*, Data Min. Knowl. Discov., 9 (2004), pp. 29–57.

[43] A. Pinar and C. Aykanat, *An effective model to decompose linear programs for parallel solution*, in Proceedings of the Third International Workshop on Applied Parallel Computing,

PARA'96, vol. 1184 of Lecture Notes in Computer Science, Springer-Verlag, 1997, pp. 592–601.

[44] A. Pinar, U. V. Çatalyürek, C. Aykanat, and M. Pinar, *Decomposing linear programs for parallel solution*, Lecture Notes in Computer Science, 1041 (1996), pp. 473–482.

[45] A. Pinar, E. Chow, and A. Pothen, *Combinatorial techniques for constructing sparse null-space bases*, Electronic Transactions on Numerical Analysis, 22 (2006), pp. 122–145. special volume on saddle point problems: numerical solution and applications.

[46] A. Pinar and B. Hendrickson, *Partitioning for complex objectives*, in Proc. Irregular 2001, 2001.

[47] A. Pothen and C. J. Fan, *Computing the block triangular form of a sparse matrix*, ACM Transactions on Mathematical Software, 16 (1990), pp. 303–324.

[48] A. Pothen, H. D. Simon, and K.-P. Liou, *Partitioning sparse matrices with eigenvectors of graphs*, SIAM Journal on Matrix Analysis and Applications, 11 (1990), pp. 430–452.

[49] S. Sahni, *General techniques for combinatorial approximation*, Operations Research, 25 (1977), pp. 920–936.

[50] S. Shekhar, C.-T. Lu, S. Chawla, and S. Ravada, *Efficient join-index-based spatial-join processing: A clustering approach*, IEEE Trans. Knowl. Data Eng., 14 (2002), pp. 1400–1421.

[51] M. M. Strout and P. D. Hovland, *Metrics and models for reordering transformations*, in Proc. of the Second ACM SIGPLAN Workshop on Memory System Performance (MSP04), Washington DC., June 2004, ACM, pp. 23–34.

[52] G. Szederknyi, *Computing sparse and dense realizations of reaction kinetic systems*, Journal of Mathematical Chemistry, 47 (2010), pp. 551–568. 10.1007/s10910-009-9525-5.

[53] A. Trifunovic and W. J. Knottenbelt, *Parkway 2.0: A parallel multilevel hypergraph partitioning tool*, in Proc. 19th International Symposium on Computer and Information Sciences (ISCIS 2004), vol. 3280 of LNCS, Springer, 2004, pp. 789–800.

[54] B. Uçar and C. Aykanat, *Encapsulating multiple communication-cost metrics in partitioning sparse rectangular matrices for parallel matrix-vector multiplies*, SIAM Journal on Scientific Computing, 26 (2004), pp. 1837–1859.

[55] ——, *Partitioning sparse matrices for parallel preconditioned iterative methods*, SIAM Journal on Scientific Computing, 29 (2007), pp. 1683–1709.

[56] ——, *Revisiting hypergraph models for sparse matrix partitioning*, SIAM Review, 49 (2007), pp. 595–603.

[57] B. Uçar, C. Aykanat, M. C. Pinar, and T. Malas, *Parallel image restoration using surrogate constraint methods*, J. Parallel Distrib. Comput., 67 (2007), pp. 186–204.

[58] B. Vastenhouw and R. H. Bisseling, *A two-dimensional data distribution method for parallel sparse matrix-vector multiplication*, SIAM Review, 47 (2005), pp. 67–95.

[59] v. Vrba, H. Espeland, P. Halvorsen, and C. Griwodz, *Limits of work-stealing scheduling*, Job Scheduling Strategies for Parallel Processing: 14th International Workshop, JSSPP 2009, Rome, Italy, May 29, 2009. Revised Papers, (2009), pp. 280–299.

[60] A. N. Yzelman and R. H. Bisseling, *Cache-oblivious sparse matrix-vector multiplication by using sparse matrix partitioning methods*, SIAM J. Sci. Comput., 31 (2009), pp. 3128–3154.

Appendix. In this section, we present the details of our experiments whose average results are given in Section 4. Table 5.1 displays the properties of the matrices we used in our experiments. Tables 5.2-5.8 display the result of 2, 4, 8, 16, 32, 64 and 128-way partitioning performance of the LP matrices for cut-net metric with net balancing. Tables 5.9-5.15 display the result of 2, 4, 8, 16, 32, 64 and 128-way partitioning performance of the PD matrices for cut-net metric with node balancing. Tables 5.16-5.22 display the result of 2, 4, 8, 16, 32, 64 and 128 -way partitioning performance of the PD matrices for connectivity metric with node balancing.

Table 5.1: Hypergraph and NIG properties for matrices of LP and PD matrix collections.

LP Collection				PD Collection		
name	$|\mathcal{N}|$	$|\mathcal{U}|$	$|\mathcal{E}|$	name	$|\mathcal{U}|$	$|\mathcal{E}|$
lp_truss	1000	8806	25122	msc01050	1050	136594
rosen2	1032	3080	31800	bcsstm08	1074	0
lp_ship12s	1042	2869	10690	bcsstm09	1083	0
lp_ship12l	1042	5533	21346	bcsstk09	1083	70206
lp_sctap2	1090	2500	11010	bcsstk10	1086	53418
lp_woodw	1098	8418	40842	1138_bus	1138	10004
lp_osa_07	1118	25067	104932	bcsstk27	1224	136882
qiulp	1192	1900	12144	mhd1280b	1280	26362
lp_sierra	1227	2735	9872	plbuckle	1282	79330
lp_ganges	1309	1706	15312	msc01440	1440	149808
model4	1337	4962	87914	bcsstk11	1473	92714
lp_pilot	1441	4860	123076	bcsstm11	1473	0
lp_sctap3	1480	3340	14772	bcsstm12	1473	52142
lp_degen3	1503	2604	100356	bcsstk12	1473	92714
fxm2-6	1520	2845	26656	ex33	1733	59050
cep1	1521	4769	196152	bcsstk14	1806	193848
primagaz	1554	10836	21658	ex3	1821	193498
pcb1000	1565	2820	32902	nasa1824	1824	140442
model3	1609	4565	43084	plat1919	1919	98990
progas	1650	1900	26210	bcsstm26	1922	0
model5	1744	11802	173646	bcsstk26	1922	90608
scrs8-2b	1820	3499	203016	bcsstk13	2003	394770
lp_cycle	1890	3371	55428	nasa2146	2146	189396
deter0	1923	5468	12466	ex10	2410	191524
lp_pilot87	2030	6680	236594	Chem97ZtZ	2541	88824
rosen10	2056	6152	47160	ex10hs	2548	202682
model6	2094	5289	62046	ex13	2568	277316
p6000	2095	7947	8964	nasa2910	2910	887840
lp_stocfor2	2157	3045	25476	bcsstk23	3134	217498
lp_d2q06c	2171	5831	53982	bcsstm23	3134	0
lp_80bau3b	2262	11934	20148	mhd3200b	3200	30944
nemspmm2	2301	8734	101804	bibd_81_2	3240	0
lp_bnl2	2324	4486	26914	ex9	3363	370452
lp_osa_14	2337	54797	227686	bcsstm24	3562	0
nemspmm1	2362	8903	111902	bcsstk24	3562	442912
lp_greenbea	2389	5598	67682	bcsstk21	3600	89472
lpi_greenbea	2390	5596	67694	bcsstm21	3600	0
lp_ken_07	2426	3602	11956	bcsstk15	3948	523740
scagr7-2c	2447	3479	257282	sts4098	4098	1085428
lpi_gran	2604	2525	194708	t2dal_e	4257	0
lpi_bgindy	2671	10880	124076	bcsstk28	4410	591662
l30	2701	16281	53428	msc04515	4515	265404
model9	2787	10939	101082	nasa4704	4704	356788
model8	2896	6464	53908	mhd4800b	4800	46552
lp_pds_02	2953	7716	20328	crystm01	4875	395322
lp22	2958	16392	221064	bcsstk16	4884	1033898
				Continued on next page		

Table 5.1 – continued from previous page

LP Collection				PD Collection		
name	$|\mathcal{N}|$	$|\mathcal{U}|$	$|\mathcal{E}|$	name	$|\mathcal{U}|$	$|\mathcal{E}|$
lp_cre_c	2986	6411	37810	s3rmt3m3	5357	540084
lpi_cplex1	3005	5224	2262516	s3rmt3m1	5489	573546
plddb	3069	5049	19586	s2rmq4m1	5489	749964
rat	3136	9408	1245198	s1rmt3m1	5489	573546
lp_maros_r7	3136	9408	660944	s1rmq4m1	5489	749964
delf	3170	5598	30338	s2rmt3m1	5489	573546
stat96v4	3173	63076	51540	s3rmq4m1	5489	749964
deter4	3235	9133	86758	ex15	6867	259938
lpl2	3294	10881	36762	Kuu	7102	1555534
model7	3358	9560	94080	Muu	7102	774216
sctap1-2c	3390	7458	273912	bcsstk38	8032	1660234
lp_cre_a	3428	7248	41496	aft01	8205	426542
lpi_ceria3d	3576	4400	1959730	fv1	9604	224652
ch	3700	8291	50464	fv3	9801	229320
aircraft	3754	7517	2834250	fv2	9801	229320
lpi_gosh	3790	13455	202218	bundle1	10581	24062342
deter8	3831	10905	34624	ted_B	10605	479178
fxm2-16	3900	7335	70906	ted_B_unscaled	10605	479178
nemsemm1	3945	75310	393474	msc10848	10848	6174798
pcb3000	3960	7732	84924	bcsstk17	10974	1395962
pgp2	4034	13254	1347842	t2dah_e	11445	602052
rlfddd	4050	61521	376536	bcsstk18	11948	701260
deter6	4255	12113	40868	cbuckle	13681	2255450
large	4282	7297	46414	crystm02	13965	1294602
lp_osa_30	4350	104374	432388	Pres_Poisson	14822	2235694
stormg2-8	4393	11322	50684	bcsstm25	15439	0
model10	4400	16819	288860	bcsstk25	15439	1153480
nsir	4453	10057	469684	Dubcova1	16129	981872
seymourl	4944	6316	1208040	olafu	16146	3372106
cq5	5048	11748	112872	gyro_m	17361	1908612
p05	5090	9590	219438	gyro	17361	5760558
deter5	5103	14529	54796	bodyy4	17546	314540
scsd8-2b	5130	35910	1408030	bodyy5	18589	333146
r05	5190	9690	400968	bodyy6	19366	346860
bas1lp	5411	9825	2591680	raefsky4	19779	5322790
deter1	5527	15737	62480	LFAT5000	19994	129928
co5	5774	12325	125918	LF10000	19998	179956
stat96v1	5995	197472	69024	t3dl_e	20360	0
lp_dfl001	6071	12230	76196	msc23052	23052	3623204
deter2	6095	17313	120428	bcsstk36	23052	3611816
fxm3_6	6200	12625	105616	crystm03	24696	2388726
deter7	6375	18153	79288	smt	25710	19418850
lp_cre_d	6476	73948	363340	thread	29736	24648426
ulevimin	6590	46937	198008	wathen100	30401	1627220
nemswrld	6647	28550	354774	ship_001	34920	25565618
nemsemm2	6943	48878	138470	nd12k	36000	90870894
nl	7039	15325	98050	wathen120	36441	1953940
lp_cre_b	7240	77137	389158	obstclae	40000	472820
deter3	7647	21777	108100	jnlbrng1	40000	476004
rlfdual	8052	74970	714646	minsurfo	40806	486844
scsd8-2r	8650	60550	3896670	bcsstm39	46772	0
cq9	9278	21534	212312	vanbody	47072	8006490
pf2177	9728	9908	715416	gridgena	48962	1638710
scagr7-2b	9743	13847	3928898	cvxbqp1	50000	1049432
lp_pds_06	9881	29351	78122	ct20stif	52329	9964622
p010	10090	19090	438228	crankseg_1	52804	75044100
ge	10099	16369	102030	nasasrb	54870	8279516
lp_osa_60	10280	243246	1006074	Andrews	60000	5451632
				Continued on next page		

Table 5.1 – continued from previous page

LP Collection				PD Collection		
name	$|\mathcal{N}|$	$|\mathcal{U}|$	$|\mathcal{E}|$	name	$|\mathcal{U}|$	$|\mathcal{E}|$
co9	10789	22924	238416	crankseg_2	63838	104526330
lpl3	10828	33686	116590	Dubcova2	65025	4027504
fome11	12142	24460	152392	qa8fm	66127	7285062
scrs8-2r	14364	27691	12404296	cfd1	70656	8088220
stormg2-27	14387	37485	205610	nd24k	72000	189118604
lp_ken_11	14694	21349	67760	oilpan	73752	11536112
sctap1-2b	15390	33858	5245512	finan512	74752	4522496
car4	16384	33052	182624	apache1	80800	1776124
lp_pds_10	16558	49932	133100	shallow_water1	81920	737280
lp_stocfor3	16675	23541	218144	shallow_water2	81920	737280
ex3sta1	17443	17516	662414	thermal1	82654	1519688
testbig	17613	31223	3274430	denormal	89400	3540180
dbir1	18804	45775	2419194	s3dkt3m2	90449	10025526
dbir2	18906	45877	2618552	s3dkq4m2	90449	13192104
scfxm1-2b	19036	33047	519242	m_t1	97578	36435564
route	20894	43019	1273910	2cubes_sphere	101492	8873034
ts-palko	22002	47235	8149338	thermomech_TK	102158	1866380
fxm4_6	22400	47185	504136	thermomech_TC	102158	1866380
fome12	24284	48920	304784	x104	108384	38593344
e18	24617	38601	780314	shipsec8	114919	22608304
pltexpa	26894	70364	242842	ship_003	121728	32654210
baxter	27441	30733	1196786	cfd2	123440	13295204
lp_ken_13	28632	42659	133172	boneS01	127224	25388478
stat96v2	29089	957432	323660	shipsec1	140874	23945538
lp_pds_20	33798	108175	286322	bmw7st_1	141347	23432912
stat96v3	33841	1113780	375972	Dubcova3	146689	17334072
world	34506	67147	547558	bmwcra_1	148770	49534938
mod2	34774	66409	570136	G2_circuit	150102	1852894
sc205-2r	35213	62423	12948830	shipsec5	179860	32159300
scfxm1-2r	37980	65943	1593802	thermomech_dM	204316	3732760
fxm3_16	41340	85575	724186	pwtk	217918	32554318
dbic1	43200	226317	2721302	hood	220542	34021638
fome13	48568	97840	609568	BenElechi1	245874	36015470
pds-30	49788	158489	418478	offshore	259789	23096456
rlfprim	58866	62712	9060730	F1	343791	224140612
stormg2-125	65935	172431	1887584	msdoor	415863	62406596
pds-40	66641	217531	571226	af_2_k101	503625	46968400
fome21	67596	216350	572644	af_5_k101	503625	46968400
pds-50	82837	275814	719666	af_1_k101	503625	46968400
pds-60	99204	336421	873016	af_4_k101	503625	46968400
pds-70	114717	390005	1008932	af_3_k101	503625	46968400
pds-80	128954	434580	1120120	af_0_k101	503625	46968400
pds-90	142596	475448	1221102	inline_1	503712	252580926
pds-100	156016	514577	1314672	af_shell8	504855	47055520
watson_1	201155	386992	1736008	af_shell3	504855	47055520
sgpf5y6	246077	312540	2530568	af_shell4	504855	47055520
watson_2	352013	677224	3038266	af_shell7	504855	47055520
stormG2_1000	526185	1377306	82461084	parabolic_fem	525825	9434110
cont11_l	1468599	1961394	16595662	apache2	715176	15848148
				tmt_sym	726713	13776468
				boneS10	914898	222646668
				ldoor	952203	144470732
				ecology2	999999	11979976
				thermal2	1228045	22790012
				G3_circuit	1585478	19681656

Table 5.2: 2-way partitioning performance of the LP matrix collection for cut-net metric with net balancing.

name	PaToH		onmetisHP		
	cutsize	%LI	cutsize	%LI	speedup
lp_truss	0.05	9.9%	0.04	2.2%	4.81
rosen2	0.01	0.0%	0.01	0.0%	1.50
lp_ship12s	0.02	0.1%	0.01	0.0%	2.47
lp_ship12l	0.01	0.1%	0.01	0.0%	3.63
lp_sctap2	0.04	1.0%	0.04	1.6%	2.17
lp_woodw	0.05	0.6%	0.06	1.6%	8.81
lp_osa_07	0.07	0.1%	0.06	1.1%	2.85
qiulp	0.11	7.2%	0.13	0.0%	2.63
lp_sierra	0.04	2.1%	0.03	0.1%	2.26
lp_ganges	0.02	0.1%	0.02	0.0%	2.74
model4	0.08	4.6%	0.07	3.2%	4.36
lp_pilot	0.16	7.9%	0.18	0.0%	2.91
lp_sctap3	0.03	1.4%	0.03	1.3%	2.45
lp_degen3	0.12	5.6%	0.16	4.7%	2.85
fxm2-6	0.03	6.9%	0.03	0.0%	1.76
cep1	0.28	0.9%	0.55	0.5%	0.35
primagaz	0.00	0.1%	0.00	99.0%	0.45
pcb1000	0.03	0.1%	0.03	0.0%	5.16
model3	0.02	9.8%	0.05	0.0%	2.11
progas	0.02	2.0%	0.02	1.8%	1.65
model5	0.00	0.1%	0.00	0.1%	13.15
scrs8-2b	0.13	11.8%	0.14	5.7%	0.41
lp_cycle	0.02	5.3%	0.03	2.9%	1.74
deter0	0.07	8.4%	0.07	0.2%	1.97
lp_pilot87	0.19	6.3%	0.31	2.1%	3.05
rosen10	0.00	0.0%	0.00	40.7%	1.06
model6	0.02	2.0%	0.04	3.2%	3.27
p6000	0.00	0.0%	0.00	47.4%	0.71
lp_stocfor2	0.00	0.9%	0.00	1.5%	1.17
lp_d2q06c	0.05	3.0%	0.06	0.0%	2.82
lp_80bau3b	0.04	9.8%	0.03	0.3%	4.14
nemspmm2	0.05	2.0%	0.03	3.1%	10.49
lp_bnl2	0.05	3.8%	0.05	2.1%	2.25
lp_osa_14	0.03	1.5%	0.03	0.0%	5.95
nemspmm1	0.07	3.2%	0.03	4.2%	5.69
lp_greenbea	0.03	0.0%	0.04	0.0%	2.81
lpi_greenbea	0.04	1.3%	0.04	0.0%	3.07
lp_ken_07	0.01	2.0%	0.01	2.0%	1.63
scagr7-2c	0.11	9.5%	0.45	6.0%	0.21
lpi_gran	0.00	6.4%	0.09	1.1%	0.43
lpi_bgindy	0.08	7.9%	0.07	1.1%	17.59
l30	0.04	5.6%	0.03	1.7%	4.06
model9	0.01	0.0%	0.03	3.6%	3.70
model8	0.05	4.7%	0.05	0.0%	3.34
lp_pds_02	0.03	1.4%	0.03	0.0%	2.29
lp22	0.32	6.7%	0.50	3.6%	2.75
lp_cre_c	0.02	0.0%	0.02	1.2%	3.06
lpi_cplex1	0.31	9.8%	0.70	9.7%	0.25
plddb	0.00	6.9%	0.00	0.0%	1.27
rat	0.22	9.2%	0.18	0.0%	1.67
lp_maros_r7	0.09	3.5%	0.09	0.0%	1.32
delf	0.01	9.0%	0.01	0.6%	1.77
stat96v4	0.01	8.3%	0.01	0.0%	20.74
deter4	0.15	9.5%	0.10	0.0%	1.01
lpl2	0.04	3.0%	0.07	3.2%	3.62
model7	0.02	6.2%	0.00	0.1%	2.55

	PaToH		onmetisHP		
name	cutsize	%LI	cutsize	%LI	speedup
sctap1-2c	0.07	0.0%	0.17	0.0%	0.35
lp_cre_a	0.02	0.0%	0.02	0.5%	2.76
lpi_ceria3d	0.29	1.9%	0.65	11.8%	0.20
ch	0.06	0.0%	0.15	1.9%	2.33
aircraft	0.20	0.0%	0.11	6.5%	0.06
lpi_gosh	0.05	3.2%	0.06	0.0%	4.64
deter8	0.07	9.9%	0.07	0.0%	1.87
fxm2-16	0.02	9.8%	0.02	2.4%	1.48
nemsemm1	0.00	5.0%	0.02	4.5%	44.06
pcb3000	0.02	5.8%	0.02	0.0%	7.17
pgp2	0.29	3.0%	0.65	0.5%	0.21
rlfddd	0.04	6.9%	0.06	0.9%	12.82
deter6	0.07	9.5%	0.07	0.0%	1.72
large	0.01	0.7%	0.01	0.0%	1.75
lp_osa_30	0.02	0.0%	0.02	2.0%	0.98
stormg2-8	0.01	0.6%	0.01	2.0%	1.83
model10	0.05	4.2%	0.09	6.7%	4.42
nsir	0.09	3.6%	0.13	7.9%	3.91
seymourl	0.28	9.8%	0.42	3.8%	0.30
cq5	0.02	1.0%	0.04	1.3%	6.40
p05	0.02	7.2%	0.07	0.0%	15.81
deter5	0.07	9.8%	0.07	0.0%	1.61
scsd8-2b	0.25	6.7%	0.84	0.9%	0.51
r05	0.04	7.0%	0.10	0.0%	17.39
bas1lp	0.07	5.4%	0.12	0.0%	1.78
deter1	0.07	9.6%	0.07	0.0%	1.53
co5	0.02	5.6%	0.05	0.7%	6.21
stat96v1	0.01	2.1%	0.01	0.0%	21.38
lp_dfl001	0.09	9.6%	0.20	1.8%	2.52
deter2	0.10	9.4%	0.09	0.0%	1.24
fxm3_6	0.00	1.9%	0.00	1.9%	1.74
deter7	0.07	9.4%	0.07	0.0%	1.44
lp_cre_d	0.05	0.0%	0.15	0.8%	18.10
ulevimin	0.04	3.8%	0.11	1.7%	3.28
nemswrld	0.08	0.0%	0.05	1.8%	7.93
nemsemm2	0.00	0.5%	0.00	3.6%	7.90
nl	0.04	0.0%	0.07	1.3%	3.48
lp_cre_b	0.05	0.2%	0.09	1.3%	17.46
deter3	0.07	9.9%	0.08	0.0%	1.49
rlfdual	0.05	8.3%	0.06	0.0%	5.85
scsd8-2r	0.25	8.0%	0.91	0.0%	0.37
cq9	0.02	8.2%	0.05	0.0%	6.73
pf2177	0.23	0.1%	0.70	0.5%	0.37
scagr7-2b	0.11	9.8%	0.47	4.0%	0.07
lp_pds_06	0.03	5.8%	0.04	2.7%	2.49
p010	0.01	0.0%	0.02	0.0%	0.36
ge	0.02	0.4%	0.02	0.0%	1.52
lp_osa_60	0.01	0.0%	0.01	7.3%	0.85
co9	0.02	6.8%	0.14	0.0%	6.58
lpl3	0.01	1.1%	0.07	2.2%	7.28
fome11	0.00	0.0%	0.00	0.0%	2.99
scrs8-2r	0.30	40.4%	0.14	10.3%	0.13
stormg2-27	0.01	0.5%	0.01	3.5%	1.81
lp_ken_11	0.00	0.8%	0.00	3.9%	2.44
sctap1-2b	0.07	0.0%	0.54	5.3%	0.13
car4	0.00	0.0%	0.00	0.0%	0.13
lp_pds_10	0.03	8.8%	0.05	0.0%	2.80
lp_stocfor3	0.00	0.2%	0.00	0.2%	0.95

Table 5.2 – continued from previous page

Table 5.2 – continued from previous page

name	PaToH cutsize	PaToH %LI	onmetisHP cutsize	onmetisHP %LI	speedup
ex3sta1	0.07	8.4%	0.07	1.4%	1.12
testbig	0.09	9.9%	0.09	3.2%	0.12
dbir1	0.06	10.0%	0.30	22.6%	5.11
dbir2	0.06	8.0%	0.37	6.8%	4.82
scfxm1-2b	0.03	9.2%	0.04	0.0%	0.67
route	0.01	0.0%	0.01	0.0%	2.21
ts-palko	0.12	9.9%	0.94	18.6%	2.08
fxm4_6	0.00	0.5%	0.00	0.5%	1.78
fome12	0.00	0.0%	0.00	0.0%	2.91
e18	0.23	9.8%	0.68	1.2%	1.18
pltexpa	0.00	0.7%	0.00	0.7%	1.90
baxter	0.01	4.3%	0.00	1.6%	0.66
lp_ken_13	0.00	0.6%	0.00	2.7%	3.35
stat96v2	0.00	1.1%	0.00	0.0%	22.45
lp_pds_20	0.02	0.9%	0.03	0.0%	3.04
stat96v3	0.00	6.3%	0.00	0.0%	11.82
world	0.00	6.3%	0.02	4.9%	2.11
mod2	0.00	6.9%	0.01	4.9%	1.97
sc205-2r	0.06	9.2%	0.20	3.6%	0.07
scfxm1-2r	0.03	9.8%	0.11	0.3%	0.56
fxm3_16	0.00	0.4%	0.00	0.5%	1.72
dbic1	0.01	0.0%	0.01	0.5%	9.51
fome13	0.00	0.0%	0.00	0.0%	2.74
pds-30	0.03	9.0%	0.02	0.0%	3.05
rlfprim	0.06	4.8%	0.08	2.2%	0.25
stormg2-125	0.02	8.9%	0.01	0.7%	1.25
pds-40	0.02	1.1%	0.02	0.9%	3.35
fome21	0.00	0.0%	0.00	0.0%	3.18
pds-50	0.03	0.3%	0.01	1.2%	3.28
pds-60	0.02	1.8%	0.01	0.4%	3.37
pds-70	0.02	6.9%	0.01	0.0%	3.44
pds-80	0.02	0.1%	0.01	0.4%	3.43
pds-90	0.02	6.2%	0.01	0.0%	3.19
pds-100	0.01	0.6%	0.01	0.0%	3.20
watson_1	0.00	0.0%	0.00	0.0%	2.91
sgpf5y6	0.00	4.1%	0.00	3.7%	1.67
watson_2	0.00	4.7%	0.00	4.8%	2.86
stormG2_1000	0.01	4.4%	0.03	3.3%	0.36
cont11_l	0.00	0.0%	0.00	0.0%	1.06

Table 5.3: 4-way partitioning performance of the LP matrix collection for cut-net metric with net balancing.

	PaToH		onmetisHP		
name	cutsize	%LI	cutsize	%LI	speedup
lp_truss	0.05	5.8%	0.14	4.8%	6.21
rosen2	0.01	0.0%	0.01	0.0%	2.64
lp_ship12s	0.02	0.1%	0.01	0.0%	3.05
lp_ship12l	0.01	0.1%	0.01	0.0%	4.92
lp_sctap2	0.04	4.5%	0.09	3.0%	2.57
lp_woodw	0.05	0.6%	0.06	2.0%	8.38
lp_osa_07	0.07	0.3%	0.07	0.0%	3.31
qiulp	0.11	3.5%	0.19	2.5%	2.51
lp_sierra	0.04	7.3%	0.07	1.7%	2.39
lp_ganges	0.02	3.2%	0.05	3.2%	2.78
model4	0.08	4.7%	0.17	12.6%	4.98
lp_pilot	0.16	8.6%	0.26	5.5%	4.19
lp_sctap3	0.03	4.0%	0.08	1.7%	2.35
lp_degen3	0.12	5.5%	0.26	8.3%	2.53
fxm2-6	0.03	3.4%	0.04	2.4%	1.96
cep1	0.28	0.0%	0.75	22.1%	0.46
primagaz	0.00	0.1%	0.00	99.1%	0.63
pcb1000	0.03	2.4%	0.06	2.3%	5.56
model3	0.02	2.7%	0.12	3.8%	2.57
progas	0.02	2.3%	0.05	2.9%	1.74
model5	0.00	0.8%	0.24	5.9%	13.51
scrs8-2b	0.13	4.7%	0.22	7.5%	0.54
lp_cycle	0.02	4.1%	0.04	7.6%	1.69
deter0	0.07	0.9%	0.11	1.1%	2.08
lp_pilot87	0.19	23.7%	0.41	13.3%	4.26
rosen10	0.00	0.0%	0.00	0.0%	1.80
model6	0.02	1.6%	0.08	6.3%	3.93
p6000	0.00	0.1%	0.00	47.4%	0.78
lp_stocfor2	0.00	4.8%	0.01	5.4%	1.54
lp_d2q06c	0.05	4.0%	0.10	4.8%	3.59
lp_80bau3b	0.04	1.8%	0.08	4.2%	3.64
nemspmm2	0.05	5.8%	0.07	4.6%	11.64
lp_bnl2	0.05	4.1%	0.12	3.0%	2.57
lp_osa_14	0.03	0.1%	0.04	3.1%	6.04
nemspmm1	0.07	3.0%	0.06	6.4%	6.99
lp_greenbea	0.03	3.0%	0.06	4.9%	3.85
lpi_greenbea	0.04	7.2%	0.06	5.4%	3.70
lp_ken_07	0.01	6.1%	0.01	6.1%	1.80
scagr7-2c	0.11	4.1%	0.49	12.0%	0.36
lpi_gran	0.00	6.1%	0.20	7.5%	0.64
lpi_bgindy	0.08	2.2%	0.07	3.5%	16.40
l30	0.04	2.6%	0.07	4.3%	4.71
model9	0.01	1.1%	0.03	6.0%	4.74
model8	0.05	7.5%	0.14	0.1%	3.59
lp_pds_02	0.03	1.1%	0.05	5.5%	2.11
lp22	0.32	7.0%	0.56	6.2%	3.68
lp_cre_c	0.02	2.4%	0.03	2.8%	2.67
lpi_cplex1	0.31	8.7%	0.91	26.3%	0.31
plddb	0.00	1.4%	0.01	1.4%	1.45
rat	0.22	8.7%	0.56	5.3%	2.29
lp_maros_r7	0.09	8.5%	0.27	0.1%	1.85
delf	0.01	5.0%	0.03	1.8%	2.18
stat96v4	0.01	6.3%	0.03	1.6%	36.69
deter4	0.15	2.4%	0.10	5.9%	1.22
lpl2	0.04	4.6%	0.10	3.8%	2.64
model7	0.02	2.7%	0.06	3.1%	2.68

	PaToH		onmetisHP		
name	cutsize	%LI	cutsize	%LI	speedup
sctap1-2c	0.07	7.6%	0.26	6.0%	0.46
lp_cre_a	0.02	0.1%	0.03	2.3%	2.57
lpi_ceria3d	0.29	7.2%	0.84	18.2%	0.21
ch	0.06	1.6%	0.23	2.9%	2.19
aircraft	0.20	7.3%	0.18	6.5%	0.08
lpi_gosh	0.05	7.3%	0.11	2.7%	5.28
deter8	0.07	0.8%	0.11	0.8%	2.12
fxm2-16	0.02	2.7%	0.03	5.6%	1.87
nemsemm1	0.00	2.7%	0.04	7.7%	75.02
pcb3000	0.02	3.0%	0.03	1.5%	7.47
pgp2	0.29	2.1%	0.73	2.2%	0.28
rlfddd	0.04	5.7%	0.11	3.2%	17.06
deter6	0.07	0.5%	0.11	1.3%	2.06
large	0.01	3.8%	0.02	1.3%	2.24
lp_osa_30	0.02	0.0%	0.02	2.8%	1.51
stormg2-8	0.01	5.5%	0.04	4.8%	2.52
model10	0.05	1.8%	0.16	11.0%	5.58
nsir	0.09	1.1%	0.29	13.8%	4.73
seymourl	0.28	22.7%	0.67	25.9%	0.50
cq5	0.02	1.0%	0.04	2.7%	6.01
p05	0.02	7.5%	0.08	4.1%	11.52
deter5	0.07	2.1%	0.11	1.6%	1.99
scsd8-2b	0.25	5.3%	0.91	46.0%	0.85
r05	0.04	8.3%	0.13	3.7%	12.52
bas1lp	0.07	3.5%	0.23	4.6%	2.58
deter1	0.07	0.5%	0.11	1.5%	1.91
co5	0.02	0.6%	0.04	5.2%	5.76
stat96v1	0.01	2.3%	0.02	1.5%	35.78
lp_dfl001	0.09	11.1%	0.28	7.4%	2.79
deter2	0.10	3.4%	0.11	4.4%	1.53
fxm3_6	0.00	5.3%	0.02	3.8%	2.22
deter7	0.07	0.6%	0.10	1.6%	1.80
lp_cre_d	0.05	0.0%	0.19	3.7%	17.90
ulevimin	0.04	5.1%	0.14	1.9%	4.14
nemswrld	0.08	0.0%	0.09	8.3%	8.23
nemsemm2	0.00	3.5%	0.00	4.3%	11.43
nl	0.04	0.9%	0.09	3.8%	3.23
lp_cre_b	0.05	0.2%	0.12	3.5%	15.77
deter3	0.07	0.4%	0.12	3.7%	1.88
rlfdual	0.05	6.1%	0.09	4.9%	7.27
scsd8-2r	0.25	7.0%	0.94	38.9%	0.65
cq9	0.02	0.5%	0.06	3.3%	6.10
pf2177	0.23	5.0%	0.88	6.2%	0.75
scagr7-2b	0.11	4.8%	0.62	9.6%	0.11
lp_pds_06	0.03	1.6%	0.05	6.5%	2.75
p010	0.01	3.1%	0.05	3.0%	0.48
ge	0.02	0.6%	0.03	5.6%	1.60
lp_osa_60	0.01	0.0%	0.01	8.0%	1.23
co9	0.02	0.5%	0.10	4.8%	6.05
lpl3	0.01	3.4%	0.09	4.1%	5.44
fome11	0.00	5.2%	0.19	4.8%	3.42
scrs8-2r	0.30	75.1%	0.26	6.7%	0.13
stormg2-27	0.01	6.1%	0.06	6.7%	2.07
lp_ken_11	0.00	2.5%	0.00	8.7%	2.43
sctap1-2b	0.07	4.6%	0.65	9.7%	0.18
car4	0.00	0.0%	0.00	0.0%	0.19
lp_pds_10	0.03	8.6%	0.09	3.1%	3.05
lp_stocfor3	0.00	0.6%	0.00	0.5%	1.14

Table 5.3 – continued from previous page					
	PaToH		*onmetisHP*		
name	cutsize	%LI	cutsize	%LI	speedup
ex3sta1	0.07	2.4%	0.13	3.9%	1.05
testbig	0.09	8.4%	0.27	7.9%	0.14
dbir1	0.06	6.3%	0.61	29.4%	6.99
dbir2	0.06	9.1%	0.64	18.5%	6.45
scfxm1-2b	0.03	6.6%	0.05	1.2%	0.85
route	0.01	0.0%	0.02	0.0%	4.34
ts-palko	0.12	3.1%	0.95	41.8%	3.43
fxm4_6	0.00	3.4%	0.00	1.5%	2.22
fome12	0.00	0.0%	0.00	0.0%	3.66
e18	0.23	2.8%	0.80	2.2%	2.08
pltexpa	0.00	3.1%	0.02	3.5%	2.07
baxter	0.01	3.0%	0.03	6.5%	1.53
lp_ken_13	0.00	1.8%	0.00	3.5%	3.16
stat96v2	0.00	6.3%	0.01	2.2%	37.92
lp_pds_20	0.02	6.8%	0.09	1.7%	3.36
stat96v3	0.00	1.1%	0.01	2.5%	21.07
world	0.00	6.4%	0.02	6.6%	2.25
mod2	0.00	5.4%	0.02	7.8%	2.12
sc205-2r	0.06	2.4%	0.39	8.5%	0.09
scfxm1-2r	0.03	7.2%	0.15	2.6%	0.73
fxm3_16	0.00	0.9%	0.00	1.2%	2.18
dbic1	0.01	0.6%	0.01	2.2%	10.49
fome13	0.00	0.0%	0.00	0.0%	3.35
pds-30	0.03	1.6%	0.06	0.2%	3.23
rlfprim	0.06	4.5%	0.19	11.4%	0.28
stormg2-125	0.02	6.1%	0.10	14.9%	1.36
pds-40	0.02	4.5%	0.05	0.8%	3.56
fome21	0.00	0.5%	0.03	0.0%	3.86
pds-50	0.03	5.1%	0.04	1.0%	3.71
pds-60	0.02	5.0%	0.03	0.8%	3.99
pds-70	0.02	5.2%	0.03	1.0%	3.79
pds-80	0.02	4.7%	0.02	1.8%	3.87
pds-90	0.02	6.0%	0.02	1.9%	3.73
pds-100	0.01	5.5%	0.02	2.4%	3.96
watson_1	0.00	0.0%	0.00	0.0%	3.42
sgpf5y6	0.00	9.1%	0.00	8.7%	1.92
watson_2	0.00	4.8%	0.00	5.1%	3.29
stormG2_1000	0.01	5.0%	0.18	18.1%	0.47
cont11_l	0.00	4.3%	0.00	0.0%	1.12

Table 5.4: 8-way partitioning performance of the LP matrix collection for cut-net metric with net balancing.

| | PaToH | | onmetisHP | | |
name	cutsize	%LI	cutsize	%LI	speedup
lp_truss	0.33	10.0%	0.30	7.0%	5.99
rosen2	0.01	0.0%	0.01	0.0%	3.67
lp_ship12s	0.06	0.1%	0.04	4.1%	2.94
lp_ship12l	0.07	0.7%	0.07	3.0%	4.51
lp_sctap2	0.10	4.9%	0.13	5.2%	2.42
lp_woodw	0.15	3.8%	0.17	7.2%	7.86
lp_osa_07	0.07	0.7%	0.07	1.7%	3.77
qiulp	0.22	5.5%	0.22	5.5%	2.50
lp_sierra	0.10	6.5%	0.10	3.4%	2.39
lp_ganges	0.08	4.3%	0.09	4.7%	2.86
model4	0.31	18.3%	0.56	46.7%	5.72
lp_pilot	0.41	31.8%	0.48	52.2%	4.52
lp_sctap3	0.09	7.0%	0.11	4.9%	2.31
lp_degen3	0.23	11.8%	0.30	15.6%	2.50
fxm2-6	0.07	3.3%	0.07	7.7%	2.28
cep1	0.51	0.5%	0.92	65.0%	0.49
primagaz	0.00	0.3%	0.00	99.1%	0.83
pcb1000	0.10	3.0%	0.09	4.8%	5.66
model3	0.12	9.6%	0.17	7.3%	3.10
progas	0.09	3.7%	0.10	4.7%	2.06
model5	0.26	0.1%	0.61	85.2%	11.98
scrs8-2b	0.41	14.8%	0.36	27.2%	0.55
lp_cycle	0.06	7.5%	0.08	15.5%	1.81
deter0	0.13	2.9%	0.13	3.8%	2.37
lp_pilot87	0.42	22.3%	0.54	36.3%	4.36
rosen10	0.00	0.0%	0.00	17.0%	2.36
model6	0.17	12.1%	0.21	16.1%	4.02
p6000	0.00	0.1%	0.00	47.5%	0.96
lp_stocfor2	0.04	3.3%	0.04	7.9%	1.85
lp_d2q06c	0.14	5.6%	0.14	7.1%	3.72
lp_80bau3b	0.09	4.1%	0.10	6.9%	3.87
nemspmm2	0.15	9.2%	0.17	9.5%	10.99
lp_bnl2	0.15	10.3%	0.17	6.5%	2.34
lp_osa_14	0.03	0.3%	0.04	2.8%	6.44
nemspmm1	0.15	5.2%	0.16	10.9%	5.86
lp_greenbea	0.10	2.2%	0.10	10.8%	4.00
lpi_greenbea	0.11	3.5%	0.10	12.6%	3.91
lp_ken_07	0.01	6.8%	0.01	10.4%	1.92
scagr7-2c	0.20	6.5%	0.67	16.3%	0.44
lpi_gran	0.21	12.4%	0.23	10.5%	0.80
lpi_bgindy	0.07	1.8%	0.07	6.5%	15.87
l30	0.16	6.0%	0.14	7.0%	4.78
model9	0.04	0.1%	0.07	9.1%	4.76
model8	0.26	4.4%	0.30	2.2%	3.29
lp_pds_02	0.08	3.9%	0.07	6.5%	2.42
lp22	0.42	15.4%	0.60	10.6%	4.02
lp_cre_c	0.03	0.2%	0.04	4.7%	2.51
lpi_cplex1	0.41	82.9%	0.95	137.7%	0.34
plddb	0.02	2.2%	0.02	3.9%	1.63
lp_maros_r7	0.79	48.7%	0.55	4.9%	4.63
rat	0.56	9.7%	0.91	44.6%	1.23
delf	0.07	5.7%	0.06	5.9%	2.15
stat96v4	0.05	0.6%	0.05	3.8%	49.28
deter4	0.27	2.0%	0.13	11.3%	1.23
lpl2	0.04	5.6%	0.11	7.3%	2.80
model7	0.07	6.6%	0.10	4.6%	2.80

	PaToH		onmetisHP		
name	cutsize	%LI	cutsize	%LI	speedup
sctap1-2c	0.21	6.3%	0.30	17.7%	0.53
lp_cre_a	0.03	0.5%	0.03	5.1%	2.44
lpi_ceria3d	0.50	13.4%	0.92	23.3%	0.23
ch	0.09	5.3%	0.32	3.8%	2.33
aircraft	0.00	220.0%	0.92	256.3%	0.11
lpi_gosh	0.15	4.6%	0.22	11.8%	4.48
deter8	0.13	0.6%	0.13	3.6%	2.24
fxm2-16	0.04	6.7%	0.04	6.8%	2.15
nemsemm1	0.16	8.6%	0.13	18.6%	93.36
pcb3000	0.06	4.9%	0.06	4.1%	7.12
pgp2	0.51	5.1%	0.97	0.0%	0.33
rlfddd	0.32	31.5%	0.25	16.1%	15.44
deter6	0.12	1.3%	0.13	2.9%	2.09
large	0.06	5.0%	0.05	5.0%	2.39
lp_osa_30	0.02	0.0%	0.02	3.8%	1.96
stormg2-8	0.07	8.2%	0.07	10.1%	2.58
model10	0.16	9.9%	0.23	19.9%	5.98
nsir	0.14	3.5%	0.35	9.8%	4.79
seymourl	0.63	67.3%	0.82	81.1%	0.67
cq5	0.04	2.0%	0.05	5.0%	5.41
p05	0.05	8.1%	0.12	5.3%	10.11
deter5	0.12	2.5%	0.12	3.5%	2.08
scsd8-2b	0.44	4.1%	0.93	87.5%	1.11
r05	0.07	10.5%	0.14	5.5%	11.57
bas1lp	0.31	21.5%	0.38	29.0%	3.26
deter1	0.13	0.7%	0.12	3.8%	2.11
co5	0.04	1.7%	0.07	6.2%	5.24
stat96v1	0.04	2.7%	0.04	2.3%	46.61
lp_dfl001	0.18	13.3%	0.37	5.6%	2.92
deter2	0.17	1.8%	0.12	7.7%	1.66
fxm3_6	0.03	5.5%	0.03	6.9%	2.45
deter7	0.13	1.1%	0.12	3.8%	1.98
lp_cre_d	0.09	0.4%	0.19	6.3%	16.71
ulevimin	0.09	8.6%	0.15	5.4%	5.64
nemswrld	0.15	0.1%	0.10	10.2%	7.68
nemsemm2	0.01	2.5%	0.01	6.9%	13.22
nl	0.06	3.6%	0.12	7.1%	3.11
lp_cre_b	0.10	1.7%	0.17	7.9%	14.59
deter3	0.12	0.6%	0.12	6.2%	1.98
rlfdual	0.26	22.5%	0.23	15.9%	7.21
scsd8-2r	0.44	3.4%	0.97	89.9%	0.78
cq9	0.04	4.7%	0.06	6.6%	5.65
pf2177	0.46	8.2%	0.93	14.3%	0.92
scagr7-2b	0.20	7.7%	0.70	17.0%	0.13
lp_pds_06	0.07	5.5%	0.07	9.3%	3.17
p010	0.02	5.5%	0.07	6.2%	0.56
ge	0.05	4.6%	0.05	7.5%	1.77
lp_osa_60	0.01	0.0%	0.01	7.5%	1.54
co9	0.04	1.3%	0.12	7.1%	5.77
lpl3	0.01	4.4%	0.09	5.6%	5.47
fome11	0.17	10.8%	0.30	8.2%	3.30
scrs8-2r	0.61	49.9%	0.36	24.7%	0.12
stormg2-27	0.06	3.4%	0.07	11.2%	2.27
lp_ken_11	0.00	5.5%	0.00	11.5%	2.44
sctap1-2b	0.27	4.0%	0.74	38.5%	0.22
car4	0.00	0.0%	0.00	0.0%	0.24
lp_pds_10	0.08	3.2%	0.10	7.7%	3.17
lp_stocfor3	0.01	2.1%	0.01	2.1%	1.24

Table 5.4 – continued from previous page

| name | PaToH | | onmetisHP | | |
	cutsize	%LI	cutsize	%LI	speedup
ex3sta1	0.21	9.0%	0.23	9.7%	1.25
testbig	0.20	5.5%	0.78	157.3%	0.17
dbir1	0.11	8.9%	0.70	13.7%	7.51
dbir2	0.11	7.2%	0.80	14.8%	6.87
scfxm1-2b	0.05	4.4%	0.06	4.5%	0.98
route	0.01	0.1%	0.03	0.5%	5.39
ts-palko	0.23	3.2%	0.98	81.8%	4.89
fxm4_6	0.01	4.8%	0.01	4.2%	2.47
fome12	0.10	4.4%	0.21	8.8%	3.62
e18	0.47	3.3%	0.84	3.8%	2.69
pltexpa	0.04	5.7%	0.06	10.9%	2.14
baxter	0.10	10.3%	0.23	26.2%	1.43
lp_ken_13	0.00	4.1%	0.00	7.6%	3.09
stat96v2	0.02	1.7%	0.02	3.5%	49.72
lp_pds_20	0.08	4.2%	0.11	6.4%	3.48
stat96v3	0.02	1.0%	0.02	4.2%	29.08
world	0.02	7.0%	0.04	8.7%	2.28
mod2	0.02	5.1%	0.04	8.1%	2.18
sc205-2r	0.20	3.7%	0.83	204.0%	0.11
scfxm1-2r	0.05	5.0%	0.16	6.6%	0.88
fxm3_16	0.00	1.9%	0.00	2.2%	2.49
dbic1	0.02	2.9%	0.02	4.9%	10.31
fome13	0.00	0.0%	0.00	0.0%	3.82
pds-30	0.08	5.2%	0.10	5.2%	3.22
rlfprim	0.24	7.4%	0.36	27.6%	0.31
stormg2-125	0.07	3.9%	0.16	21.1%	1.48
pds-40	0.07	6.0%	0.10	3.7%	3.60
fome21	0.05	3.7%	0.09	3.1%	3.88
pds-50	0.07	5.7%	0.09	2.2%	3.71
pds-60	0.06	3.7%	0.07	1.2%	3.94
pds-70	0.06	4.7%	0.06	1.5%	3.92
pds-80	0.05	3.9%	0.06	1.7%	4.01
pds-90	0.05	7.5%	0.05	2.2%	3.80
pds-100	0.05	5.1%	0.05	2.4%	4.11
watson_1	0.00	0.1%	0.00	0.2%	3.67
sgpf5y6	0.01	8.7%	0.01	12.1%	2.00
watson_2	0.00	2.5%	0.00	5.2%	3.55
stormG2_1000	0.08	6.1%	0.28	35.5%	0.44
cont11_l	0.00	2.6%	0.00	0.0%	1.15

Table 5.5: 16-way partitioning performance of the LP matrix collection for cut-net metric with net balancing.

name	$PaToH$		$onmetisHP$		speedup
	cutsize	$\%LI$	cutsize	$\%LI$	
lp_truss	0.51	11.9%	0.48	11.7%	5.35
rosen2	0.01	0.0%	0.02	0.0%	4.91
lp_ship12s	0.11	3.5%	0.07	6.1%	2.76
lp_ship12l	0.17	1.7%	0.18	8.1%	3.95
lp_sctap2	0.14	6.4%	0.16	7.6%	2.23
lp_woodw	0.29	8.4%	0.30	11.2%	6.35
lp_osa_07	0.07	1.4%	0.07	4.2%	4.26
qiulp	0.30	9.6%	0.33	10.7%	2.30
lp_sierra	0.15	5.8%	0.15	9.8%	2.32
lp_ganges	0.15	9.6%	0.15	10.9%	2.55
model4	0.44	44.9%	0.62	39.4%	5.87
lp_pilot	0.48	49.1%	0.61	78.0%	4.75
lp_sctap3	0.12	6.4%	0.14	8.3%	2.36
lp_degen3	0.27	16.0%	0.36	24.7%	2.62
fxm2-6	0.08	5.8%	0.09	9.9%	2.52
cep1	0.55	9.5%	0.95	163.3%	0.59
primagaz	0.00	0.3%	0.00	99.6%	1.03
pcb1000	0.15	5.8%	0.15	10.1%	4.89
model3	0.22	18.2%	0.26	19.2%	2.91
progas	0.16	6.7%	0.17	8.2%	2.11
model5	0.35	14.1%	0.71	110.5%	11.40
scrs8-2b	0.50	40.3%	0.48	30.4%	0.75
lp_cycle	0.20	5.3%	0.33	26.8%	1.92
deter0	0.14	1.9%	0.14	7.3%	2.75
lp_pilot87	0.51	56.8%	0.67	61.7%	4.28
rosen10	0.00	0.0%	0.00	0.0%	3.02
model6	0.28	12.7%	0.33	28.6%	3.62
p6000	0.00	0.1%	0.00	47.5%	1.13
lp_stocfor2	0.09	5.6%	0.09	11.8%	2.11
lp_d2q06c	0.19	9.5%	0.20	13.3%	3.98
lp_80bau3b	0.11	7.8%	0.13	11.2%	4.13
nemspmm2	0.27	12.9%	0.30	28.3%	12.36
lp_bnl2	0.18	12.4%	0.21	10.7%	2.39
lp_osa_14	0.03	0.6%	0.03	2.6%	6.60
nemspmm1	0.28	12.9%	0.38	44.0%	5.77
lp_greenbea	0.22	11.8%	0.36	66.0%	3.93
lpi_greenbea	0.22	12.0%	0.35	69.3%	3.96
lp_ken_07	0.01	4.3%	0.01	11.9%	2.14
scagr7-2c	0.21	8.5%	0.65	27.7%	0.55
lpi_gran	0.27	20.1%	0.26	14.7%	0.68
lpi_bgindy	0.08	2.6%	0.08	10.9%	14.64
l30	0.24	4.8%	0.21	7.7%	5.34
model9	0.15	6.4%	0.15	14.8%	5.13
model8	0.30	3.8%	0.41	8.5%	3.20
lp_pds_02	0.09	5.2%	0.08	9.8%	2.39
lp22	0.53	24.7%	0.61	25.9%	3.87
lp_cre_c	0.04	2.1%	0.05	9.2%	2.48
lpi_cplex1	0.41	261.3%	0.97	156.7%	0.35
plddb	0.04	2.3%	0.04	4.8%	1.89
lp_maros_r7	0.88	182.9%	0.88	57.7%	4.46
rat	0.83	79.8%	0.97	88.3%	1.46
delf	0.09	4.1%	0.12	7.4%	2.09
stat96v4	0.09	2.8%	0.09	5.0%	59.36
deter4	0.29	5.6%	0.31	45.7%	1.27
lpl2	0.05	4.1%	0.12	9.8%	3.04
model7	0.14	12.9%	0.16	12.2%	3.02
				Continued on next page	

	PaToH		onmetisHP		
name	cutsize	%LI	cutsize	%LI	speedup
sctap1-2c	0.27	7.3%	0.48	28.8%	0.68
lp_cre_a	0.04	0.2%	0.04	7.4%	2.32
lpi_ceria3d	0.52	18.2%	0.95	60.7%	0.27
ch	0.11	4.7%	0.29	6.4%	2.40
aircraft	0.00	540.0%	1.00	465.0%	0.12
lpi_gosh	0.20	6.5%	0.27	25.7%	5.00
deter8	0.14	3.4%	0.14	6.5%	2.39
fxm2-16	0.06	6.8%	0.04	8.6%	2.62
nemsemm1	0.26	19.5%	0.38	48.9%	100.43
pcb3000	0.10	4.3%	0.10	8.0%	6.47
pgp2	0.54	7.1%	0.98	42.9%	0.38
rlfddd	0.47	77.9%	0.47	64.6%	16.92
deter6	0.14	1.0%	0.14	5.6%	2.29
large	0.09	4.5%	0.10	7.3%	2.23
lp_osa_30	0.02	0.0%	0.02	5.7%	2.46
stormg2-8	0.11	8.1%	0.11	12.6%	2.76
model10	0.24	12.4%	0.37	46.2%	6.66
nsir	0.18	7.5%	0.38	15.3%	5.05
seymourl	0.75	93.1%	0.88	180.2%	0.58
cq5	0.06	6.2%	0.07	10.8%	5.07
p05	0.08	3.8%	0.13	9.4%	9.35
deter5	0.14	4.9%	0.14	7.1%	2.28
scsd8-2b	0.48	7.7%	0.94	91.2%	1.33
r05	0.10	6.3%	0.16	10.2%	10.97
bas1lp	0.46	119.5%	0.59	71.3%	3.70
deter1	0.14	3.3%	0.14	6.3%	2.30
co5	0.06	3.7%	0.07	9.1%	5.17
stat96v1	0.07	6.6%	0.07	3.7%	54.22
lp_dfl001	0.24	12.7%	0.40	8.9%	3.03
deter2	0.19	3.1%	0.13	10.2%	1.66
fxm3_6	0.05	4.4%	0.04	7.6%	2.64
deter7	0.14	3.3%	0.13	7.1%	2.14
lp_cre_d	0.12	1.9%	0.25	11.9%	16.27
ulevimin	0.11	4.8%	0.18	7.6%	5.51
nemswrld	0.19	6.9%	0.18	14.1%	7.13
nemsemm2	0.03	5.1%	0.03	13.9%	14.06
nl	0.07	2.5%	0.13	10.6%	3.05
lp_cre_b	0.12	1.7%	0.18	11.2%	13.41
deter3	0.14	1.4%	0.13	9.1%	2.08
rlfdual	0.42	49.3%	0.39	40.4%	6.77
scsd8-2r	0.48	9.5%	0.96	124.5%	0.91
cq9	0.06	3.7%	0.07	8.3%	5.40
pf2177	0.62	7.7%	0.95	21.5%	1.25
scagr7-2b	0.20	5.8%	0.81	73.7%	0.15
lp_pds_06	0.08	3.6%	0.08	9.8%	3.35
p010	0.05	5.4%	0.07	10.5%	0.81
ge	0.06	3.7%	0.06	10.9%	1.93
lp_osa_60	0.01	0.1%	0.01	10.0%	1.79
co9	0.05	3.5%	0.13	8.5%	5.64
lpl3	0.02	6.7%	0.08	9.1%	5.45
fome11	0.20	13.8%	0.36	12.4%	3.12
scrs8-2r	0.64	72.0%	0.48	31.4%	0.12
stormg2-27	0.09	5.6%	0.12	11.2%	2.46
lp_ken_11	0.01	6.2%	0.01	14.2%	2.46
sctap1-2b	0.28	6.0%	0.78	66.3%	0.26
car4	0.00	0.0%	0.03	2.6%	0.30
lp_pds_10	0.08	5.3%	0.13	13.7%	3.31
lp_stocfor3	0.01	4.0%	0.01	4.5%	1.36
				Continued on next page	

	PaToH		onmetisHP		
name	cutsize	%LI	cutsize	%LI	speedup
ex3sta1	0.30	7.1%	0.31	12.1%	1.35
testbig	0.22	2.8%	0.84	178.5%	0.21
dbir1	0.11	5.7%	0.72	13.9%	9.16
dbir2	0.13	9.7%	0.80	16.2%	8.25
scfxm1-2b	0.05	3.9%	0.06	6.3%	1.14
route	0.01	0.3%	0.03	0.0%	6.06
ts-palko	0.29	22.7%	0.98	134.5%	6.31
fxm4_6	0.02	3.7%	0.02	8.5%	2.65
fome12	0.18	10.7%	0.31	11.8%	3.57
e18	0.53	3.6%	0.82	5.3%	2.96
pltexpa	0.06	5.9%	0.09	11.9%	2.32
baxter	0.19	18.6%	0.38	29.8%	1.52
lp_ken_13	0.01	4.5%	0.00	10.7%	3.04
stat96v2	0.03	3.1%	0.03	4.6%	58.58
lp_pds_20	0.10	2.7%	0.13	9.9%	3.63
stat96v3	0.03	3.6%	0.03	7.3%	35.83
world	0.06	6.8%	0.09	12.5%	2.24
mod2	0.06	9.5%	0.08	13.3%	2.23
sc205-2r	0.22	5.6%	0.96	83.9%	0.11
scfxm1-2r	0.05	3.6%	0.25	9.4%	1.04
fxm3_16	0.00	3.7%	0.00	4.9%	2.72
dbic1	0.02	1.1%	0.02	8.5%	10.06
fome13	0.10	4.3%	0.20	9.6%	3.66
pds-30	0.11	6.8%	0.12	8.4%	3.30
rlfprim	0.35	16.0%	0.59	81.8%	0.32
stormg2-125	0.09	5.4%	0.25	34.2%	1.70
pds-40	0.08	5.3%	0.13	8.3%	3.78
fome21	0.09	5.0%	0.12	7.9%	3.76
pds-50	0.10	6.9%	0.12	7.1%	3.67
pds-60	0.09	3.9%	0.12	6.3%	3.92
pds-70	0.07	6.5%	0.12	7.1%	3.95
pds-80	0.08	4.2%	0.11	6.5%	4.07
pds-90	0.07	6.3%	0.10	6.1%	3.84
pds-100	0.06	6.6%	0.09	6.9%	4.06
watson_1	0.00	0.4%	0.00	0.3%	3.81
sgpf5y6	0.01	5.4%	0.01	16.4%	2.10
watson_2	0.00	3.8%	0.00	10.6%	3.68
stormG2_1000	0.10	7.3%	0.39	60.8%	0.47
cont11_l	0.01	2.3%	0.01	0.7%	1.20

Table 5.5 – continued from previous page

Table 5.6: 32-way partitioning performance of the LP matrix collection for cut-net metric with net balancing.

| name | PaToH | | onmetisHP | | |
	cutsize	%LI	cutsize	%LI	speedup
model3	0.27	25.9%	0.31	28.0%	2.97
progas	0.26	10.6%	0.25	14.3%	2.14
model5	0.40	62.8%	0.76	156.7%	11.24
scrs8-2b	0.58	171.5%	0.88	279.2%	0.53
lp_cycle	0.30	31.9%	0.40	46.1%	2.02
deter0	0.19	5.1%	0.21	10.2%	2.51
lp_pilot87	0.57	36.1%	0.72	105.4%	4.21
rosen10	0.00	0.0%	0.02	74.1%	3.65
model6	0.31	24.3%	0.38	31.6%	3.66
p6000	0.00	0.9%	0.00	48.3%	1.37
lp_stocfor2	0.20	11.3%	0.20	18.7%	2.20
lp_d2q06c	0.28	13.0%	0.30	28.0%	3.43
lp_80bau3b	0.14	9.1%	0.16	14.4%	3.79
nemspmm2	0.37	33.0%	0.43	38.1%	9.67
lp_bnl2	0.21	11.2%	0.24	13.1%	2.54
lp_osa_14	0.03	0.6%	0.03	6.7%	7.12
nemspmm1	0.37	20.3%	0.49	53.1%	5.32
lp_greenbea	0.28	17.1%	0.52	69.6%	3.50
lpi_greenbea	0.28	10.0%	0.53	79.0%	3.61
lp_ken_07	0.04	7.6%	0.04	16.8%	2.19
scagr7-2c	0.25	16.8%	0.77	59.1%	0.74
lpi_gran	0.27	46.3%	0.29	34.2%	0.79
lpi_bgindy	0.10	3.9%	0.10	16.8%	13.79
l30	0.37	13.4%	0.34	14.0%	5.20
model9	0.30	13.8%	0.41	45.2%	4.06
model8	0.36	16.4%	0.47	12.5%	2.98
lp_pds_02	0.11	5.8%	0.11	15.1%	2.23
lp22	0.61	86.1%	0.73	71.4%	3.69
lp_cre_c	0.07	0.8%	0.07	11.4%	2.40
lpi_cplex1	0.41	604.0%	0.98	203.3%	0.37
plddb	0.09	7.8%	0.09	8.2%	2.43
lp_maros_r7	0.90	374.4%	0.96	122.2%	2.20
rat	0.85	656.2%	0.99	103.8%	2.91
delf	0.11	5.0%	0.14	9.3%	2.10
stat96v4	0.13	2.4%	0.13	8.1%	63.60
deter4	0.31	5.4%	0.85	333.8%	1.31
lpl2	0.06	3.0%	0.12	12.4%	3.33
model7	0.20	47.5%	0.28	28.3%	3.26
sctap1-2c	0.30	17.3%	0.40	22.9%	0.66
lp_cre_a	0.06	0.2%	0.06	10.4%	2.21
lpi_ceria3d	0.53	19.2%	0.97	118.6%	0.29
ch	0.13	9.4%	0.29	9.7%	2.61
aircraft	0.00	1180.0%	1.00	540.0%	0.11
lpi_gosh	0.22	9.6%	0.31	33.5%	4.91
deter8	0.16	4.1%	0.15	12.2%	2.66
fxm2-16	0.09	7.0%	0.06	10.1%	2.78
nemsemm1	0.46	45.5%	0.77	177.1%	102.11
pcb3000	0.15	6.6%	0.15	11.4%	5.83
pgp2	0.56	12.5%	0.98	55.6%	0.45
rlfddd	0.69	89.0%	0.70	124.1%	14.86
deter6	0.16	5.3%	0.15	9.5%	2.51
large	0.13	5.1%	0.14	11.4%	2.24
lp_osa_30	0.02	0.4%	0.02	5.0%	2.90
stormg2-8	0.16	15.2%	0.17	16.1%	2.93
model10	0.37	61.6%	0.62	88.5%	6.50
nsir	0.24	14.3%	0.46	27.3%	5.28
				Continued on next page	

Table 5.6 – continued from previous page				
	PaToH		*onmetisHP*		
name	cutsize	%LI	cutsize	%LI	speedup
seymourl	0.82	216.5%	0.90	215.9%	0.77
cq5	0.09	7.5%	0.11	17.7%	4.81
p05	0.12	5.6%	0.17	13.9%	8.59
deter5	0.16	5.7%	0.16	8.1%	2.34
scsd8-2b	0.49	24.6%	0.95	144.0%	1.50
r05	0.14	8.0%	0.19	14.1%	10.32
bas1lp	0.58	203.2%	0.74	168.3%	3.64
deter1	0.16	4.8%	0.16	8.7%	2.32
co5	0.10	9.9%	0.13	15.1%	4.89
stat96v1	0.11	3.3%	0.11	5.8%	59.50
lp_dfl001	0.32	16.7%	0.42	11.3%	3.08
deter2	0.20	3.9%	0.18	14.7%	1.75
fxm3_6	0.07	4.9%	0.06	9.0%	2.92
deter7	0.15	6.6%	0.14	9.4%	2.30
lp_cre_d	0.17	9.7%	0.42	30.2%	16.39
ulevimin	0.14	11.0%	0.20	13.1%	6.01
nemswrld	0.27	4.1%	0.48	76.4%	6.89
nemsemm2	0.09	11.3%	0.10	22.7%	13.12
nl	0.09	4.0%	0.14	14.9%	3.08
lp_cre_b	0.15	7.7%	0.25	18.4%	12.60
deter3	0.15	3.4%	0.14	10.0%	2.10
rlfdual	0.63	77.8%	0.64	103.8%	6.77
scsd8-2r	0.49	12.9%	0.97	162.5%	1.05
cq9	0.07	8.1%	0.09	12.1%	5.15
pf2177	0.73	32.2%	0.96	35.3%	1.53
scagr7-2b	0.24	12.0%	0.85	91.2%	0.21
lp_pds_06	0.11	8.0%	0.12	17.2%	3.07
p010	0.07	7.9%	0.10	12.8%	0.89
ge	0.08	6.9%	0.08	13.3%	1.91
lp_osa_60	0.01	0.1%	0.02	16.1%	2.05
co9	0.08	4.6%	0.17	11.3%	5.58
lpl3	0.03	7.5%	0.08	12.4%	5.54
fome11	0.25	14.1%	0.41	14.2%	3.37
scrs8-2r	0.70	277.6%	0.90	406.0%	0.13
stormg2-27	0.12	8.5%	0.13	16.7%	2.52
lp_ken_11	0.01	6.8%	0.01	14.5%	2.47
sctap1-2b	0.30	6.5%	0.85	76.6%	0.32
car4	0.02	2.0%	0.04	5.0%	0.37
lp_pds_10	0.13	4.2%	0.14	15.4%	3.02
lp_stocfor3	0.04	5.0%	0.03	6.9%	1.42
ex3sta1	0.35	8.6%	0.37	17.7%	1.35
testbig	0.22	11.0%	0.86	198.8%	0.22
dbir1	0.14	7.7%	0.84	16.7%	8.83
dbir2	0.14	10.2%	0.76	19.9%	7.47
scfxm1-2b	0.06	2.6%	0.06	10.1%	1.34
route	0.09	3.0%	0.10	12.5%	5.83
ts-palko	0.39	43.7%	0.99	189.7%	7.39
fxm4_6	0.04	6.3%	0.02	12.2%	2.82
fome12	0.20	9.9%	0.37	13.4%	3.43
e18	0.58	9.0%	0.84	8.3%	3.21
pltexpa	0.07	4.2%	0.11	13.6%	2.41
baxter	0.24	21.1%	0.41	41.7%	1.44
lp_ken_13	0.01	4.3%	0.00	12.6%	3.00
stat96v2	0.05	4.3%	0.05	5.5%	65.24
lp_pds_20	0.12	6.1%	0.16	12.5%	3.68
stat96v3	0.04	2.8%	0.04	7.0%	41.35
world	0.09	5.8%	0.12	14.2%	2.21
mod2	0.08	5.1%	0.11	14.7%	2.18
Continued on next page					

Table 5.6 – continued from previous page					
	PaToH		*onmetisHP*		
name	cutsize	%*LI*	cutsize	%*LI*	speedup
sc205-2r	0.22	7.1%	0.97	62.0%	0.13
scfxm1-2r	0.06	4.3%	0.19	11.6%	1.12
fxm3_16	0.03	3.3%	0.03	5.4%	2.78
dbic1	0.03	1.9%	0.03	10.8%	9.63
fome13	0.18	9.7%	0.32	14.7%	3.70
pds-30	0.10	6.0%	0.15	12.7%	3.79
rlfprim	0.49	21.1%	0.72	132.7%	0.42
stormg2-125	0.12	6.3%	0.28	44.2%	1.80
pds-40	0.10	6.2%	0.15	11.0%	3.80
fome21	0.11	7.1%	0.13	10.9%	3.72
pds-50	0.11	8.8%	0.13	10.6%	3.65
pds-60	0.11	7.6%	0.13	10.7%	3.70
pds-70	0.10	8.9%	0.13	9.7%	4.00
pds-80	0.09	4.7%	0.13	11.4%	4.00
pds-90	0.08	3.7%	0.13	11.1%	3.79
pds-100	0.08	6.1%	0.12	12.0%	4.18
watson_1	0.00	0.8%	0.00	1.8%	3.90
sgpf5y6	0.02	9.1%	0.02	20.7%	2.06
watson_2	0.00	3.6%	0.00	13.8%	3.73
stormG2_1000	0.12	10.9%	0.50	100.1%	0.55
cont11_l	0.01	3.9%	0.01	3.4%	1.20

Table 5.7: 64-way partitioning performance of the LP matrix collection for cut-net metric with net balancing.

| | PaToH | | onmetisHP | | |
name	cutsize	%LI	cutsize	%LI	speedup
deter4	0.33	7.0%	0.85	338.5%	1.60
lpl2	0.12	13.1%	0.15	14.0%	3.93
model7	0.28	37.9%	0.32	36.1%	3.25
sctap1-2c	0.32	16.9%	0.39	22.9%	0.78
lp_cre_a	0.09	6.0%	0.09	18.6%	2.22
lpi_ceria3d	0.54	24.5%	0.98	189.6%	0.32
ch	0.17	16.9%	0.30	12.9%	3.02
aircraft	0.00	2460.0%	1.00	1180.0%	0.12
lpi_gosh	0.24	17.9%	0.33	41.7%	5.29
deter8	0.20	11.0%	0.22	14.3%	2.33
fxm2-16	0.22	19.8%	0.20	26.9%	2.26
nemsemm1	0.53	55.5%	0.80	204.3%	98.13
pcb3000	0.22	8.4%	0.22	13.0%	4.93
pgp2	0.57	13.7%	0.99	52.3%	0.53
rlfddd	0.83	310.3%	0.84	290.7%	13.01
deter6	0.21	4.5%	0.22	12.9%	2.32
large	0.17	11.1%	0.18	14.7%	2.35
lp_osa_30	0.02	0.4%	0.02	3.4%	3.26
stormg2-8	0.25	28.2%	0.25	25.8%	2.79
model10	0.44	68.9%	0.65	97.9%	6.38
nsir	0.28	17.2%	0.58	35.0%	5.57
seymourl	0.86	362.4%	0.93	279.1%	1.07
cq5	0.15	12.8%	0.16	22.7%	4.47
p05	0.18	10.8%	0.22	15.8%	8.00
deter5	0.20	5.5%	0.21	13.4%	2.35
scsd8-2b	0.52	18.4%	0.96	169.3%	1.76
r05	0.20	9.2%	0.24	18.0%	9.84
bas1lp	0.65	1289.7%	0.86	296.0%	3.84
deter1	0.20	7.6%	0.20	16.4%	2.33
co5	0.14	13.4%	0.16	21.9%	4.50
stat96v1	0.18	10.5%	0.17	10.2%	59.23
lp_dfl001	0.37	17.3%	0.47	14.1%	3.25
deter2	0.22	5.9%	0.24	20.2%	1.79
fxm3_6	0.09	9.2%	0.08	14.0%	2.93
deter7	0.16	9.2%	0.15	12.6%	2.60
lp_cre_d	0.23	11.5%	0.48	47.2%	13.96
ulevimin	0.17	7.6%	0.24	18.3%	5.77
nemswrld	0.30	7.3%	0.58	68.7%	6.25
nemsemm2	0.16	13.9%	0.17	21.0%	12.29
nl	0.12	7.1%	0.15	17.9%	3.03
lp_cre_b	0.20	31.8%	0.36	34.6%	11.63
deter3	0.16	2.4%	0.16	15.9%	2.31
rlfdual	0.81	184.1%	0.79	184.7%	5.53
scsd8-2r	0.50	16.1%	0.98	205.9%	1.18
cq9	0.11	13.7%	0.16	19.9%	4.97
pf2177	0.81	36.3%	0.98	119.3%	1.97
scagr7-2b	0.26	126.6%	0.86	118.5%	0.26
lp_pds_06	0.14	8.9%	0.17	21.3%	3.25
p010	0.11	9.9%	0.16	15.9%	1.11
ge	0.11	10.8%	0.12	19.3%	2.08
lp_osa_60	0.01	0.4%	0.01	10.1%	2.29
co9	0.11	11.7%	0.23	21.0%	5.24
lpl3	0.04	3.5%	0.10	15.2%	5.71
fome11	0.33	18.9%	0.43	16.7%	3.47
scrs8-2r	0.75	798.7%	0.99	321.9%	0.14
stormg2-27	0.15	7.9%	0.15	20.0%	2.71
				Continued on next page	

Table 5.7 – continued from previous page

name	PaToH cutsize	PaToH %LI	onmetisHP cutsize	onmetisHP %LI	speedup
lp_ken_11	0.02	7.8%	0.02	21.6%	2.58
sctap1-2b	0.30	7.5%	0.83	84.1%	0.33
car4	0.02	2.6%	0.05	5.0%	0.41
lp_pds_10	0.14	8.9%	0.18	20.5%	3.16
lp_stocfor3	0.05	4.6%	0.04	8.2%	1.65
ex3sta1	0.43	16.8%	0.44	30.7%	1.42
testbig	0.23	12.3%	0.88	262.1%	0.26
dbir1	0.17	12.6%	0.84	23.0%	8.76
dbir2	0.17	11.6%	0.86	24.4%	7.94
scfxm1-2b	0.06	4.8%	0.06	10.6%	1.39
route	0.18	8.5%	0.20	17.6%	5.17
ts-palko	0.60	139.1%	0.99	290.2%	8.47
fxm4_6	0.05	4.9%	0.04	16.0%	2.90
fome12	0.24	14.6%	0.40	15.1%	3.60
e18	0.62	12.6%	0.85	14.9%	3.64
pltexpa	0.15	4.0%	0.21	20.7%	2.35
baxter	0.28	27.3%	0.43	47.4%	0.87
lp_ken_13	0.02	5.1%	0.02	15.4%	2.92
stat96v2	0.07	3.0%	0.07	8.1%	70.20
lp_pds_20	0.14	9.0%	0.18	17.8%	3.81
stat96v3	0.06	2.4%	0.07	8.3%	45.83
world	0.11	9.4%	0.16	15.6%	2.27
mod2	0.12	6.5%	0.16	16.5%	2.14
sc205-2r	0.23	10.1%	0.97	65.6%	0.15
scfxm1-2r	0.06	4.3%	0.24	17.3%	1.25
fxm3_16	0.05	5.1%	0.05	7.9%	2.89
dbic1	0.04	2.7%	0.04	13.6%	9.43
fome13	0.20	13.2%	0.38	15.7%	3.59
pds-30	0.13	10.0%	0.16	15.9%	3.44
rlfprim	0.63	56.5%	0.80	173.6%	0.45
stormg2-125	0.13	8.0%	0.29	44.2%	1.90
pds-40	0.12	8.3%	0.17	16.9%	3.92
fome21	0.12	8.4%	0.16	15.1%	3.85
pds-50	0.12	9.0%	0.16	15.3%	3.70
pds-60	0.12	10.1%	0.16	15.3%	3.82
pds-70	0.11	6.5%	0.16	15.7%	3.94
pds-80	0.11	6.2%	0.15	15.1%	4.03
pds-90	0.10	6.7%	0.14	13.6%	3.79
pds-100	0.10	7.9%	0.13	14.7%	4.04
watson_1	0.02	1.0%	0.01	4.2%	3.95
sgpf5y6	0.03	7.2%	0.03	25.8%	1.97
watson_2	0.01	3.6%	0.01	16.4%	3.80
stormG2_1000	0.13	11.9%	0.54	113.3%	0.57
cont11_l	0.01	3.2%	0.01	5.9%	1.21

Table 5.8: 128-way partitioning performance of the LP matrix collection for cut-net metric with net balancing.

name	PaToH		onmetisHP		speedup
	cutsize	%LI	cutsize	%LI	
lp_cre_d	0.27	24.3%	0.50	59.1%	12.01
ulevimin	0.23	28.1%	0.30	28.9%	5.76
nemswrld	0.34	36.3%	0.61	81.3%	6.06
nemsemm2	0.21	14.3%	0.24	26.9%	10.63
nl	0.17	13.5%	0.20	24.9%	3.09
lp_cre_b	0.25	33.5%	0.41	59.4%	10.32
deter3	0.21	8.1%	0.22	20.8%	2.28
rlfdual	0.87	276.1%	0.90	290.7%	5.57
scsd8-2r	0.53	21.8%	0.98	268.3%	1.33
cq9	0.18	21.3%	0.21	32.2%	4.67
pf2177	0.90	104.8%	0.98	157.7%	2.16
scagr7-2b	0.29	153.3%	0.87	147.1%	0.31
lp_pds_06	0.17	9.1%	0.20	23.1%	3.21
p010	0.18	9.3%	0.19	19.5%	1.43
ge	0.19	17.3%	0.21	34.9%	2.24
lp_osa_60	0.01	0.4%	0.01	8.1%	2.57
co9	0.17	16.3%	0.28	26.8%	4.91
lpl3	0.07	4.8%	0.13	19.7%	5.95
fome11	0.38	23.5%	0.45	17.5%	3.35
scrs8-2r	0.76	1783.4%	0.99	276.7%	0.14
stormg2-27	0.20	14.7%	0.20	24.6%	2.84
lp_ken_11	0.04	9.4%	0.03	17.0%	2.64
sctap1-2b	0.31	12.3%	0.86	79.2%	0.41
car4	0.03	2.9%	0.06	6.9%	0.45
lp_pds_10	0.16	8.9%	0.22	26.3%	3.04
lp_stocfor3	0.11	5.9%	0.09	11.9%	1.80
ex3sta1	0.48	28.6%	0.49	33.6%	1.46
testbig	0.23	12.5%	0.85	194.4%	0.30
dbir1	0.19	17.7%	0.83	32.1%	8.94
dbir2	0.19	16.6%	0.84	25.6%	8.63
scfxm1-2b	0.07	4.6%	0.07	17.1%	1.61
route	0.43	37.8%	0.54	77.9%	4.67
ts-palko	0.85	1195.9%	1.00	576.4%	8.88
fxm4_6	0.07	5.6%	0.07	20.3%	3.08
fome12	0.33	17.0%	0.44	19.6%	3.63
e18	0.66	10.3%	0.85	21.8%	3.63
pltexpa	0.19	8.1%	0.23	25.9%	2.42
baxter	0.31	40.6%	0.47	70.0%	0.94
lp_ken_13	0.03	5.5%	0.03	16.5%	2.89
stat96v2	0.11	3.8%	0.10	9.0%	72.51
lp_pds_20	0.16	7.7%	0.21	21.5%	3.43
stat96v3	0.10	2.9%	0.10	9.4%	49.37
world	0.14	9.2%	0.19	22.2%	2.19
mod2	0.15	12.1%	0.20	23.2%	2.16
sc205-2r	0.23	11.2%	0.97	82.4%	0.17
scfxm1-2r	0.06	4.7%	0.17	16.5%	1.31
fxm3_16	0.07	5.7%	0.05	10.1%	2.93
dbic1	0.05	4.1%	0.04	15.8%	9.22
fome13	0.25	15.3%	0.42	24.9%	3.68
pds-30	0.15	9.6%	0.20	22.6%	3.54
rlfprim	0.72	97.6%	0.87	243.0%	0.51
stormg2-125	0.15	11.7%	0.29	44.0%	2.03
pds-40	0.15	10.3%	0.19	20.6%	3.72
fome21	0.14	9.4%	0.18	19.0%	3.62
pds-50	0.15	9.1%	0.18	18.7%	3.77
pds-60	0.15	13.0%	0.17	17.6%	3.72

name	PaToH cutsize	PaToH %LI	onmetisHP cutsize	onmetisHP %LI	speedup
Table 5.8 – continued from previous page					
pds-70	0.14	10.3%	0.18	18.6%	3.91
pds-80	0.13	9.6%	0.17	18.7%	4.03
pds-90	0.13	9.7%	0.17	18.8%	3.79
pds-100	0.12	10.0%	0.15	20.8%	3.84
watson_1	0.04	2.7%	0.02	8.7%	3.89
sgpf5y6	0.03	7.7%	0.04	27.8%	1.87
watson_2	0.02	3.2%	0.02	18.4%	3.79
stormG2_1000	0.14	11.3%	0.55	114.6%	0.58
cont11_l	0.02	2.7%	0.02	8.2%	1.21

Table 5.9: 2-way partitioning performance of the PD matrix collection for cut-net metric with node balancing.

name	PaToH		onmetisHP				speedup
	cutsize	%LI	cutsize	$exp\%LI_p$	$act\%LI_p$	$act\%LI_c$	
msc01050	0.21	2.3%	0.30	1.7%	3.2%	3.1%	1.27
bcsstm08	0.00	0.0%	0.00	0.0%	0.0%	0.0%	2.45
bcsstm09	0.00	0.1%	0.00	0.1%	0.1%	0.1%	2.39
bcsstk09	0.11	3.7%	0.12	0.2%	0.2%	0.2%	1.94
bcsstk10	0.03	1.3%	0.03	1.3%	1.3%	1.3%	1.66
1138_bus	0.02	0.0%	0.02	0.9%	1.0%	0.9%	1.91
bcsstk27	0.06	2.8%	0.06	3.0%	2.8%	2.8%	1.97
mhd1280b	0.01	0.4%	0.01	0.1%	0.4%	0.2%	1.14
plbuckle	0.00	2.6%	0.00	2.6%	2.6%	2.6%	1.65
msc01440	0.11	0.3%	0.11	0.3%	0.2%	0.2%	1.74
bcsstk11	0.04	3.6%	0.04	4.0%	3.8%	3.8%	1.64
bcsstm11	0.00	0.1%	0.00	0.1%	0.1%	0.1%	2.56
bcsstm12	0.05	0.0%	0.05	0.1%	0.1%	0.1%	1.64
bcsstk12	0.04	3.6%	0.04	4.0%	3.8%	3.8%	1.64
ex33	0.04	6.0%	0.05	2.0%	2.1%	2.1%	1.64
bcsstk14	0.11	0.0%	0.12	0.2%	0.2%	0.1%	1.49
ex3	0.06	0.0%	0.06	0.8%	0.8%	0.0%	1.59
nasa1824	0.11	0.2%	0.12	0.1%	0.1%	0.1%	1.31
plat1919	0.04	2.1%	0.04	1.4%	1.8%	1.4%	1.42
bcsstm26	0.00	0.0%	0.00	0.0%	0.0%	0.0%	2.49
bcsstk26	0.07	1.0%	0.08	0.3%	0.8%	0.8%	1.42
bcsstk13	0.22	1.6%	0.26	1.4%	2.7%	2.7%	1.39
nasa2146	0.07	2.3%	0.07	3.3%	3.2%	3.2%	1.70
ex10	0.02	0.9%	0.02	1.4%	1.3%	0.8%	1.28
Chem97ZtZ	0.00	0.0%	0.00	0.1%	0.1%	0.1%	0.50
ex10hs	0.02	0.3%	0.02	0.6%	0.6%	0.0%	1.27
ex13	0.04	0.0%	0.04	0.1%	0.1%	0.0%	1.26
nasa2910	0.17	0.0%	0.18	1.7%	3.6%	0.1%	1.38
bcsstk23	0.18	0.0%	0.18	0.0%	0.4%	0.4%	1.71
bcsstm23	0.00	0.0%	0.00	0.0%	0.0%	0.0%	2.58
mhd3200b	0.00	0.0%	0.00	1.9%	1.9%	1.8%	1.18
bibd_81_2	0.00	0.0%	0.00	0.0%	0.0%	0.0%	2.62
ex9	0.03	0.9%	0.03	1.6%	1.5%	0.6%	1.28
bcsstm24	0.00	0.0%	0.00	0.0%	0.0%	0.0%	2.63
bcsstk24	0.08	0.0%	0.11	0.0%	0.0%	0.0%	1.66
bcsstk21	0.00	0.0%	0.00	0.0%	0.0%	0.0%	1.25
bcsstm21	0.00	0.0%	0.00	0.0%	0.0%	0.0%	2.62
bcsstk15	0.10	2.7%	0.10	1.5%	1.3%	1.3%	1.36
sts4098	0.11	0.0%	0.19	3.7%	19.7%	18.9%	0.68
t2dal_e	0.00	0.0%	0.00	0.0%	0.0%	0.0%	2.64
bcsstk28	0.05	6.5%	0.05	4.0%	4.3%	4.3%	1.63
msc04515	0.04	1.7%	0.04	2.3%	2.6%	2.6%	1.20
nasa4704	0.08	0.1%	0.08	0.1%	0.1%	0.1%	1.23
mhd4800b	0.00	0.0%	0.00	4.3%	4.3%	4.3%	1.16
crystm01	0.03	1.4%	0.03	1.4%	1.4%	1.4%	1.24
bcsstk16	0.05	0.0%	0.05	0.0%	0.0%	0.0%	1.51
s3rmt3m3	0.06	0.0%	0.06	0.0%	0.0%	0.0%	1.54
s3rmt3m1	0.07	0.0%	0.07	0.1%	0.1%	0.1%	1.52
s2rmq4m1	0.07	0.3%	0.07	1.3%	1.2%	1.2%	1.55
s1rmt3m1	0.07	0.0%	0.07	0.1%	0.1%	0.1%	1.45
s1rmq4m1	0.07	1.2%	0.07	2.2%	2.0%	2.0%	1.54
s2rmt3m1	0.07	0.0%	0.07	0.0%	0.0%	0.0%	1.55
s3rmq4m1	0.07	0.4%	0.07	1.3%	1.2%	1.2%	1.54
ex15	0.01	0.3%	0.01	0.3%	0.3%	0.3%	1.21
Kuu	0.06	0.1%	0.06	3.6%	3.4%	0.8%	1.19
Muu	0.00	0.0%	0.00	0.0%	0.0%	0.0%	0.98

Table 5.9 – continued from previous page

	PaToH		onmetisHP				
name	cutsize	%LI	cutsize	$exp\%LI_p$	$act\%LI_p$	$act\%LI_c$	speedup
bcsstk38	0.03	3.1%	0.04	2.5%	2.1%	2.1%	1.17
aft01	0.03	0.0%	0.03	3.6%	3.6%	3.1%	1.17
fv1	0.02	0.0%	0.02	0.0%	0.0%	0.0%	1.42
fv3	0.02	0.0%	0.02	0.6%	0.6%	0.6%	1.42
fv2	0.02	0.0%	0.02	0.6%	0.6%	0.6%	1.42
bundle1	0.13	0.2%	0.10	3.4%	10.1%	1.9%	0.22
ted_B	0.00	0.0%	0.00	0.1%	0.1%	0.0%	0.64
ted_B_unscaled	0.00	0.0%	0.00	0.1%	0.1%	0.0%	0.64
msc10848	0.09	0.0%	0.09	3.8%	1.3%	0.0%	1.82
bcsstk17	0.04	0.0%	0.04	2.5%	2.5%	2.5%	1.30
t2dah_e	0.02	0.0%	0.02	1.0%	1.0%	0.7%	1.10
bcsstk18	0.04	0.0%	0.04	1.0%	0.9%	0.9%	1.00
cbuckle	0.05	1.2%	0.05	4.0%	2.4%	2.4%	1.33
crystm02	0.02	1.3%	0.02	1.0%	1.0%	1.0%	1.11
Pres_Poisson	0.03	0.5%	0.03	0.7%	0.7%	0.7%	1.41
bcsstm25	0.00	0.0%	0.00	0.0%	0.0%	0.0%	2.61
bcsstk25	0.02	4.4%	0.02	0.6%	0.8%	0.8%	1.05
Dubcova1	0.03	0.0%	0.02	1.6%	1.6%	1.0%	1.10
olafu	0.05	0.1%	0.04	0.5%	0.8%	0.8%	1.50
gyro_m	0.00	0.2%	0.00	0.4%	0.6%	0.4%	0.88
gyro	0.01	0.1%	0.01	0.3%	0.4%	0.1%	1.27
bodyy4	0.01	0.0%	0.01	0.0%	0.0%	0.0%	1.30
bodyy5	0.01	0.0%	0.01	0.0%	0.0%	0.0%	1.32
bodyy6	0.01	0.0%	0.01	0.0%	0.0%	0.0%	1.31
raefsky4	0.05	1.5%	0.05	1.8%	1.7%	1.7%	1.46
LFAT5000	0.00	0.0%	0.00	0.0%	0.0%	0.0%	1.14
LF10000	0.00	0.0%	0.00	0.0%	0.0%	0.0%	1.09
t3dl_e	0.00	0.0%	0.00	0.0%	0.0%	0.0%	2.65
msc23052	0.03	2.7%	0.03	2.5%	2.3%	2.3%	1.52
bcsstk36	0.03	1.0%	0.03	2.0%	1.8%	1.8%	1.44
crystm03	0.01	1.8%	0.01	0.7%	0.7%	0.7%	1.19
smt	0.07	0.3%	0.06	1.4%	1.1%	0.1%	1.87
thread	0.10	0.0%	0.10	0.3%	0.3%	0.0%	1.87
wathen100	0.02	0.0%	0.02	0.4%	0.4%	0.2%	0.99
ship_001	0.03	2.5%	0.03	1.0%	1.0%	0.7%	1.83
nd12k	0.31	1.0%	0.29	0.9%	0.9%	0.7%	2.58
wathen120	0.02	0.0%	0.01	0.5%	0.5%	0.3%	1.01
obstclae	0.01	0.0%	0.01	0.0%	0.0%	0.0%	1.29
jnlbrng1	0.01	0.0%	0.01	0.0%	0.0%	0.0%	1.28
minsurfo	0.01	0.0%	0.01	0.0%	0.0%	0.0%	1.30
bcsstm39	0.00	0.0%	0.00	0.0%	0.0%	0.0%	2.86
vanbody	0.02	1.5%	0.02	1.9%	1.8%	1.7%	1.42
gridgena	0.01	0.0%	0.01	1.0%	1.0%	1.0%	1.08
cvxbqp1	0.02	0.0%	0.02	0.0%	0.0%	0.0%	1.48
ct20stif	0.04	4.4%	0.04	3.4%	3.5%	3.3%	1.40
crankseg_1	0.04	0.0%	0.03	2.4%	1.9%	1.2%	1.94
nasasrb	0.01	0.5%	0.01	0.2%	0.2%	0.2%	1.46
Andrews	0.07	0.5%	0.10	1.5%	1.5%	1.5%	1.21
crankseg_2	0.04	2.0%	0.03	1.0%	0.1%	0.0%	1.97
Dubcova2	0.01	0.0%	0.01	0.1%	0.1%	0.0%	1.05
qa8fm	0.01	0.1%	0.01	0.0%	0.0%	0.0%	1.16
cfd1	0.02	0.8%	0.03	1.7%	1.7%	1.7%	1.14
nd24k	0.24	0.9%	0.23	1.7%	1.6%	0.0%	2.56
oilpan	0.02	1.0%	0.02	0.2%	0.2%	0.0%	1.42
finan512	0.00	0.0%	0.00	0.0%	0.0%	0.0%	0.81
apache1	0.02	0.0%	0.02	0.0%	0.0%	0.0%	1.48
shallow_water1	0.01	0.0%	0.01	0.0%	0.0%	0.0%	1.32
shallow_water2	0.01	0.0%	0.01	0.0%	0.0%	0.0%	1.32

Table 5.9 – continued from previous page						
	$PaToH$		$onmetisHP$			
name	cutsize	%LI	cutsize	$exp\%LI_p$	$act\%LI_p$	$act\%LI_c$	speedup
thermal1	0.00	0.0%	0.00	0.2%	0.2%	0.2%	1.24
denormal	0.01	0.0%	0.01	0.0%	0.0%	0.0%	1.12
s3dkt3m2	0.01	0.0%	0.01	0.0%	0.0%	0.0%	1.36
s3dkq4m2	0.01	0.0%	0.01	0.7%	0.7%	0.7%	1.56
m_t1	0.02	4.0%	0.02	0.4%	0.7%	0.1%	1.92
2cubes_sphere	0.04	6.5%	0.04	1.9%	1.8%	0.0%	1.11
thermomech_TK	0.00	0.0%	0.00	0.9%	0.9%	0.9%	1.42
thermomech_TC	0.00	0.6%	0.00	0.3%	0.4%	0.3%	1.42
x104	0.03	0.0%	0.03	0.1%	0.3%	0.0%	1.82
shipsec8	0.03	3.0%	0.03	0.1%	0.3%	0.3%	1.52
ship_003	0.02	0.9%	0.02	2.3%	2.3%	2.3%	1.52
cfd2	0.02	1.1%	0.02	0.7%	0.9%	0.9%	1.11
boneS01	0.04	0.3%	0.03	1.5%	1.7%	1.4%	1.43
shipsec1	0.02	0.1%	0.02	0.3%	0.5%	0.5%	1.59
bmw7st_1	0.01	2.3%	0.01	0.4%	0.6%	0.5%	1.52
Dubcova3	0.01	0.0%	0.01	0.0%	0.0%	0.0%	1.04
bmwcra_1	0.01	3.5%	0.01	0.0%	0.0%	0.0%	1.42
G2_circuit	0.00	0.0%	0.00	0.0%	0.0%	0.0%	1.42
shipsec5	0.01	5.4%	0.02	0.7%	1.1%	1.1%	1.56
thermomech_dM	0.00	0.0%	0.00	0.0%	0.0%	0.0%	1.56
pwtk	0.01	0.1%	0.01	0.1%	0.1%	0.1%	1.56
hood	0.01	0.6%	0.01	0.7%	0.8%	0.6%	1.48
BenElechi1	0.01	0.0%	0.01	1.0%	1.0%	1.0%	1.57
offshore	0.02	4.3%	0.02	2.5%	2.4%	1.7%	1.17
F1	0.01	0.0%	0.01	1.0%	1.0%	0.0%	1.21
msdoor	0.00	0.5%	0.00	0.2%	0.2%	0.1%	1.48
af_2_k101	0.00	0.0%	0.00	0.0%	0.0%	0.0%	1.27
af_5_k101	0.00	0.0%	0.00	0.0%	0.0%	0.0%	1.28
af_1_k101	0.00	0.0%	0.00	0.0%	0.0%	0.0%	1.28
af_4_k101	0.00	0.0%	0.00	0.0%	0.0%	0.0%	1.27
af_3_k101	0.00	0.0%	0.00	0.0%	0.0%	0.0%	1.28
af_0_k101	0.00	0.0%	0.00	0.0%	0.0%	0.0%	1.28
inline_1	0.01	2.1%	0.01	1.3%	1.3%	0.9%	1.26
af_shell8	0.00	0.0%	0.00	0.0%	0.0%	0.0%	1.28
af_shell3	0.00	0.0%	0.00	0.0%	0.0%	0.0%	1.28
af_shell4	0.00	0.0%	0.00	0.0%	0.0%	0.0%	1.28
af_shell7	0.00	0.0%	0.00	0.0%	0.0%	0.0%	1.28
parabolic_fem	0.00	0.0%	0.00	0.0%	0.0%	0.0%	1.67
apache2	0.01	0.0%	0.01	0.0%	0.0%	0.0%	1.47
tmt_sym	0.00	0.9%	0.00	0.0%	0.1%	0.1%	1.22
boneS10	0.01	3.1%	0.01	0.5%	0.5%	0.0%	1.46
ldoor	0.00	0.0%	0.00	0.3%	0.3%	0.3%	1.47
ecology2	0.00	0.0%	0.00	0.0%	0.0%	0.0%	1.29
thermal2	0.00	1.7%	0.00	0.2%	0.2%	0.2%	1.30
G3_circuit	0.00	0.0%	0.00	0.0%	0.0%	0.0%	1.39

Table 5.10: 4-way partitioning performance of the PD matrix collection for cut-net metric with node balancing.

name	PaToH		onmetisHP				speedup
	cutsize	%LI	cutsize	$exp\%LI_p$	$act\%LI_p$	$act\%LI_c$	
msc01050	0.33	5.0%	0.44	12.6%	16.3%	8.7%	1.68
bcsstm08	0.00	0.2%	0.00	0.2%	0.2%	0.2%	3.18
bcsstm09	0.00	0.1%	0.00	0.1%	0.1%	0.1%	3.11
bcsstk09	0.21	0.6%	0.21	0.9%	0.6%	0.4%	1.85
bcsstk10	0.09	1.5%	0.09	4.0%	4.9%	4.9%	2.10
1138_bus	0.04	1.3%	0.04	2.8%	2.4%	2.3%	2.09
bcsstk27	0.18	3.2%	0.17	4.6%	10.3%	10.3%	2.33
mhd1280b	0.02	2.0%	0.02	2.0%	2.8%	2.4%	1.63
plbuckle	0.11	2.9%	0.10	3.1%	3.5%	3.5%	1.89
msc01440	0.23	1.2%	0.23	2.8%	1.5%	1.5%	1.92
bcsstk11	0.14	3.9%	0.14	7.4%	5.4%	5.4%	1.84
bcsstm11	0.00	0.2%	0.00	0.2%	0.2%	0.2%	3.28
bcsstm12	0.11	1.6%	0.11	4.8%	7.7%	7.6%	2.00
bcsstk12	0.14	3.8%	0.14	7.4%	5.4%	5.4%	1.84
ex33	0.08	4.6%	0.08	5.2%	7.1%	7.1%	1.92
bcsstk14	0.21	0.1%	0.21	3.4%	2.9%	1.1%	1.80
ex3	0.20	0.1%	0.21	3.1%	5.8%	0.5%	1.60
nasa1824	0.24	1.2%	0.26	4.2%	7.1%	7.1%	1.52
plat1919	0.13	2.2%	0.13	5.9%	5.7%	5.0%	1.71
bcsstm26	0.00	0.1%	0.00	0.1%	0.1%	0.1%	3.18
bcsstk26	0.14	1.2%	0.15	3.3%	5.9%	5.6%	1.66
bcsstk13	0.46	3.3%	0.55	44.0%	38.4%	27.1%	1.91
nasa2146	0.19	2.2%	0.18	4.0%	4.1%	4.1%	1.84
ex10	0.07	2.0%	0.05	6.0%	7.5%	6.0%	1.49
Chem97ZtZ	0.00	0.1%	0.00	4.0%	4.0%	4.0%	0.60
ex10hs	0.06	2.8%	0.05	8.6%	6.3%	4.7%	1.48
ex13	0.11	0.3%	0.11	4.8%	4.9%	1.7%	1.65
nasa2910	0.28	0.0%	0.26	5.6%	9.4%	0.4%	1.79
bcsstk23	0.35	0.6%	0.37	4.5%	3.8%	1.4%	1.50
bcsstm23	0.00	0.1%	0.00	0.1%	0.1%	0.1%	3.27
mhd3200b	0.00	0.3%	0.00	3.4%	3.3%	3.1%	1.61
bibd_81_2	0.00	0.0%	0.00	0.0%	0.0%	0.0%	3.31
ex9	0.10	0.8%	0.10	6.4%	9.0%	6.2%	1.64
bcsstm24	0.00	0.1%	0.00	0.1%	0.1%	0.1%	3.31
bcsstk24	0.16	0.2%	0.19	0.9%	1.7%	0.9%	2.16
bcsstk21	0.07	0.0%	0.07	0.1%	0.0%	0.0%	1.58
bcsstm21	0.00	0.0%	0.00	0.0%	0.0%	0.0%	3.32
bcsstk15	0.24	1.7%	0.24	3.6%	4.2%	4.0%	1.48
sts4098	0.22	5.1%	0.26	12.3%	11.7%	9.9%	0.76
t2dal_e	0.00	0.1%	0.00	0.1%	0.1%	0.1%	3.35
bcsstk28	0.14	2.4%	0.13	3.5%	6.7%	6.7%	2.20
msc04515	0.09	3.9%	0.09	3.8%	4.9%	4.9%	1.58
nasa4704	0.17	1.6%	0.16	2.7%	4.8%	4.8%	1.50
mhd4800b	0.00	0.0%	0.00	4.5%	4.4%	4.4%	1.52
crystm01	0.08	2.5%	0.08	3.3%	5.4%	5.4%	1.54
bcsstk16	0.14	4.3%	0.14	1.4%	3.5%	3.5%	2.13
s3rmt3m3	0.13	0.2%	0.13	0.7%	3.1%	2.9%	1.97
s3rmt3m1	0.14	0.2%	0.15	0.5%	4.1%	4.0%	1.95
s2rmq4m1	0.14	1.1%	0.13	4.2%	3.3%	2.9%	2.20
s1rmt3m1	0.14	0.1%	0.15	0.6%	4.4%	4.3%	1.95
s1rmq4m1	0.14	1.8%	0.13	4.9%	4.0%	4.0%	2.18
s2rmt3m1	0.14	0.2%	0.15	0.6%	4.0%	3.8%	1.94
s3rmq4m1	0.14	1.4%	0.13	4.4%	3.8%	3.6%	2.18
ex15	0.04	2.1%	0.04	3.9%	4.1%	4.1%	1.55
Kuu	0.14	0.3%	0.14	3.9%	4.1%	0.0%	1.59
Muu	0.07	0.0%	0.06	4.9%	4.7%	2.1%	1.22

Continued on next page

Table 5.10 – continued from previous page

name	PaToH		onmetisHP				speedup
	cutsize	%LI	cutsize	$exp\%LI_p$	$act\%LI_p$	$act\%LI_c$	
bcsstk38	0.14	3.7%	0.14	5.0%	6.3%	6.0%	1.52
aft01	0.07	0.0%	0.06	4.6%	5.5%	4.4%	1.37
fv1	0.04	0.6%	0.04	0.0%	0.0%	0.0%	1.67
fv3	0.04	0.7%	0.04	2.1%	2.0%	2.0%	1.66
fv2	0.04	0.7%	0.04	2.1%	2.0%	2.0%	1.66
bundle1	0.33	0.0%	0.52	75.6%	58.2%	15.4%	0.26
ted_B	0.01	0.0%	0.01	0.5%	0.5%	0.0%	0.83
ted_B_unscaled	0.01	0.1%	0.01	0.5%	0.6%	0.2%	0.82
msc10848	0.24	0.0%	0.22	5.9%	5.1%	0.3%	2.57
bcsstk17	0.08	0.8%	0.08	3.0%	7.7%	7.4%	1.76
t2dah_e	0.06	0.0%	0.05	1.8%	1.7%	0.8%	1.37
bcsstk18	0.08	4.6%	0.08	4.7%	7.0%	6.8%	1.06
cbuckle	0.10	1.5%	0.10	5.9%	4.1%	4.1%	1.84
crystm02	0.06	2.8%	0.06	1.7%	2.3%	2.3%	1.39
Pres_Poisson	0.09	1.5%	0.08	1.9%	4.6%	4.6%	1.93
bcsstm25	0.00	0.0%	0.00	0.0%	0.0%	0.0%	3.25
bcsstk25	0.07	2.0%	0.07	2.3%	2.9%	2.9%	1.22
Dubcova1	0.06	0.0%	0.05	3.0%	2.9%	1.1%	1.33
olafu	0.09	2.0%	0.08	4.5%	5.3%	5.2%	2.10
gyro_m	0.01	2.0%	0.01	5.0%	4.7%	4.5%	1.07
gyro	0.05	0.9%	0.05	5.1%	6.2%	4.7%	1.54
bodyy4	0.03	0.1%	0.03	0.5%	0.8%	0.8%	1.55
bodyy5	0.03	0.0%	0.03	0.6%	0.8%	0.8%	1.54
bodyy6	0.03	0.0%	0.03	0.5%	0.5%	0.5%	1.55
raefsky4	0.11	2.0%	0.12	4.6%	4.0%	4.0%	1.92
LFAT5000	0.00	0.0%	0.00	0.0%	0.0%	0.0%	1.33
LF10000	0.00	0.0%	0.00	0.0%	0.0%	0.0%	1.29
t3dl_e	0.00	0.0%	0.00	0.0%	0.0%	0.0%	3.27
msc23052	0.09	2.0%	0.08	5.0%	5.7%	5.6%	2.05
bcsstk36	0.09	3.6%	0.08	3.8%	5.0%	4.9%	1.91
crystm03	0.04	1.5%	0.04	1.7%	3.0%	3.0%	1.40
smt	0.21	0.3%	0.19	6.2%	8.8%	5.7%	2.57
thread	0.31	0.0%	0.28	3.8%	12.5%	8.1%	2.58
wathen100	0.04	0.0%	0.03	1.8%	1.8%	1.1%	1.21
ship_001	0.09	2.3%	0.08	3.5%	2.8%	1.6%	2.53
nd12k	0.52	0.8%	0.50	8.3%	6.1%	1.8%	3.75
wathen120	0.03	0.0%	0.03	1.9%	1.9%	1.4%	1.19
obstclae	0.02	0.0%	0.02	0.1%	0.2%	0.2%	1.48
jnlbrng1	0.02	0.0%	0.02	0.0%	0.2%	0.2%	1.47
minsurfo	0.02	0.0%	0.02	0.1%	0.2%	0.2%	1.48
bcsstm39	0.00	0.0%	0.00	0.0%	0.0%	0.0%	3.48
vanbody	0.04	3.6%	0.04	4.7%	5.0%	4.9%	1.90
gridgena	0.02	1.7%	0.02	1.8%	2.2%	2.2%	1.26
cvxbqp1	0.03	0.9%	0.03	2.1%	2.8%	2.8%	1.66
ct20stif	0.08	3.1%	0.08	4.5%	5.2%	4.9%	1.80
crankseg_1	0.11	3.4%	0.10	7.5%	5.3%	3.4%	2.81
nasasrb	0.03	2.7%	0.03	0.5%	1.4%	1.4%	1.94
Andrews	0.14	6.2%	0.18	8.5%	10.2%	9.7%	1.29
crankseg_2	0.11	2.1%	0.10	2.7%	1.5%	0.0%	2.87
Dubcova2	0.03	0.0%	0.02	1.7%	1.7%	0.6%	1.27
qa8fm	0.08	0.8%	0.08	2.4%	2.7%	2.7%	1.38
cfd1	0.06	2.4%	0.05	4.2%	4.2%	4.2%	1.37
nd24k	0.42	1.4%	0.41	5.4%	4.3%	2.6%	3.80
oilpan	0.04	1.2%	0.04	2.1%	2.2%	1.7%	1.88
finan512	0.00	0.0%	0.00	0.0%	0.0%	0.0%	0.91
apache1	0.04	0.0%	0.04	0.1%	0.4%	0.4%	1.55
shallow_water1	0.02	0.0%	0.02	0.0%	0.2%	0.2%	1.48
shallow_water2	0.02	0.0%	0.02	0.0%	0.3%	0.3%	1.48

Table 5.10 – continued from previous page

| name | PaToH | | onmetisHP | | | | |
	cutsize	%LI	cutsize	$exp\%LI_p$	$act\%LI_p$	$act\%LI_c$	speedup
thermal1	0.01	1.9%	0.01	1.9%	2.1%	2.1%	1.43
denormal	0.03	0.0%	0.03	0.0%	0.2%	0.2%	1.33
s3dkt3m2	0.04	0.0%	0.04	0.1%	1.1%	1.1%	1.80
s3dkq4m2	0.04	0.2%	0.03	2.7%	3.3%	3.3%	2.09
m_t1	0.07	4.0%	0.06	4.2%	3.1%	1.7%	2.67
2cubes_sphere	0.11	4.6%	0.11	2.7%	3.8%	2.5%	1.26
thermomech_TK	0.01	1.6%	0.01	2.9%	2.9%	2.9%	1.69
thermomech_TC	0.01	1.5%	0.01	0.9%	1.3%	1.3%	1.69
x104	0.06	1.9%	0.06	3.7%	3.9%	2.6%	2.56
shipsec8	0.07	2.4%	0.07	1.9%	2.9%	2.8%	1.98
ship_003	0.07	3.0%	0.07	4.7%	5.4%	5.4%	1.98
cfd2	0.05	1.5%	0.05	4.5%	4.4%	4.4%	1.31
boneS01	0.08	2.6%	0.07	2.4%	1.9%	0.7%	1.82
shipsec1	0.05	1.8%	0.04	2.3%	2.0%	2.0%	2.11
bmw7st_1	0.03	2.7%	0.03	3.3%	3.2%	3.2%	2.01
Dubcova3	0.03	0.0%	0.02	1.5%	1.4%	0.3%	1.27
bmwcra_1	0.02	7.3%	0.03	3.5%	5.5%	5.5%	1.85
G2_circuit	0.01	0.0%	0.01	3.0%	3.0%	3.0%	1.51
shipsec5	0.05	3.6%	0.05	1.5%	2.0%	2.0%	2.07
thermomech_dM	0.00	1.2%	0.00	1.1%	1.1%	1.1%	1.87
pwtk	0.01	0.6%	0.01	0.7%	0.7%	0.7%	2.14
hood	0.02	0.9%	0.02	2.3%	2.3%	2.1%	1.99
BenElechi1	0.02	0.3%	0.01	1.5%	1.8%	1.8%	2.15
offshore	0.04	2.9%	0.04	3.8%	4.4%	3.8%	1.38
F1	0.03	3.5%	0.02	2.6%	2.8%	0.9%	1.54
msdoor	0.01	0.6%	0.01	2.1%	1.9%	1.5%	2.03
af_2_k101	0.01	0.0%	0.01	0.0%	0.3%	0.3%	1.68
af_5_k101	0.01	0.0%	0.01	0.0%	0.3%	0.3%	1.67
af_1_k101	0.01	0.0%	0.01	0.0%	0.3%	0.3%	1.67
af_4_k101	0.01	0.0%	0.01	0.0%	0.3%	0.3%	1.68
af_3_k101	0.01	0.0%	0.01	0.0%	0.3%	0.3%	1.67
af_0_k101	0.01	0.0%	0.01	0.0%	0.3%	0.3%	1.67
inline_1	0.02	2.3%	0.02	4.4%	4.6%	4.0%	1.65
af_shell8	0.01	0.0%	0.01	0.1%	0.1%	0.1%	1.68
af_shell3	0.01	0.0%	0.01	0.1%	0.2%	0.2%	1.68
af_shell4	0.01	0.0%	0.01	0.0%	0.1%	0.1%	1.68
af_shell7	0.01	0.0%	0.01	0.1%	0.1%	0.1%	1.68
parabolic_fem	0.01	0.0%	0.01	0.0%	0.2%	0.2%	1.92
apache2	0.01	0.0%	0.01	0.0%	0.1%	0.1%	1.55
tmt_sym	0.01	1.6%	0.01	1.0%	1.0%	1.0%	1.39
boneS10	0.01	2.3%	0.01	3.0%	3.0%	3.0%	1.95
ldoor	0.01	2.1%	0.01	2.4%	2.4%	2.4%	2.03
ecology2	0.00	0.0%	0.00	0.0%	0.0%	0.0%	1.40
thermal2	0.00	2.1%	0.00	1.2%	1.3%	1.3%	1.53
G3_circuit	0.00	0.0%	0.00	0.0%	0.1%	0.1%	1.52

Table 5.11: 8-way partitioning performance of the PD matrix collection for cut-net metric with node balancing.

name	PaToH		onmetisHP				speedup
	cutsize	%LI	cutsize	$exp\%LI_p$	$act\%LI_p$	$act\%LI_c$	
msc01050	0.44	3.5%	0.47	27.4%	37.5%	33.8%	1.82
bcsstm08	0.00	0.6%	0.00	0.6%	0.6%	0.6%	3.52
bcsstm09	0.00	0.5%	0.00	0.5%	0.5%	0.5%	3.47
bcsstk09	0.41	3.0%	0.41	9.9%	16.8%	16.3%	2.00
bcsstk10	0.23	4.1%	0.22	20.9%	13.1%	13.0%	2.21
1138_bus	0.07	2.1%	0.07	5.3%	6.1%	5.8%	2.21
bcsstk27	0.46	3.5%	0.45	25.9%	18.3%	17.7%	2.74
mhd1280b	0.06	2.8%	0.05	7.1%	5.8%	4.8%	1.97
plbuckle	0.31	3.7%	0.32	9.1%	12.9%	12.3%	2.16
msc01440	0.46	2.8%	0.45	10.3%	11.4%	11.3%	2.21
bcsstk11	0.26	2.8%	0.25	11.7%	11.6%	11.5%	2.16
bcsstm11	0.00	0.5%	0.00	0.5%	0.5%	0.5%	3.63
bcsstm12	0.21	1.9%	0.20	11.1%	15.8%	15.4%	2.18
bcsstk12	0.26	2.8%	0.25	10.9%	11.0%	10.9%	2.16
ex33	0.15	4.6%	0.13	13.6%	18.0%	17.9%	2.10
bcsstk14	0.42	2.2%	0.41	10.3%	19.9%	16.7%	2.11
ex3	0.36	0.1%	0.34	10.1%	24.0%	10.8%	1.82
nasa1824	0.37	1.6%	0.39	17.4%	16.3%	13.5%	1.78
plat1919	0.25	2.4%	0.26	9.2%	12.9%	11.6%	2.02
bcsstm26	0.00	0.3%	0.00	0.3%	0.3%	0.3%	3.53
bcsstk26	0.24	2.6%	0.26	8.9%	14.1%	12.9%	1.79
bcsstk13	0.66	4.3%	0.72	53.6%	56.3%	27.5%	1.99
nasa2146	0.32	2.4%	0.31	10.0%	15.2%	14.7%	2.07
ex10	0.20	1.4%	0.17	15.7%	15.2%	8.7%	1.72
Chem97ZtZ	0.00	0.2%	0.00	1.8%	1.8%	1.8%	0.67
ex10hs	0.18	1.5%	0.15	25.4%	9.7%	4.3%	1.73
ex13	0.29	0.2%	0.29	4.2%	7.2%	0.1%	1.81
nasa2910	0.48	0.1%	0.45	46.4%	22.1%	1.6%	2.00
bcsstk23	0.49	0.5%	0.53	13.7%	24.9%	17.1%	1.62
bcsstm23	0.00	0.1%	0.00	0.1%	0.1%	0.1%	3.65
mhd3200b	0.01	0.2%	0.01	5.2%	4.7%	4.5%	1.82
bibd_81_2	0.00	0.0%	0.00	0.0%	0.0%	0.0%	3.67
ex9	0.26	0.8%	0.26	10.5%	10.0%	2.6%	1.77
bcsstm24	0.00	0.2%	0.00	0.2%	0.2%	0.2%	3.65
bcsstk24	0.32	1.4%	0.33	6.1%	17.9%	16.5%	2.45
bcsstk21	0.16	0.2%	0.15	0.9%	2.3%	2.2%	1.74
bcsstm21	0.00	0.0%	0.00	0.0%	0.0%	0.0%	3.67
bcsstk15	0.39	2.8%	0.38	7.5%	10.2%	9.4%	1.63
sts4098	0.32	4.5%	0.37	24.2%	25.8%	21.4%	0.90
t2dal_e	0.00	0.2%	0.00	0.2%	0.2%	0.2%	3.68
bcsstk28	0.26	3.1%	0.25	8.9%	11.9%	11.0%	2.47
msc04515	0.17	3.2%	0.16	6.3%	10.1%	10.0%	1.76
nasa4704	0.25	3.1%	0.24	10.8%	9.4%	9.2%	1.70
mhd4800b	0.01	0.2%	0.00	3.9%	3.5%	3.3%	1.73
crystm01	0.19	4.0%	0.18	7.2%	7.5%	7.5%	1.71
bcsstk16	0.35	4.8%	0.35	8.9%	11.5%	11.4%	2.38
s3rmt3m3	0.23	0.5%	0.22	5.0%	9.7%	9.1%	2.26
s3rmt3m1	0.25	0.4%	0.24	4.2%	9.8%	9.4%	2.28
s2rmq4m1	0.27	1.5%	0.26	6.5%	12.0%	12.0%	2.57
s1rmt3m1	0.25	0.7%	0.25	3.4%	10.1%	9.6%	2.27
s1rmq4m1	0.27	2.1%	0.26	6.5%	11.5%	11.4%	2.59
s2rmt3m1	0.24	0.3%	0.25	4.5%	9.3%	8.8%	2.28
s3rmq4m1	0.27	1.6%	0.26	6.9%	12.7%	12.5%	2.60
ex15	0.08	2.5%	0.08	4.5%	8.2%	8.2%	1.82
Kuu	0.26	0.1%	0.26	11.8%	13.9%	1.2%	1.81
Muu	0.14	0.1%	0.14	5.5%	5.2%	0.0%	1.40

Table 5.11 – continued from previous page

| name | PaToH | | onmetisHP | | | | |
	cutsize	%LI	cutsize	$exp\%LI_p$	$act\%LI_p$	$act\%LI_c$	speedup
bcsstk38	0.26	3.2%	0.27	14.9%	17.3%	16.2%	1.72
aft01	0.12	0.1%	0.11	7.5%	7.6%	5.5%	1.49
fv1	0.08	2.2%	0.08	1.0%	3.1%	3.1%	1.91
fv3	0.08	2.0%	0.08	3.5%	3.1%	3.1%	1.93
fv2	0.09	1.6%	0.08	3.5%	3.1%	3.1%	1.93
bundle1	0.55	0.2%	0.95	163.6%	110.3%	1.6%	0.28
ted_B	0.02	0.6%	0.02	0.7%	0.9%	0.0%	0.99
ted_B_unscaled	0.02	0.0%	0.02	0.6%	0.9%	0.0%	1.00
msc10848	0.36	0.1%	0.33	15.0%	26.7%	18.7%	2.98
bcsstk17	0.15	3.3%	0.16	6.8%	12.7%	12.5%	2.07
t2dah_e	0.10	0.0%	0.09	4.7%	4.3%	2.6%	1.55
bcsstk18	0.13	4.6%	0.14	7.4%	12.6%	12.3%	1.27
cbuckle	0.18	2.2%	0.17	8.1%	6.6%	6.6%	2.22
crystm02	0.13	3.2%	0.13	5.3%	5.0%	5.0%	1.55
Pres_Poisson	0.16	1.5%	0.15	4.7%	6.2%	6.2%	2.29
bcsstm25	0.00	0.0%	0.00	0.0%	0.0%	0.0%	3.58
bcsstk25	0.15	2.5%	0.15	8.1%	7.5%	7.4%	1.30
Dubcova1	0.10	0.0%	0.09	5.6%	3.8%	1.3%	1.48
olafu	0.16	2.2%	0.14	9.3%	11.5%	11.4%	2.43
gyro_m	0.03	2.4%	0.03	7.5%	7.6%	6.8%	1.18
gyro	0.12	1.7%	0.10	7.4%	18.7%	15.4%	1.71
bodyy4	0.05	0.6%	0.05	0.8%	1.7%	1.7%	1.77
bodyy5	0.05	0.2%	0.05	1.6%	2.6%	2.5%	1.77
bodyy6	0.05	0.3%	0.05	1.3%	1.8%	1.8%	1.76
raefsky4	0.20	2.7%	0.21	8.0%	8.3%	8.3%	2.20
LFAT5000	0.00	0.0%	0.00	0.1%	0.1%	0.1%	1.47
LF10000	0.00	0.0%	0.00	0.0%	0.0%	0.0%	1.45
t3dl_e	0.00	0.0%	0.00	0.0%	0.0%	0.0%	3.62
msc23052	0.16	2.7%	0.14	6.3%	7.4%	7.3%	2.38
bcsstk36	0.16	3.0%	0.15	6.2%	8.5%	8.4%	2.22
crystm03	0.10	2.8%	0.10	5.5%	4.5%	4.5%	1.52
smt	0.35	0.5%	0.31	16.5%	19.2%	13.7%	3.04
thread	0.47	0.0%	0.44	15.8%	21.1%	11.3%	3.05
wathen100	0.07	0.0%	0.07	3.2%	4.6%	3.5%	1.35
ship_001	0.22	2.7%	0.21	10.6%	6.4%	2.3%	2.93
nd12k	0.72	0.4%	0.70	20.6%	13.9%	1.3%	4.47
wathen120	0.07	0.0%	0.06	3.0%	4.2%	3.2%	1.34
obstclae	0.04	0.0%	0.03	0.8%	2.6%	2.6%	1.63
jnlbrng1	0.04	0.0%	0.04	0.3%	1.9%	1.9%	1.62
minsurfo	0.04	0.0%	0.03	0.8%	2.1%	2.1%	1.64
bcsstm39	0.00	0.0%	0.00	0.0%	0.0%	0.0%	3.77
vanbody	0.08	3.5%	0.08	10.3%	8.5%	8.3%	2.15
gridgena	0.04	1.6%	0.04	4.1%	3.7%	3.6%	1.38
cvxbqp1	0.05	0.0%	0.06	2.5%	3.3%	3.3%	1.78
ct20stif	0.13	4.3%	0.13	10.0%	11.2%	10.8%	2.06
crankseg_1	0.35	1.5%	0.30	19.2%	14.3%	2.0%	3.33
nasasrb	0.08	2.9%	0.08	3.3%	3.7%	3.7%	2.21
Andrews	0.23	6.3%	0.26	7.3%	24.6%	23.1%	1.32
crankseg_2	0.35	2.1%	0.29	10.5%	13.1%	4.8%	3.41
Dubcova2	0.05	0.0%	0.05	3.6%	2.8%	1.4%	1.42
qa8fm	0.15	1.8%	0.14	3.9%	4.2%	4.1%	1.46
cfd1	0.09	3.4%	0.09	6.5%	9.3%	9.2%	1.47
nd24k	0.59	0.4%	0.57	13.8%	10.4%	5.0%	4.55
oilpan	0.07	1.0%	0.07	6.2%	5.9%	5.3%	2.15
finan512	0.01	0.0%	0.01	0.0%	0.0%	0.0%	0.98
apache1	0.07	0.0%	0.07	0.5%	3.1%	3.1%	1.70
shallow_water1	0.03	0.0%	0.03	2.2%	2.2%	2.2%	1.61
shallow_water2	0.03	0.0%	0.03	2.6%	2.7%	2.7%	1.61

Table 5.11 – continued from previous page						
	PaToH		*onmetisHP*			
name	cutsize	%LI	cutsize	$exp\%LI_p$	$act\%LI_p$	$act\%LI_c$	speedup
thermal1	0.02	1.6%	0.02	4.3%	4.2%	4.2%	1.56
denormal	0.05	0.0%	0.05	0.7%	2.9%	2.9%	1.46
s3dkt3m2	0.06	0.0%	0.06	1.6%	2.9%	2.8%	2.09
s3dkq4m2	0.07	0.6%	0.06	3.8%	5.0%	5.0%	2.43
m_t1	0.11	3.7%	0.10	9.4%	5.7%	3.8%	3.10
2cubes_sphere	0.18	2.8%	0.19	4.1%	4.6%	1.5%	1.34
thermomech_TK	0.02	2.2%	0.02	4.3%	4.3%	4.3%	1.81
thermomech_TC	0.02	2.4%	0.02	4.9%	4.6%	4.6%	1.84
x104	0.09	2.2%	0.08	8.5%	8.0%	6.3%	2.97
shipsec8	0.11	2.1%	0.10	5.8%	6.7%	6.6%	2.23
ship_003	0.13	3.7%	0.12	8.7%	7.0%	7.0%	2.20
cfd2	0.08	2.2%	0.08	6.6%	7.9%	7.9%	1.43
boneS01	0.12	2.3%	0.11	6.1%	5.8%	5.0%	2.04
shipsec1	0.09	1.5%	0.08	4.9%	4.8%	4.8%	2.38
bmw7st_1	0.05	3.7%	0.05	7.5%	7.8%	7.8%	2.27
Dubcova3	0.05	0.0%	0.04	2.7%	2.7%	0.5%	1.37
bmwcra_1	0.07	5.9%	0.08	8.2%	10.7%	10.7%	2.07
G2_circuit	0.02	0.1%	0.02	4.4%	4.7%	4.7%	1.57
shipsec5	0.08	3.5%	0.08	4.0%	5.6%	5.6%	2.34
thermomech_dM	0.01	1.5%	0.01	4.0%	4.0%	4.0%	2.00
pwtk	0.03	1.4%	0.03	1.3%	1.3%	1.3%	2.47
hood	0.03	2.0%	0.03	3.3%	3.2%	3.0%	2.25
BenElechi1	0.04	0.3%	0.03	4.6%	4.5%	4.5%	2.46
offshore	0.07	2.7%	0.07	4.7%	5.0%	4.1%	1.42
F1	0.08	2.0%	0.07	10.0%	8.7%	6.4%	1.69
msdoor	0.02	1.5%	0.02	4.5%	4.5%	4.4%	2.31
af_2_k101	0.02	0.0%	0.02	0.2%	0.5%	0.5%	1.86
af_5_k101	0.02	0.0%	0.02	0.2%	0.5%	0.5%	1.86
af_1_k101	0.02	0.0%	0.02	0.2%	0.6%	0.6%	1.87
af_4_k101	0.02	0.0%	0.02	0.2%	0.5%	0.5%	1.87
af_3_k101	0.02	0.0%	0.02	0.4%	0.8%	0.8%	1.86
af_0_k101	0.02	0.0%	0.02	0.1%	0.4%	0.4%	1.88
inline_1	0.04	2.3%	0.04	6.8%	7.3%	6.1%	1.85
af_shell8	0.02	0.0%	0.02	0.2%	1.3%	1.3%	1.87
af_shell3	0.02	0.0%	0.02	0.2%	1.3%	1.3%	1.88
af_shell4	0.02	0.0%	0.02	0.4%	1.6%	1.6%	1.88
af_shell7	0.02	0.0%	0.02	0.3%	1.3%	1.3%	1.88
parabolic_fem	0.01	0.0%	0.01	0.5%	1.2%	1.2%	2.01
apache2	0.03	0.0%	0.02	0.1%	0.8%	0.8%	1.59
tmt_sym	0.01	2.0%	0.01	2.0%	2.1%	2.1%	1.50
boneS10	0.02	3.0%	0.02	5.1%	5.3%	5.2%	2.20
ldoor	0.01	2.4%	0.01	4.7%	4.8%	4.7%	2.31
ecology2	0.01	0.0%	0.01	0.0%	0.3%	0.3%	1.46
thermal2	0.01	2.6%	0.01	2.1%	2.1%	2.1%	1.64
G3_circuit	0.01	0.0%	0.01	0.1%	0.3%	0.3%	1.57

Table 5.12: 16-way partitioning performance of the PD matrix collection for cut-net metric with node balancing.

name	PaToH		onmetisHP				speedup
	cutsize	%LI	cutsize	$exp\%LI_p$	$act\%LI_p$	$act\%LI_c$	
msc01050	0.62	3.4%	0.85	109.5%	124.7%	27.8%	0.73
bcsstm08	0.00	1.3%	0.00	1.3%	1.3%	1.3%	3.83
bcsstm09	0.00	0.5%	0.00	0.5%	0.5%	0.5%	3.78
bcsstk09	0.59	3.7%	0.23	15.4%	20.9%	20.2%	0.18
bcsstk10	0.45	3.2%	0.99	422.5%	184.6%	3.3%	0.01
1138_bus	0.11	2.6%	0.02	8.5%	16.5%	15.2%	0.93
bcsstk27	0.71	2.2%	0.64	76.2%	43.1%	37.7%	2.73
mhd1280b	0.14	3.3%	0.11	21.1%	20.6%	17.8%	1.96
plbuckle	0.51	4.5%	0.49	30.1%	24.0%	20.7%	2.10
msc01440	0.65	3.9%	0.62	38.2%	34.1%	30.2%	2.30
bcsstk11	0.50	3.1%	0.51	34.8%	31.2%	28.3%	2.15
bcsstm11	0.00	1.0%	0.00	1.0%	1.0%	1.0%	3.90
bcsstm12	0.34	2.5%	0.35	34.6%	35.3%	33.8%	2.06
bcsstk12	0.49	3.1%	0.51	36.3%	33.0%	30.1%	2.15
ex33	0.30	3.0%	0.29	42.0%	27.2%	26.6%	2.23
bcsstk14	0.59	1.5%	0.57	34.9%	38.9%	28.2%	2.23
ex3	0.56	0.5%	0.54	59.3%	33.0%	7.3%	1.87
nasa1824	0.55	2.3%	0.59	59.7%	41.1%	25.8%	1.86
plat1919	0.41	2.5%	0.42	20.4%	26.4%	23.2%	2.12
bcsstm26	0.00	0.7%	0.00	0.7%	0.7%	0.7%	3.79
bcsstk26	0.38	2.8%	0.39	23.2%	22.0%	18.4%	1.87
bcsstk13	0.78	2.7%	0.85	109.5%	124.7%	27.8%	2.22
nasa2146	0.53	3.1%	0.50	24.6%	28.8%	27.7%	2.17
ex10	0.35	1.2%	0.33	57.5%	25.8%	10.9%	1.82
Chem97ZtZ	0.00	0.4%	0.00	11.5%	11.5%	11.5%	0.73
ex10hs	0.35	1.4%	0.32	55.4%	24.1%	10.8%	1.85
ex13	0.45	0.3%	0.44	30.9%	26.1%	8.4%	1.99
nasa2910	0.68	0.3%	0.74	234.9%	82.5%	12.7%	2.26
bcsstk23	0.63	1.1%	0.68	35.7%	40.7%	22.8%	1.69
bcsstm23	0.00	0.1%	0.00	0.1%	0.1%	0.1%	3.85
mhd3200b	0.02	0.5%	0.02	6.0%	5.2%	4.8%	2.16
bibd_81_2	0.00	0.2%	0.00	0.2%	0.2%	0.2%	3.88
ex9	0.41	0.9%	0.39	13.7%	17.8%	1.9%	1.94
bcsstm24	0.00	0.2%	0.00	0.2%	0.2%	0.2%	3.86
bcsstk24	0.48	2.0%	0.48	26.7%	46.9%	42.0%	2.71
bcsstk21	0.27	0.8%	0.27	3.9%	12.0%	11.5%	1.90
bcsstm21	0.00	0.0%	0.00	0.0%	0.0%	0.0%	3.86
bcsstk15	0.56	2.6%	0.56	30.9%	19.2%	15.8%	1.80
sts4098	0.41	4.8%	0.46	45.7%	34.9%	27.2%	0.97
t2dal_e	0.00	0.4%	0.00	0.4%	0.4%	0.4%	3.91
bcsstk28	0.43	2.3%	0.40	18.3%	30.2%	27.4%	2.72
msc04515	0.27	2.9%	0.27	14.4%	20.1%	19.9%	1.92
nasa4704	0.37	2.8%	0.38	17.7%	20.6%	19.7%	1.78
mhd4800b	0.01	0.6%	0.01	5.5%	4.8%	4.5%	1.94
crystm01	0.32	4.7%	0.31	12.9%	20.4%	20.2%	1.84
bcsstk16	0.60	3.5%	0.59	45.1%	44.2%	38.4%	2.66
s3rmt3m3	0.36	1.0%	0.35	11.1%	19.8%	17.9%	2.46
s3rmt3m1	0.39	0.9%	0.38	7.5%	17.3%	15.5%	2.50
s2rmq4m1	0.42	2.1%	0.38	13.0%	21.9%	21.1%	2.81
s1rmt3m1	0.39	0.7%	0.38	7.6%	16.5%	14.9%	2.51
s1rmq4m1	0.42	2.3%	0.38	11.0%	19.7%	19.1%	2.80
s2rmt3m1	0.39	0.7%	0.38	8.8%	18.1%	16.4%	2.48
s3rmq4m1	0.41	2.2%	0.38	10.8%	20.4%	19.8%	2.81
ex15	0.15	2.6%	0.15	7.3%	9.2%	9.2%	2.01
Kuu	0.41	0.1%	0.39	17.0%	24.9%	1.1%	1.94
Muu	0.26	0.1%	0.26	11.2%	14.2%	1.7%	1.46

Table 5.12 – continued from previous page

name	PaToH		onmetisHP				
	cutsize	%LI	cutsize	$exp\%LI_p$	$act\%LI_p$	$act\%LI_c$	speedup
bcsstk38	0.41	3.2%	0.40	23.9%	38.8%	34.5%	1.85
aft01	0.20	0.2%	0.19	11.0%	12.3%	8.1%	1.56
fv1	0.13	3.0%	0.12	2.4%	5.8%	5.8%	2.14
fv3	0.13	2.9%	0.12	4.6%	4.0%	4.0%	2.15
fv2	0.13	3.0%	0.12	4.6%	3.7%	3.7%	2.14
bundle1	0.80	1.8%	0.99	422.5%	184.6%	3.3%	0.31
ted_B	0.04	0.4%	0.04	1.9%	1.7%	0.2%	1.11
ted_B_unscaled	0.04	0.2%	0.04	1.8%	2.6%	0.2%	1.12
msc10848	0.56	0.1%	0.52	43.6%	59.1%	40.2%	3.27
bcsstk17	0.28	2.8%	0.26	15.7%	16.5%	16.0%	2.24
t2dah_e	0.18	0.1%	0.16	8.1%	8.6%	5.6%	1.68
bcsstk18	0.23	4.9%	0.23	15.4%	20.9%	20.2%	1.37
cbuckle	0.29	2.0%	0.27	13.0%	11.6%	11.5%	2.47
crystm02	0.23	4.5%	0.22	8.8%	12.1%	12.1%	1.67
Pres_Poisson	0.28	2.5%	0.25	9.3%	13.2%	13.2%	2.50
bcsstm25	0.00	0.0%	0.00	0.0%	0.0%	0.0%	3.82
bcsstk25	0.29	1.4%	0.31	10.1%	10.0%	9.4%	1.40
Dubcova1	0.16	0.1%	0.14	8.9%	4.1%	0.4%	1.60
olafu	0.26	2.9%	0.23	20.3%	16.1%	15.9%	2.69
gyro_m	0.08	2.5%	0.06	11.0%	11.9%	9.8%	1.23
gyro	0.23	1.6%	0.17	20.5%	44.6%	37.7%	1.81
bodyy4	0.09	1.6%	0.09	3.5%	3.9%	3.8%	1.97
bodyy5	0.09	0.5%	0.09	3.4%	4.3%	4.2%	1.98
bodyy6	0.09	1.1%	0.09	3.9%	4.1%	4.0%	1.97
raefsky4	0.35	3.1%	0.34	23.4%	14.5%	14.4%	2.40
LFAT5000	0.00	0.1%	0.00	0.3%	0.3%	0.3%	1.58
LF10000	0.00	0.0%	0.00	0.0%	0.1%	0.1%	1.58
t3dl_e	0.00	0.0%	0.00	0.0%	0.0%	0.0%	3.87
msc23052	0.25	2.8%	0.23	13.1%	13.3%	13.1%	2.61
bcsstk36	0.24	3.4%	0.23	9.9%	13.6%	13.4%	2.43
crystm03	0.18	3.3%	0.18	7.4%	10.8%	10.8%	1.66
smt	0.53	0.5%	0.50	39.4%	35.2%	23.3%	3.38
thread	0.63	0.0%	0.60	26.3%	30.5%	16.7%	3.32
wathen100	0.11	0.0%	0.10	4.8%	7.3%	5.5%	1.47
ship_001	0.44	1.5%	0.43	22.2%	20.6%	10.8%	3.28
nd12k	0.89	0.1%	0.91	174.9%	68.0%	13.9%	4.96
wathen120	0.10	0.0%	0.09	4.6%	6.7%	5.1%	1.45
obstclae	0.06	0.0%	0.05	4.6%	4.9%	4.9%	1.77
jnlbrng1	0.06	0.0%	0.05	2.9%	3.8%	3.8%	1.76
minsurfo	0.06	0.1%	0.05	3.6%	4.7%	4.7%	1.77
bcsstm39	0.00	0.0%	0.00	0.0%	0.0%	0.0%	3.98
vanbody	0.13	4.4%	0.12	13.3%	14.2%	13.9%	2.36
gridgena	0.07	1.2%	0.07	6.5%	6.8%	6.7%	1.50
cvxbqp1	0.07	1.7%	0.09	4.5%	4.5%	4.4%	1.88
ct20stif	0.19	4.0%	0.18	13.9%	18.8%	18.1%	2.23
crankseg_1	0.56	0.1%	0.47	36.3%	28.4%	10.5%	3.63
nasasrb	0.16	2.6%	0.16	6.0%	7.0%	7.0%	2.42
Andrews	0.35	6.8%	0.38	19.0%	27.2%	24.3%	1.42
crankseg_2	0.54	1.6%	0.45	30.9%	33.6%	15.0%	3.74
Dubcova2	0.08	0.0%	0.07	4.9%	3.1%	0.8%	1.51
qa8fm	0.21	3.5%	0.20	7.3%	7.9%	7.8%	1.54
cfd1	0.15	4.2%	0.15	9.8%	16.2%	16.2%	1.54
nd24k	0.78	0.3%	0.77	59.0%	35.2%	18.2%	5.06
oilpan	0.13	1.1%	0.12	6.4%	7.0%	5.9%	2.34
finan512	0.02	0.1%	0.02	0.0%	0.0%	0.0%	1.02
apache1	0.11	0.0%	0.11	5.5%	6.4%	6.4%	1.79
shallow_water1	0.04	0.0%	0.04	5.8%	5.5%	5.5%	1.72
shallow_water2	0.04	0.0%	0.04	5.3%	5.2%	5.1%	1.72

Table 5.12 – continued from previous page

name	PaToH		onmetisHP				speedup
	cutsize	%LI	cutsize	$exp\%LI_p$	$act\%LI_p$	$act\%LI_c$	
thermal1	0.04	1.9%	0.04	7.1%	7.0%	7.0%	1.67
denormal	0.08	0.1%	0.07	3.5%	4.2%	4.2%	1.56
s3dkt3m2	0.10	0.1%	0.10	2.4%	4.4%	4.3%	2.27
s3dkq4m2	0.11	1.4%	0.10	5.7%	7.8%	7.8%	2.68
m_t1	0.20	2.5%	0.18	11.9%	14.0%	10.6%	3.41
2cubes_sphere	0.25	2.0%	0.26	6.7%	6.8%	1.5%	1.43
thermomech_TK	0.03	2.0%	0.03	8.0%	7.2%	7.1%	1.91
thermomech_TC	0.03	2.4%	0.03	8.6%	7.8%	7.8%	1.92
x104	0.15	1.6%	0.14	14.0%	13.9%	11.1%	3.25
shipsec8	0.16	2.6%	0.16	8.4%	9.6%	9.5%	2.44
ship_003	0.22	3.4%	0.21	12.3%	10.8%	10.5%	2.41
cfd2	0.13	2.8%	0.12	8.8%	9.9%	9.9%	1.50
boneS01	0.18	2.6%	0.17	10.4%	10.6%	9.2%	2.23
shipsec1	0.14	2.1%	0.13	7.8%	9.1%	9.0%	2.57
bmw7st_1	0.09	3.4%	0.08	8.4%	9.9%	9.8%	2.48
Dubcova3	0.08	0.0%	0.10	8.3%	7.5%	2.6%	1.45
bmwcra_1	0.18	6.0%	0.17	20.3%	15.4%	15.4%	2.19
G2_circuit	0.04	0.0%	0.04	4.3%	5.1%	5.1%	1.64
shipsec5	0.12	3.0%	0.11	8.5%	9.9%	9.9%	2.54
thermomech_dM	0.02	1.6%	0.02	6.7%	6.4%	6.4%	2.04
pwtk	0.06	1.8%	0.05	4.9%	5.5%	5.5%	2.68
hood	0.05	1.9%	0.05	6.4%	6.1%	5.7%	2.40
BenElechi1	0.06	1.2%	0.06	6.5%	7.0%	7.0%	2.66
offshore	0.11	4.5%	0.11	9.0%	8.3%	6.7%	1.46
F1	0.14	1.5%	0.14	13.2%	12.4%	7.6%	1.75
msdoor	0.03	2.3%	0.03	6.2%	6.5%	6.3%	2.47
af_2_k101	0.04	0.0%	0.04	0.8%	1.3%	1.3%	1.98
af_5_k101	0.04	0.0%	0.04	1.2%	1.3%	1.3%	1.99
af_1_k101	0.04	0.0%	0.04	1.0%	1.4%	1.4%	1.99
af_4_k101	0.04	0.0%	0.04	0.5%	1.1%	1.0%	1.99
af_3_k101	0.04	0.0%	0.04	1.1%	1.6%	1.6%	1.99
af_0_k101	0.04	0.0%	0.04	1.4%	1.9%	1.9%	1.99
inline_1	0.07	1.9%	0.07	9.9%	10.5%	8.5%	1.95
af_shell8	0.03	0.0%	0.03	1.5%	2.7%	2.6%	1.98
af_shell3	0.03	0.0%	0.03	1.6%	2.8%	2.8%	1.99
af_shell4	0.03	0.0%	0.03	1.4%	2.3%	2.3%	1.99
af_shell7	0.03	0.0%	0.03	2.4%	3.3%	3.3%	1.98
parabolic_fem	0.02	0.0%	0.02	2.8%	3.4%	3.4%	2.02
apache2	0.04	0.0%	0.04	0.9%	2.5%	2.5%	1.64
tmt_sym	0.02	2.5%	0.02	3.9%	3.8%	3.8%	1.54
boneS10	0.04	2.7%	0.03	8.3%	8.2%	8.1%	2.36
ldoor	0.02	2.6%	0.02	7.1%	7.0%	7.0%	2.50
ecology2	0.01	0.0%	0.01	0.1%	0.6%	0.6%	1.51
thermal2	0.01	2.5%	0.01	3.4%	3.4%	3.4%	1.70
G3_circuit	0.01	0.0%	0.01	1.9%	2.1%	2.1%	1.61

Table 5.13: 32-way partitioning performance of the PD matrix collection for cut-net metric with node balancing.

name	PaToH		onmetisHP				speedup
	cutsize	%LI	cutsize	$exp\%LI_p$	$act\%LI_p$	$act\%LI_c$	
ex33	0.48	2.7%	0.45	65.2%	42.3%	39.0%	2.12
bcsstk14	0.84	1.9%	0.86	193.9%	124.4%	40.0%	2.14
ex3	0.76	0.9%	0.76	157.9%	84.5%	31.6%	1.88
nasa1824	0.68	2.9%	0.72	115.3%	82.6%	41.5%	1.86
plat1919	0.62	2.8%	0.64	60.0%	43.5%	31.4%	1.99
bcsstm26	0.00	1.6%	0.00	1.6%	1.6%	1.6%	3.99
bcsstk26	0.54	3.3%	0.55	60.9%	57.0%	42.2%	1.79
bcsstk13	0.86	2.8%	0.93	366.2%	442.3%	103.5%	2.24
nasa2146	0.75	2.5%	0.70	63.0%	48.8%	42.3%	2.11
ex10	0.55	1.9%	0.56	164.2%	59.2%	25.1%	1.83
Chem97ZtZ	0.02	3.0%	0.05	39.6%	35.1%	30.9%	0.79
ex10hs	0.56	1.1%	0.55	152.1%	62.6%	29.4%	1.86
ex13	0.69	0.5%	0.69	120.2%	57.8%	18.6%	1.98
nasa2910	0.83	0.5%	0.93	440.5%	286.0%	24.4%	2.40
bcsstm23	0.00	0.1%	0.00	0.1%	0.1%	0.1%	3.99
bcsstk23	0.75	1.5%	0.81	61.5%	72.1%	25.5%	1.75
mhd3200b	0.05	0.9%	0.04	7.8%	6.2%	5.3%	2.40
bibd_81_2	0.00	0.7%	0.00	0.7%	0.7%	0.7%	4.08
ex9	0.63	1.0%	0.64	83.1%	46.2%	14.5%	2.03
bcsstm24	0.00	0.6%	0.00	0.6%	0.6%	0.6%	4.02
bcsstk24	0.69	1.6%	0.65	77.2%	77.4%	61.5%	2.70
bcsstk21	0.41	1.8%	0.42	10.0%	21.4%	19.8%	1.94
bcsstm21	0.00	0.4%	0.00	0.4%	0.4%	0.4%	4.05
bcsstk15	0.75	3.1%	0.80	95.6%	44.2%	22.1%	1.90
sts4098	0.56	3.1%	0.62	98.2%	103.0%	75.4%	1.17
t2dal_e	0.00	0.7%	0.00	0.7%	0.7%	0.7%	4.08
bcsstk28	0.63	2.8%	0.60	69.9%	60.5%	52.2%	2.85
msc04515	0.42	3.0%	0.41	32.7%	31.4%	30.4%	2.02
nasa4704	0.52	2.9%	0.55	66.5%	39.6%	33.2%	1.85
mhd4800b	0.03	0.6%	0.03	7.0%	5.8%	5.2%	2.23
crystm01	0.50	4.7%	0.51	79.9%	36.5%	33.7%	1.95
bcsstk16	0.77	2.8%	0.75	118.0%	85.0%	60.9%	2.80
s3rmt3m3	0.53	1.3%	0.52	32.9%	35.5%	29.6%	2.54
s2rmq4m1	0.63	2.2%	0.60	48.1%	36.2%	33.6%	2.90
s1rmq4m1	0.63	2.0%	0.59	50.1%	37.7%	34.5%	2.91
s1rmt3m1	0.57	1.2%	0.56	25.1%	27.8%	22.3%	2.56
s2rmt3m1	0.57	1.0%	0.56	24.8%	33.4%	27.7%	2.54
s3rmq4m1	0.63	2.2%	0.59	50.6%	43.0%	40.1%	2.92
s3rmt3m1	0.57	1.2%	0.56	28.7%	31.7%	25.7%	2.55
ex15	0.25	2.4%	0.24	22.1%	19.9%	19.5%	2.19
Kuu	0.60	0.6%	0.60	112.5%	47.7%	2.8%	2.08
Muu	0.40	0.3%	0.39	25.1%	29.4%	6.0%	1.56
bcsstk38	0.56	2.5%	0.56	52.0%	56.1%	43.7%	1.97
aft01	0.31	0.4%	0.28	16.2%	17.8%	11.4%	1.68
fv1	0.20	3.0%	0.20	7.9%	10.6%	10.6%	2.22
fv3	0.20	2.5%	0.20	8.5%	8.7%	8.7%	2.21
fv2	0.20	2.5%	0.20	7.8%	8.4%	8.4%	2.21
bundle1	0.98	1.8%	1.00	921.9%	475.2%	81.6%	0.34
ted_B	0.09	0.5%	0.08	7.2%	11.3%	5.3%	1.20
ted_B_unscaled	0.09	0.5%	0.08	7.0%	10.8%	4.9%	1.20
msc10848	0.74	0.1%	0.73	166.9%	99.5%	49.7%	3.56
bcsstk17	0.44	3.4%	0.42	34.3%	24.6%	23.1%	2.38
t2dah_e	0.26	0.2%	0.24	11.8%	11.5%	6.7%	1.77
bcsstk18	0.32	4.2%	0.34	25.0%	30.8%	28.0%	1.46
cbuckle	0.43	2.8%	0.39	18.5%	13.5%	13.3%	2.63
crystm02	0.36	4.3%	0.35	24.7%	26.6%	26.5%	1.77

Table 5.13 – continued from previous page

| name | PaToH | | onmetisHP | | | | speedup |
	cutsize	%LI	cutsize	$exp\%LI_p$	$act\%LI_p$	$act\%LI_c$	
Pres_Poisson	0.41	2.8%	0.38	14.7%	19.4%	19.3%	2.67
bcsstk25	0.42	1.9%	0.44	17.7%	20.4%	17.4%	1.51
bcsstm25	0.00	0.1%	0.00	0.1%	0.1%	0.1%	3.98
Dubcova1	0.25	0.1%	0.23	10.9%	7.4%	0.6%	1.70
olafu	0.41	3.1%	0.37	44.9%	32.3%	31.5%	2.87
gyro_m	0.15	2.0%	0.13	22.2%	28.0%	23.0%	1.29
gyro	0.39	1.7%	0.36	68.9%	78.4%	56.1%	1.94
bodyy4	0.14	1.4%	0.14	7.0%	7.5%	7.3%	2.06
bodyy5	0.14	1.3%	0.14	4.8%	5.4%	5.3%	2.06
bodyy6	0.14	1.2%	0.13	5.4%	6.4%	6.2%	2.14
raefsky4	0.52	3.3%	0.50	50.4%	30.7%	29.9%	2.60
LFAT5000	0.01	0.1%	0.00	0.6%	0.5%	0.5%	1.71
LF10000	0.01	0.2%	0.01	0.3%	0.4%	0.4%	1.69
t3dl_e	0.00	0.1%	0.00	0.1%	0.1%	0.1%	4.02
bcsstk36	0.36	2.9%	0.34	18.3%	21.4%	20.5%	2.57
msc23052	0.36	2.7%	0.34	15.9%	22.5%	21.8%	2.77
crystm03	0.29	4.5%	0.27	14.2%	22.0%	21.9%	1.76
smt	0.70	0.2%	0.66	82.9%	66.6%	41.0%	3.70
thread	0.76	0.0%	0.74	89.9%	58.5%	32.8%	3.52
wathen100	0.18	0.1%	0.16	5.2%	7.8%	4.7%	1.54
ship_001	0.63	1.4%	0.62	75.6%	42.6%	21.5%	3.52
nd12k	0.97	0.1%	0.99	298.0%	162.8%	0.3%	5.05
wathen120	0.16	0.3%	0.14	7.9%	10.2%	7.5%	1.55
obstclae	0.09	0.5%	0.08	6.0%	6.2%	6.2%	1.93
jnlbrng1	0.09	0.6%	0.08	5.6%	6.6%	6.6%	1.91
minsurfo	0.09	1.1%	0.08	5.6%	5.9%	5.9%	1.93
bcsstm39	0.00	0.0%	0.00	0.0%	0.0%	0.0%	4.14
vanbody	0.22	4.2%	0.21	19.1%	21.9%	21.3%	2.46
gridgena	0.11	1.4%	0.11	8.7%	9.2%	9.0%	1.63
cvxbqp1	0.10	2.0%	0.12	7.7%	7.3%	7.3%	1.97
ct20stif	0.27	3.3%	0.25	20.4%	26.1%	25.0%	2.39
crankseg_1	0.72	0.1%	0.66	117.3%	65.7%	26.1%	3.86
nasasrb	0.24	3.1%	0.23	9.6%	11.1%	11.0%	2.60
Andrews	0.50	6.1%	0.54	46.7%	38.2%	30.1%	1.46
crankseg_2	0.70	0.0%	0.63	133.7%	57.6%	25.4%	3.97
Dubcova2	0.13	0.0%	0.12	8.1%	5.0%	0.7%	1.57
qa8fm	0.32	3.6%	0.31	11.8%	20.4%	20.3%	1.63
cfd1	0.27	4.5%	0.27	19.0%	24.9%	24.8%	1.62
nd24k	0.89	0.2%	0.93	258.0%	97.6%	26.5%	5.39
oilpan	0.20	1.5%	0.19	12.6%	12.2%	10.5%	2.50
finan512	0.03	0.3%	0.03	0.0%	0.0%	0.0%	1.06
apache1	0.17	0.8%	0.16	9.2%	10.5%	10.5%	1.90
shallow_water2	0.06	0.0%	0.06	6.3%	6.3%	6.3%	1.84
shallow_water1	0.06	0.7%	0.06	7.6%	7.5%	7.5%	1.83
thermal1	0.06	1.9%	0.06	9.2%	9.5%	9.5%	1.77
denormal	0.12	0.6%	0.11	6.0%	8.0%	8.0%	1.66
s3dkt3m2	0.15	0.7%	0.15	5.0%	6.9%	6.6%	2.42
s3dkq4m2	0.17	1.5%	0.15	5.8%	8.5%	8.5%	2.84
m_t1	0.29	1.4%	0.28	12.4%	18.1%	12.2%	3.67
2cubes_sphere	0.34	1.5%	0.34	11.4%	10.2%	4.3%	1.48
thermomech_TC	0.05	1.8%	0.05	8.8%	9.3%	9.3%	1.99
thermomech_TK	0.05	2.2%	0.05	10.1%	10.1%	10.1%	1.99
x104	0.24	1.2%	0.22	18.0%	22.1%	17.0%	3.44
shipsec8	0.23	2.5%	0.22	13.6%	14.5%	14.2%	2.58
ship_003	0.31	3.0%	0.29	13.6%	14.4%	13.8%	2.53
cfd2	0.20	3.0%	0.19	13.3%	14.5%	14.5%	1.57
boneS01	0.25	2.7%	0.23	12.2%	17.6%	15.5%	2.35
shipsec1	0.20	2.7%	0.19	10.4%	14.5%	14.5%	2.75

Table 5.13 – continued from previous page

| name | PaToH | | onmetisHP | | | | |
	cutsize	%LI	cutsize	$exp\%LI_p$	$act\%LI_p$	$act\%LI_c$	speedup
bmw7st_1	0.13	3.3%	0.12	13.4%	15.8%	15.7%	2.63
Dubcova3	0.12	0.0%	0.10	7.2%	6.8%	1.5%	1.49
bmwcra_1	0.28	5.4%	0.27	20.0%	20.1%	19.9%	2.32
G2_circuit	0.06	0.4%	0.06	6.6%	7.8%	7.8%	1.71
shipsec5	0.17	3.2%	0.16	9.7%	12.0%	12.0%	2.68
thermomech_dM	0.03	2.2%	0.03	8.8%	8.7%	8.7%	2.08
pwtk	0.12	1.9%	0.11	10.1%	9.4%	9.4%	2.84
hood	0.09	1.6%	0.08	11.2%	11.2%	10.4%	2.54
BenElechi1	0.10	1.4%	0.09	8.1%	8.3%	8.3%	2.83
offshore	0.16	3.0%	0.17	12.1%	11.3%	8.8%	1.49
F1	0.22	0.9%	0.22	20.3%	18.3%	10.1%	1.79
msdoor	0.05	2.1%	0.05	9.2%	9.7%	9.4%	2.60
af_4_k101	0.06	0.1%	0.06	4.4%	4.5%	4.4%	2.09
af_0_k101	0.06	0.3%	0.06	4.0%	3.7%	3.7%	2.10
af_5_k101	0.06	0.1%	0.06	4.5%	4.7%	4.7%	2.09
af_1_k101	0.06	0.2%	0.06	3.0%	3.8%	3.7%	2.10
af_2_k101	0.06	0.2%	0.06	4.2%	4.2%	4.2%	2.09
af_3_k101	0.06	0.2%	0.06	4.4%	4.4%	4.4%	2.10
inline_1	0.12	1.7%	0.11	13.9%	14.1%	10.6%	2.01
af_shell8	0.06	0.1%	0.05	4.4%	4.8%	4.7%	2.08
af_shell3	0.06	0.3%	0.05	3.3%	4.3%	4.2%	2.10
af_shell7	0.06	0.3%	0.05	5.1%	5.3%	5.3%	2.11
af_shell4	0.06	0.3%	0.05	4.4%	5.2%	5.2%	2.08
parabolic_fem	0.03	0.0%	0.03	5.0%	5.3%	5.3%	2.04
apache2	0.06	0.0%	0.06	4.3%	5.0%	5.0%	1.68
tmt_sym	0.02	2.4%	0.02	6.5%	6.2%	6.2%	1.60
boneS10	0.06	3.2%	0.05	12.1%	12.3%	12.1%	2.44
ldoor	0.04	2.4%	0.04	8.2%	8.2%	8.0%	2.60
ecology2	0.02	0.0%	0.02	0.7%	1.2%	1.2%	1.55
thermal2	0.02	2.3%	0.02	4.9%	4.7%	4.7%	1.78
G3_circuit	0.02	0.3%	0.02	5.4%	5.1%	5.1%	1.64

Table 5.14: 64-way partitioning performance of the PD matrix collection for cut-net metric with node balancing.

	PaToH		onmetisHP				
name	cutsize	%LI	cutsize	$exp\%LI_p$	$act\%LI_p$	$act\%LI_c$	speedup
bcsstk13	0.94	1.8%	0.98	375.6%	664.8%	78.3%	3.06
Chem97ZtZ	0.20	3.5%	0.20	79.2%	55.2%	33.9%	0.93
mhd3200b	0.09	1.2%	0.08	13.4%	10.1%	8.1%	2.46
bibd_81_2	0.00	0.7%	0.00	0.7%	0.7%	0.7%	4.19
ex9	0.81	1.3%	0.81	222.1%	99.3%	31.1%	2.02
bcsstm24	0.00	0.6%	0.00	0.6%	0.6%	0.6%	4.14
bcsstk24	0.87	1.5%	0.85	307.7%	191.4%	98.9%	2.73
bcsstm21	0.00	1.3%	0.00	1.3%	1.3%	1.3%	4.19
bcsstk21	0.58	2.0%	0.61	34.4%	33.1%	25.6%	1.89
bcsstk15	0.92	2.7%	0.94	401.2%	157.2%	36.0%	1.94
sts4098	0.67	11.3%	0.72	156.6%	271.8%	175.8%	1.18
t2dal_e	0.00	0.7%	0.00	0.7%	0.7%	0.7%	4.23
bcsstk28	0.86	2.3%	0.80	225.7%	121.0%	69.8%	2.81
msc04515	0.61	2.8%	0.59	70.9%	61.4%	57.2%	1.96
nasa4704	0.65	2.8%	0.67	113.0%	82.1%	62.0%	1.86
mhd4800b	0.06	1.6%	0.06	10.1%	8.7%	7.4%	2.38
crystm01	0.72	4.7%	0.74	114.6%	59.7%	45.9%	1.97
bcsstk16	0.91	2.2%	0.91	420.4%	214.2%	76.9%	2.87
s3rmt3m3	0.73	1.5%	0.69	92.7%	83.6%	61.4%	2.53
s2rmq4m1	0.83	2.3%	0.78	121.7%	72.0%	58.1%	2.93
s1rmt3m1	0.77	1.4%	0.75	93.8%	67.6%	45.1%	2.53
s1rmq4m1	0.83	2.4%	0.77	134.6%	72.0%	58.9%	2.91
s3rmt3m1	0.77	1.4%	0.75	94.5%	73.7%	50.2%	2.52
s3rmq4m1	0.83	1.9%	0.77	130.1%	75.6%	61.0%	2.92
s2rmt3m1	0.77	1.4%	0.75	93.1%	75.0%	53.0%	2.53
ex15	0.40	2.9%	0.39	42.1%	32.4%	31.2%	2.25
Muu	0.59	0.9%	0.60	84.1%	52.2%	5.8%	1.60
Kuu	0.77	0.9%	0.79	248.7%	112.5%	14.5%	2.17
bcsstk38	0.72	2.5%	0.73	165.1%	111.9%	68.5%	2.08
aft01	0.45	0.8%	0.43	27.5%	27.7%	16.8%	1.69
fv1	0.29	3.3%	0.28	14.5%	14.6%	14.4%	2.43
fv3	0.29	3.2%	0.28	11.6%	12.8%	12.6%	2.42
fv2	0.29	3.1%	0.28	12.2%	12.9%	12.8%	2.41
bundle1	1.00	2.9%	1.00	1458.9%	974.9%	258.9%	0.31
ted_B	0.18	1.2%	0.16	21.8%	51.2%	35.1%	1.26
ted_B_unscaled	0.18	1.1%	0.16	20.3%	47.7%	31.8%	1.25
msc10848	0.88	0.2%	0.91	592.1%	238.4%	73.4%	3.64
bcsstk17	0.61	3.2%	0.62	86.9%	53.3%	44.7%	2.47
t2dah_e	0.39	0.9%	0.37	15.5%	17.6%	9.3%	1.89
bcsstk18	0.44	4.9%	0.47	80.7%	56.4%	42.7%	1.50
cbuckle	0.60	2.9%	0.56	36.0%	32.5%	31.4%	2.81
crystm02	0.54	4.9%	0.54	49.6%	52.2%	49.9%	1.89
Pres_Poisson	0.60	3.6%	0.57	42.2%	32.1%	31.0%	2.81
bcsstk25	0.54	2.2%	0.57	50.0%	37.0%	28.4%	1.62
bcsstm25	0.00	0.3%	0.00	0.3%	0.3%	0.3%	4.09
Dubcova1	0.36	0.3%	0.32	15.2%	13.6%	2.9%	1.81
olafu	0.60	3.0%	0.57	106.8%	66.4%	56.0%	3.05
gyro	0.57	1.1%	0.60	301.4%	118.4%	57.0%	2.09
gyro_m	0.31	2.6%	0.30	61.5%	55.1%	39.7%	1.37
bodyy4	0.20	1.7%	0.20	9.1%	9.2%	8.8%	2.18
bodyy5	0.20	1.5%	0.20	8.6%	8.5%	8.1%	2.20
bodyy6	0.20	1.3%	0.20	8.2%	7.8%	7.4%	2.26
raefsky4	0.69	3.6%	0.68	138.1%	61.1%	51.4%	2.77
LFAT5000	0.01	0.1%	0.01	0.9%	0.8%	0.8%	1.89
LF10000	0.01	0.5%	0.01	0.7%	1.0%	1.0%	1.85
t3dl_e	0.00	0.3%	0.00	0.3%	0.3%	0.3%	4.14

Table 5.14 – continued from previous page

name	PaToH		onmetisHP				speedup
	cutsize	%LI	cutsize	$exp\%LI_p$	$act\%LI_p$	$act\%LI_c$	
bcsstk36	0.49	3.2%	0.47	35.2%	34.1%	31.7%	2.70
msc23052	0.49	2.4%	0.47	36.0%	32.4%	29.9%	2.90
crystm03	0.45	4.8%	0.43	24.6%	36.2%	35.8%	1.85
smt	0.85	0.1%	0.87	394.0%	136.6%	50.4%	3.83
thread	0.86	0.3%	0.89	313.3%	112.3%	38.5%	3.72
wathen100	0.26	0.2%	0.22	6.5%	8.7%	4.3%	1.61
ship_001	0.79	1.2%	0.81	367.6%	107.1%	41.9%	3.72
nd12k	0.99	0.3%	1.00	459.7%	461.2%	2.2%	5.13
wathen120	0.24	0.3%	0.20	8.6%	10.5%	6.6%	1.59
obstclae	0.12	1.5%	0.12	8.0%	8.6%	8.5%	2.06
jnlbrng1	0.12	1.4%	0.12	8.9%	9.3%	9.3%	2.06
minsurfo	0.12	1.4%	0.12	8.6%	9.4%	9.4%	2.06
bcsstm39	0.00	0.0%	0.00	0.0%	0.0%	0.0%	4.22
vanbody	0.33	3.6%	0.32	32.6%	30.4%	28.8%	2.58
gridgena	0.17	1.8%	0.16	10.0%	12.7%	12.3%	1.76
cvxbqp1	0.13	2.3%	0.16	11.3%	12.6%	12.3%	2.03
ct20stif	0.37	3.0%	0.35	30.4%	48.1%	45.5%	2.50
crankseg_1	0.83	0.0%	0.86	522.3%	120.2%	23.3%	4.02
nasasrb	0.34	3.0%	0.31	14.9%	17.8%	17.6%	2.72
Andrews	0.65	5.0%	0.70	66.3%	53.6%	31.2%	1.50
crankseg_2	0.80	0.2%	0.84	482.2%	123.2%	32.1%	4.19
Dubcova2	0.19	0.0%	0.16	10.7%	6.0%	0.4%	1.65
qa8fm	0.42	4.3%	0.40	15.5%	27.8%	27.5%	1.73
cfd1	0.40	5.0%	0.39	22.7%	27.3%	27.1%	1.69
nd24k	0.97	0.8%	0.99	600.6%	273.2%	8.7%	5.54
oilpan	0.29	1.8%	0.28	15.0%	16.5%	13.5%	2.62
finan512	0.16	1.4%	0.12	5.0%	5.3%	1.8%	1.14
apache1	0.24	1.8%	0.23	12.2%	13.2%	13.1%	2.02
shallow_water2	0.08	0.7%	0.08	7.3%	6.9%	6.8%	1.98
shallow_water1	0.08	1.2%	0.08	7.2%	6.8%	6.7%	1.98
thermal1	0.09	2.3%	0.09	10.9%	10.8%	10.8%	1.91
denormal	0.17	1.8%	0.15	9.7%	10.9%	10.9%	1.78
s3dkt3m2	0.23	0.6%	0.22	6.8%	8.6%	8.1%	2.57
s3dkq4m2	0.26	1.9%	0.22	10.4%	11.6%	11.6%	3.00
m_t1	0.42	1.4%	0.39	25.8%	29.1%	20.0%	3.88
2cubes_sphere	0.43	1.4%	0.44	18.5%	17.6%	9.0%	1.54
thermomech_TK	0.08	2.4%	0.08	12.3%	12.0%	11.9%	2.07
thermomech_TC	0.08	2.2%	0.08	12.8%	12.7%	12.7%	2.07
x104	0.34	1.1%	0.33	29.4%	31.2%	22.8%	3.63
shipsec8	0.32	2.6%	0.31	22.5%	23.1%	22.5%	2.71
ship_003	0.41	2.4%	0.40	22.4%	23.8%	22.4%	2.66
cfd2	0.29	3.7%	0.27	19.7%	21.0%	20.9%	1.66
boneS01	0.33	2.5%	0.31	17.4%	27.3%	24.2%	2.47
shipsec1	0.27	2.5%	0.26	15.5%	19.1%	18.9%	2.83
bmw7st_1	0.20	3.6%	0.19	18.9%	21.4%	21.2%	2.75
Dubcova3	0.18	0.1%	0.14	10.3%	8.6%	1.5%	1.54
bmwcra_1	0.39	4.8%	0.38	27.7%	34.9%	34.3%	2.44
G2_circuit	0.10	1.0%	0.10	9.0%	9.1%	9.0%	1.81
shipsec5	0.25	3.2%	0.24	18.9%	18.7%	18.6%	2.81
thermomech_dM	0.05	1.9%	0.05	11.0%	11.1%	11.1%	2.13
pwtk	0.18	1.7%	0.16	10.7%	9.5%	9.5%	2.99
hood	0.14	1.6%	0.14	15.3%	14.9%	13.3%	2.67
BenElechi1	0.15	1.4%	0.13	10.9%	11.8%	11.8%	2.96
offshore	0.23	3.3%	0.23	17.2%	18.6%	14.5%	1.51
F1	0.31	0.4%	0.31	25.2%	28.1%	15.3%	1.84
msdoor	0.08	2.7%	0.08	12.0%	13.1%	12.7%	2.70
af_2_k101	0.09	0.5%	0.09	5.6%	5.8%	5.8%	2.19
af_3_k101	0.09	0.6%	0.09	5.1%	6.0%	5.9%	2.20

name	PaToH		onmetisHP				speedup
	cutsize	%LI	cutsize	$exp\%LI_p$	$act\%LI_p$	$act\%LI_c$	
af_5_k101	0.09	1.0%	0.09	5.6%	6.3%	6.2%	2.17
af_0_k101	0.09	0.4%	0.09	5.9%	6.0%	5.9%	2.17
af_1_k101	0.09	0.7%	0.09	6.2%	6.7%	6.7%	2.20
af_4_k101	0.09	0.5%	0.09	5.7%	6.2%	6.1%	2.17
inline_1	0.18	1.0%	0.17	15.8%	18.5%	13.0%	2.04
af_shell4	0.09	0.7%	0.08	6.3%	6.3%	6.3%	2.18
af_shell7	0.09	1.0%	0.08	5.8%	6.2%	6.2%	2.19
af_shell8	0.09	0.9%	0.08	6.3%	6.9%	6.8%	2.18
af_shell3	0.09	0.7%	0.08	5.5%	6.4%	6.3%	2.18
parabolic_fem	0.04	0.2%	0.04	6.8%	7.0%	6.9%	2.05
apache2	0.09	0.3%	0.08	7.7%	8.1%	8.1%	1.74
tmt_sym	0.03	2.2%	0.03	9.6%	9.6%	9.5%	1.63
boneS10	0.08	3.3%	0.08	16.5%	16.1%	15.8%	2.50
ldoor	0.06	2.2%	0.06	11.3%	11.2%	10.9%	2.67
ecology2	0.03	0.0%	0.03	4.7%	4.8%	4.8%	1.59
thermal2	0.02	2.2%	0.02	7.6%	7.7%	7.7%	1.79
G3_circuit	0.03	0.6%	0.02	6.5%	6.3%	6.3%	1.67

Table 5.14 – continued from previous page

Table 5.15: 128-way partitioning performance of the PD matrix collection for cut-net metric with node balancing.

name	PaToH		onmetisHP				speedup
	cutsize	%LI	cutsize	$exp\%LI_p$	$act\%LI_p$	$act\%LI_c$	
bcsstk13	0.97	1.6%	0.98	931.4%	1480.7%	353.6%	2.43
Chem97ZtZ	0.49	75.6%	0.56	216.7%	187.0%	79.1%	0.94
sts4098	0.79	38.7%	0.84	321.0%	326.9%	136.4%	1.20
ex15	0.57	3.1%	0.54	76.3%	61.8%	57.6%	2.08
Muu	0.77	1.2%	0.78	203.9%	98.4%	12.3%	1.60
Kuu	0.91	0.9%	0.91	1008.2%	244.6%	12.8%	2.24
bcsstk38	0.85	2.3%	0.87	460.8%	237.6%	88.2%	2.10
aft01	0.62	1.6%	0.60	52.6%	48.6%	28.3%	1.65
fv1	0.42	3.1%	0.43	17.5%	18.9%	18.3%	2.25
fv2	0.42	3.4%	0.43	16.2%	20.0%	19.4%	2.30
fv3	0.42	3.3%	0.43	16.2%	20.0%	19.4%	2.30
bundle1	1.00	5.9%	1.00	3222.4%	1918.4%	621.5%	0.34
ted_B_unscaled	0.38	1.5%	0.35	180.0%	98.1%	48.4%	1.24
ted_B	0.38	1.5%	0.34	175.1%	64.9%	24.1%	1.23
msc10848	0.97	0.4%	0.96	1372.4%	440.5%	89.9%	3.71
bcsstk17	0.79	3.0%	0.78	238.4%	126.7%	78.6%	2.49
t2dah_e	0.54	0.9%	0.52	33.7%	37.3%	22.5%	1.90
bcsstk18	0.53	3.6%	0.57	131.5%	117.6%	80.7%	1.57
cbuckle	0.80	2.6%	0.74	94.2%	56.6%	50.6%	2.80
crystm02	0.70	5.5%	0.71	69.8%	65.4%	54.1%	1.95
Pres_Poisson	0.81	3.6%	0.76	71.4%	54.3%	47.9%	2.80
bcsstm25	0.00	0.3%	0.00	0.3%	0.3%	0.3%	4.18
bcsstk25	0.66	2.0%	0.70	91.3%	66.8%	44.4%	1.69
Dubcova1	0.50	0.6%	0.48	33.5%	27.8%	10.2%	1.84
olafu	0.81	2.5%	0.79	309.3%	136.6%	80.8%	3.13
gyro_m	0.45	2.0%	0.49	160.4%	92.7%	52.9%	1.45
gyro	0.72	1.0%	0.81	790.8%	255.5%	70.1%	2.14
bodyy4	0.29	1.8%	0.30	11.7%	14.1%	13.1%	2.28
bodyy5	0.29	1.7%	0.29	11.3%	12.4%	11.4%	2.38
bodyy6	0.29	1.6%	0.29	10.8%	11.9%	11.0%	2.44
raefsky4	0.85	3.6%	0.83	264.8%	107.9%	71.5%	2.87
LFAT5000	0.02	0.8%	0.02	2.0%	1.1%	1.1%	2.20
LF10000	0.03	1.2%	0.03	1.8%	2.4%	2.4%	2.14
t3dl_e	0.00	0.6%	0.00	0.6%	0.6%	0.6%	4.22
bcsstk36	0.65	2.8%	0.62	85.1%	58.7%	49.4%	2.80
msc23052	0.65	2.6%	0.62	72.9%	61.9%	53.7%	2.98
crystm03	0.61	4.5%	0.61	45.8%	47.0%	43.6%	1.93
smt	0.94	0.4%	0.97	1277.2%	298.9%	54.4%	3.92
thread	0.95	0.5%	0.97	882.5%	282.9%	54.8%	3.74
wathen100	0.36	0.9%	0.35	12.8%	15.2%	7.6%	1.67
ship_001	0.90	0.6%	0.94	712.7%	265.4%	55.5%	3.81
nd12k	1.00	0.6%	1.00	701.4%	937.0%	101.7%	5.11
wathen120	0.34	0.8%	0.31	11.6%	13.9%	7.2%	1.64
obstclae	0.18	1.7%	0.16	11.3%	11.1%	11.0%	2.17
jnlbrng1	0.18	1.8%	0.17	11.6%	12.4%	12.4%	2.16
minsurfo	0.17	1.5%	0.17	11.8%	13.0%	12.9%	2.17
bcsstm39	0.00	0.2%	0.00	0.2%	0.2%	0.2%	4.30
vanbody	0.48	3.2%	0.46	45.6%	54.3%	49.6%	2.69
gridgena	0.25	1.8%	0.24	12.8%	16.0%	15.2%	1.87
cvxbqp1	0.17	2.2%	0.19	18.1%	17.7%	16.6%	2.13
ct20stif	0.50	3.2%	0.47	50.4%	71.2%	65.4%	2.60
crankseg_1	0.91	0.1%	0.95	932.0%	293.2%	26.2%	4.11
nasasrb	0.49	3.2%	0.45	24.9%	26.7%	26.2%	2.85
Andrews	0.77	4.3%	0.85	162.6%	98.9%	31.1%	1.53
crankseg_2	0.90	0.4%	0.94	800.4%	298.9%	48.5%	4.31
Dubcova2	0.27	0.2%	0.25	13.1%	9.2%	0.8%	1.72
						Continued on next page	

Table 5.15 – continued from previous page

	PaToH		onmetisHP				
name	cutsize	%LI	cutsize	$exp\%LI_p$	$act\%LI_p$	$act\%LI_c$	speedup
qa8fm	0.53	4.7%	0.51	25.0%	37.1%	36.2%	1.79
cfd1	0.52	5.2%	0.51	30.5%	39.0%	38.2%	1.77
nd24k	0.99	0.5%	1.00	615.4%	454.5%	0.3%	5.56
oilpan	0.41	1.5%	0.39	23.1%	22.3%	17.5%	2.70
finan512	0.31	1.8%	0.25	9.4%	11.0%	3.9%	1.16
apache1	0.33	2.0%	0.32	18.6%	17.8%	17.4%	2.00
shallow_water1	0.11	1.3%	0.11	10.1%	10.0%	9.8%	2.12
shallow_water2	0.11	0.9%	0.11	11.7%	11.1%	10.9%	2.11
thermal1	0.14	2.5%	0.13	15.2%	14.9%	14.8%	2.03
denormal	0.23	1.6%	0.22	12.7%	12.7%	12.6%	1.89
s3dkt3m2	0.33	0.8%	0.32	9.5%	10.7%	9.4%	2.68
s3dkq4m2	0.37	2.1%	0.32	11.4%	13.3%	13.2%	3.09
m_t1	0.57	1.0%	0.52	45.3%	51.6%	35.9%	4.05
2cubes_sphere	0.53	1.7%	0.54	25.5%	24.1%	11.4%	1.56
thermomech_TK	0.12	2.2%	0.12	15.2%	15.4%	15.2%	2.18
thermomech_TC	0.12	2.2%	0.12	15.6%	15.3%	15.2%	2.17
x104	0.47	0.8%	0.46	39.6%	60.4%	45.4%	3.79
shipsec8	0.43	2.6%	0.42	33.9%	36.6%	34.6%	2.81
ship_003	0.53	2.9%	0.53	40.1%	34.9%	31.5%	2.74
cfd2	0.39	4.4%	0.37	25.8%	29.8%	29.6%	1.72
boneS01	0.42	2.0%	0.40	27.5%	35.4%	30.7%	2.56
shipsec1	0.36	2.8%	0.35	24.0%	30.7%	30.3%	2.95
bmw7st_1	0.29	3.5%	0.27	28.6%	28.7%	28.1%	2.82
Dubcova3	0.26	0.2%	0.22	12.3%	12.4%	1.5%	1.58
bmwcra_1	0.52	5.0%	0.50	47.7%	49.3%	48.0%	2.53
G2_circuit	0.14	1.3%	0.14	9.4%	11.9%	11.8%	1.90
shipsec5	0.34	3.3%	0.33	22.2%	26.5%	26.2%	2.90
thermomech_dM	0.08	2.3%	0.08	13.4%	13.2%	13.2%	2.19
pwtk	0.25	2.1%	0.23	15.3%	16.0%	15.9%	3.11
hood	0.21	1.5%	0.21	18.9%	18.4%	15.8%	2.77
BenElechi1	0.23	1.8%	0.20	14.7%	16.0%	16.0%	3.09
offshore	0.32	3.4%	0.32	24.8%	27.6%	21.0%	1.55
F1	0.43	0.8%	0.43	43.4%	56.6%	33.9%	1.90
msdoor	0.12	2.4%	0.12	17.7%	17.4%	16.8%	2.78
af_3_k101	0.13	0.9%	0.13	7.6%	7.2%	7.1%	2.26
af_1_k101	0.13	0.8%	0.13	7.2%	7.7%	7.5%	2.27
af_2_k101	0.13	0.9%	0.13	6.7%	7.5%	7.4%	2.27
af_4_k101	0.13	0.8%	0.13	7.2%	7.8%	7.7%	2.25
af_0_k101	0.13	0.9%	0.13	7.2%	7.7%	7.6%	2.26
af_5_k101	0.13	0.8%	0.13	7.9%	8.1%	8.0%	2.25
inline_1	0.27	0.8%	0.26	25.0%	26.0%	16.8%	2.09
af_shell7	0.13	1.0%	0.12	7.2%	7.6%	7.4%	2.26
af_shell3	0.13	1.0%	0.12	7.8%	8.2%	8.1%	2.27
af_shell4	0.13	0.9%	0.12	8.2%	8.8%	8.6%	2.25
af_shell8	0.13	1.1%	0.12	9.3%	9.8%	9.6%	2.25
parabolic_fem	0.06	0.6%	0.06	10.1%	10.2%	10.1%	2.10
apache2	0.13	1.0%	0.12	12.2%	12.0%	11.9%	1.79
tmt_sym	0.05	2.3%	0.05	12.2%	12.3%	12.3%	1.66
boneS10	0.13	3.7%	0.12	20.6%	23.3%	22.8%	2.58
ldoor	0.09	2.3%	0.09	13.8%	13.2%	12.8%	2.75
ecology2	0.04	0.3%	0.04	8.0%	8.0%	8.0%	1.63
thermal2	0.04	2.3%	0.04	10.2%	10.1%	10.1%	1.80
G3_circuit	0.04	0.6%	0.04	7.6%	7.2%	7.2%	1.68

Table 5.16: 2-way partitioning performance of the PD matrix collection for connectivity metric with node balancing.

name	PaToH		onmetisHP		speedup
	cutsize	%LI	cutsize	%LI	
msc01050	1.21	3.1%	1.29	0.0%	0.77
bcsstm08	1.00	0.0%	1.00	0.0%	2.31
bcsstm09	1.00	0.1%	1.00	0.1%	2.30
bcsstk09	1.11	5.4%	1.12	0.1%	1.71
bcsstk10	1.03	1.3%	1.03	1.3%	1.49
1138_bus	1.02	0.0%	1.02	1.4%	1.77
bcsstk27	1.07	2.7%	1.06	2.8%	1.78
mhd1280b	1.01	0.2%	1.01	0.1%	1.03
plbuckle	1.00	2.6%	1.00	2.6%	1.53
msc01440	1.11	0.2%	1.11	0.1%	1.49
bcsstk11	1.04	3.6%	1.04	3.7%	1.46
bcsstm11	1.00	0.1%	1.00	0.1%	2.38
bcsstm12	1.05	0.0%	1.05	0.1%	1.49
bcsstk12	1.04	3.6%	1.04	3.7%	1.46
ex33	1.04	3.4%	1.04	3.2%	1.48
bcsstk14	1.11	0.0%	1.11	0.2%	1.27
ex3	1.06	0.1%	1.06	0.9%	1.45
nasa1824	1.11	0.1%	1.13	0.1%	1.15
plat1919	1.04	4.3%	1.04	2.8%	1.31
bcsstm26	1.00	0.0%	1.00	0.0%	2.32
bcsstk26	1.07	1.5%	1.08	0.0%	1.26
bcsstk13	1.22	3.7%	1.29	1.8%	0.81
nasa2146	1.07	2.0%	1.07	2.3%	1.55
ex10	1.02	1.2%	1.02	1.1%	1.20
Chem97ZtZ	1.00	0.0%	1.00	0.0%	0.48
ex10hs	1.02	0.7%	1.02	0.0%	1.19
ex13	1.04	0.1%	1.04	0.9%	1.19
nasa2910	1.18	0.0%	1.16	3.2%	1.06
bcsstk23	1.18	0.0%	1.18	0.5%	1.43
bcsstm23	1.00	0.0%	1.00	0.0%	2.39
mhd3200b	1.00	0.0%	1.00	4.3%	1.08
bibd_81_2	1.00	0.0%	1.00	0.0%	2.41
ex9	1.03	0.5%	1.03	0.6%	1.20
bcsstm24	1.00	0.0%	1.00	0.0%	2.40
bcsstk24	1.08	0.0%	1.11	0.1%	1.37
bcsstk21	1.00	0.0%	1.00	0.0%	1.19
bcsstm21	1.00	0.0%	1.00	0.0%	2.42
bcsstk15	1.09	1.4%	1.09	3.5%	1.15
sts4098	1.10	0.3%	1.11	6.3%	0.46
t2dal_e	1.00	0.0%	1.00	0.0%	2.44
bcsstk28	1.05	5.7%	1.05	3.8%	1.51
msc04515	1.04	3.1%	1.04	3.8%	1.11
nasa4704	1.08	0.2%	1.08	0.3%	1.11
mhd4800b	1.00	0.0%	1.00	1.6%	1.09
crystm01	1.03	1.4%	1.03	1.4%	1.17
bcsstk16	1.05	0.0%	1.05	0.0%	1.39
s3rmt3m3	1.06	0.0%	1.06	0.0%	1.39
s3rmt3m1	1.07	0.0%	1.07	0.0%	1.38
s2rmq4m1	1.07	0.3%	1.07	0.7%	1.40
s1rmt3m1	1.07	0.0%	1.07	0.1%	1.39
s1rmq4m1	1.07	0.4%	1.07	1.2%	1.39
s2rmt3m1	1.07	0.0%	1.07	0.1%	1.37
s3rmq4m1	1.07	0.2%	1.07	1.0%	1.39
ex15	1.01	0.3%	1.01	0.2%	1.16
Kuu	1.07	0.0%	1.06	2.1%	1.10
Muu	1.00	0.0%	1.00	0.0%	0.97
Continued on next page					

name	PaToH		onmetisHP		speedup
	cutsize	%LI	cutsize	%LI	
bcsstk38	1.04	3.3%	1.04	2.0%	1.10
aft01	1.03	0.0%	1.03	2.6%	1.16
fv1	1.02	0.0%	1.02	0.0%	1.33
fv3	1.02	0.1%	1.02	1.0%	1.33
fv2	1.02	0.1%	1.02	1.0%	1.33
bundle1	1.14	0.1%	1.11	18.8%	0.17
ted_B	1.00	0.0%	1.00	0.0%	0.63
ted_B_unscaled	1.00	0.0%	1.00	0.1%	0.63
msc10848	1.09	0.0%	1.09	0.4%	1.51
bcsstk17	1.04	0.0%	1.04	1.0%	1.20
t2dah_e	1.02	0.0%	1.02	0.7%	1.06
bcsstk18	1.04	1.7%	1.04	0.3%	0.93
cbuckle	1.05	2.3%	1.05	2.4%	1.19
crystm02	1.02	1.3%	1.02	1.0%	1.08
Pres_Poisson	1.03	0.8%	1.03	0.7%	1.35
bcsstm25	1.00	0.0%	1.00	0.0%	2.36
bcsstk25	1.02	1.4%	1.02	0.8%	1.04
Dubcova1	1.03	0.0%	1.02	1.0%	1.10
olafu	1.05	0.1%	1.05	0.7%	1.34
gyro_m	1.00	0.0%	1.00	0.1%	0.86
gyro	1.01	0.0%	1.01	0.7%	1.25
bodyy4	1.01	0.0%	1.01	0.0%	1.22
bodyy5	1.01	0.0%	1.01	0.0%	1.22
bodyy6	1.01	0.0%	1.01	0.0%	1.24
raefsky4	1.05	1.0%	1.05	1.4%	1.33
LFAT5000	1.00	0.0%	1.00	0.0%	1.06
LF10000	1.00	0.0%	1.00	0.0%	1.03
t3dl_e	1.00	0.0%	1.00	0.0%	2.41
msc23052	1.03	1.7%	1.03	2.4%	1.44
bcsstk36	1.03	2.5%	1.03	1.8%	1.36
crystm03	1.01	1.6%	1.01	0.7%	1.15
smt	1.07	2.8%	1.06	0.9%	1.63
thread	1.10	0.4%	1.10	1.0%	1.40
wathen100	1.02	0.0%	1.02	0.7%	0.97
ship_001	1.03	2.0%	1.03	0.7%	1.71
nd12k	1.30	1.2%	1.29	2.1%	0.99
wathen120	1.02	0.0%	1.01	0.6%	0.97
obstclae	1.01	0.0%	1.01	0.0%	1.23
jnlbrng1	1.01	0.0%	1.01	0.0%	1.22
minsurfo	1.01	0.0%	1.01	0.0%	1.23
bcsstm39	1.00	0.0%	1.00	0.0%	2.60
vanbody	1.02	2.1%	1.02	1.7%	1.37
gridgena	1.01	0.0%	1.01	0.1%	1.03
cvxbqp1	1.02	0.0%	1.02	0.0%	1.40
ct20stif	1.04	2.3%	1.04	3.0%	1.27
crankseg_1	1.04	0.0%	1.03	1.8%	1.71
nasasrb	1.01	1.6%	1.01	0.2%	1.41
Andrews	1.07	1.8%	1.11	2.8%	1.13
crankseg_2	1.04	2.0%	1.03	0.5%	1.68
Dubcova2	1.01	0.0%	1.01	0.7%	1.02
qa8fm	1.01	0.3%	1.01	0.0%	1.14
cfd1	1.02	0.2%	1.03	1.7%	1.08
nd24k	1.24	2.6%	1.23	1.1%	1.13
oilpan	1.02	0.0%	1.02	0.1%	1.35
finan512	1.00	0.0%	1.00	0.0%	0.79
apache1	1.02	0.0%	1.02	0.0%	1.38
shallow_water1	1.01	0.0%	1.01	0.0%	1.28
shallow_water2	1.01	0.0%	1.01	0.0%	1.26

Table 5.16 – continued from previous page

Table 5.16 – continued from previous page

name	PaToH		onmetisHP		
	cutsize	%LI	cutsize	%LI	speedup
thermal1	1.00	0.9%	1.00	0.8%	1.19
denormal	1.01	0.0%	1.01	0.0%	1.09
s3dkt3m2	1.01	0.0%	1.01	0.0%	1.29
s3dkq4m2	1.01	0.0%	1.01	0.2%	1.48
m_t1	1.03	1.5%	1.02	0.9%	1.81
2cubes_sphere	1.04	6.4%	1.04	0.7%	1.05
thermomech_TK	1.00	1.6%	1.00	0.7%	1.38
thermomech_TC	1.00	1.5%	1.00	0.1%	1.39
x104	1.03	0.0%	1.03	0.9%	1.69
shipsec8	1.03	0.1%	1.03	0.4%	1.41
ship_003	1.02	0.7%	1.02	1.2%	1.44
cfd2	1.02	0.6%	1.02	0.6%	1.08
boneS01	1.04	0.0%	1.04	0.8%	1.30
shipsec1	1.02	0.2%	1.02	0.4%	1.52
bmw7st_1	1.01	1.2%	1.01	0.7%	1.46
Dubcova3	1.01	0.0%	1.01	0.4%	1.02
bmwcra_1	1.01	3.5%	1.01	0.2%	1.36
G2_circuit	1.01	0.0%	1.00	0.4%	1.36
shipsec5	1.01	4.1%	1.02	0.7%	1.48
thermomech_dM	1.00	0.0%	1.00	0.0%	1.50
pwtk	1.01	0.2%	1.01	0.1%	1.51
hood	1.01	0.4%	1.01	0.3%	1.42
BenElechi1	1.01	0.0%	1.01	0.2%	1.52
offshore	1.02	2.9%	1.02	1.6%	1.18
F1	1.01	0.0%	1.01	0.5%	1.16
msdoor	1.00	0.3%	1.00	0.3%	1.43
af_2_k101	1.00	0.0%	1.00	0.0%	1.24
af_5_k101	1.00	0.0%	1.00	0.0%	1.23
af_1_k101	1.00	0.0%	1.00	0.0%	1.24
af_4_k101	1.00	0.0%	1.00	0.0%	1.23
af_3_k101	1.00	0.0%	1.00	0.0%	1.23
af_0_k101	1.00	0.0%	1.00	0.0%	1.23
inline_1	1.01	0.0%	1.01	0.9%	1.22
af_shell8	1.00	0.0%	1.00	0.0%	1.24
af_shell3	1.00	0.0%	1.00	0.0%	1.23
af_shell4	1.00	0.0%	1.00	0.0%	1.24
af_shell7	1.00	0.0%	1.00	0.0%	1.23
parabolic_fem	1.00	0.0%	1.00	0.0%	1.60
apache2	1.01	0.0%	1.01	0.0%	1.43
tmt_sym	1.00	0.9%	1.00	0.1%	1.18
boneS10	1.01	3.0%	1.01	0.4%	1.42
ldoor	1.00	0.4%	1.00	0.4%	1.44
ecology2	1.00	0.0%	1.00	0.0%	1.24
thermal2	1.00	1.6%	1.00	0.3%	1.25
G3_circuit	1.00	0.0%	1.00	0.0%	1.36

Table 5.17: 4-way partitioning performance of the PD matrix collection for connectivity metric with node balancing.

name	PaToH		onmetisHP		speedup
	cutsize	%LI	cutsize	%LI	
msc01050	1.44	4.7%	1.52	11.0%	0.79
bcsstm08	1.00	0.2%	1.00	0.2%	2.78
bcsstm09	1.00	0.1%	1.00	0.1%	2.77
bcsstk09	1.24	0.9%	1.25	0.8%	1.50
bcsstk10	1.09	1.5%	1.09	1.6%	1.82
1138_bus	1.04	1.7%	1.05	3.4%	1.86
bcsstk27	1.18	3.3%	1.17	3.3%	1.89
mhd1280b	1.03	1.1%	1.02	1.4%	1.45
plbuckle	1.11	2.8%	1.11	2.8%	1.60
msc01440	1.23	1.2%	1.22	2.1%	1.49
bcsstk11	1.14	4.1%	1.14	4.0%	1.61
bcsstm11	1.00	0.2%	1.00	0.2%	2.80
bcsstm12	1.12	2.6%	1.12	2.3%	1.69
bcsstk12	1.14	4.0%	1.14	4.0%	1.60
ex33	1.08	5.3%	1.07	5.3%	1.70
bcsstk14	1.24	0.5%	1.24	2.0%	1.37
ex3	1.20	0.1%	1.19	4.3%	1.36
nasa1824	1.26	2.1%	1.26	4.8%	1.31
plat1919	1.13	3.4%	1.13	3.6%	1.53
bcsstm26	1.00	0.1%	1.00	0.1%	2.75
bcsstk26	1.15	2.1%	1.16	3.0%	1.40
bcsstk13	1.52	7.2%	1.61	12.8%	0.86
nasa2146	1.20	4.2%	1.20	2.7%	1.58
ex10	1.07	1.2%	1.05	7.4%	1.36
Chem97ZtZ	1.00	0.0%	1.00	0.7%	0.54
ex10hs	1.06	2.3%	1.05	3.9%	1.40
ex13	1.11	1.0%	1.10	1.8%	1.45
nasa2910	1.35	0.0%	1.31	6.3%	1.20
bcsstk23	1.40	1.9%	1.42	2.2%	1.18
bcsstm23	1.00	0.1%	1.00	0.1%	2.79
mhd3200b	1.00	0.0%	1.00	4.4%	1.40
bibd_81_2	1.00	0.0%	1.00	0.0%	2.80
ex9	1.10	1.1%	1.10	0.8%	1.45
bcsstm24	1.00	0.1%	1.00	0.1%	2.85
bcsstk24	1.18	0.1%	1.21	0.8%	1.59
bcsstk21	1.07	0.0%	1.07	0.0%	1.45
bcsstm21	1.00	0.0%	1.00	0.0%	2.85
bcsstk15	1.27	2.5%	1.27	3.2%	1.17
sts4098	1.25	5.0%	1.43	29.4%	0.43
t2dal_e	1.00	0.1%	1.00	0.1%	2.86
bcsstk28	1.14	2.0%	1.14	5.7%	1.81
msc04515	1.09	4.0%	1.09	4.6%	1.38
nasa4704	1.17	2.5%	1.18	2.8%	1.31
mhd4800b	1.00	0.1%	1.00	4.4%	1.35
crystm01	1.08	2.5%	1.08	2.5%	1.38
bcsstk16	1.14	3.3%	1.14	3.5%	1.70
s3rmt3m3	1.14	0.2%	1.14	0.5%	1.61
s3rmt3m1	1.14	0.1%	1.15	0.4%	1.59
s2rmq4m1	1.15	1.5%	1.14	4.4%	1.81
s1rmt3m1	1.15	0.1%	1.16	0.6%	1.59
s1rmq4m1	1.14	1.8%	1.14	4.4%	1.82
s2rmt3m1	1.14	0.1%	1.15	0.3%	1.60
s3rmq4m1	1.14	3.2%	1.14	4.4%	1.82
ex15	1.04	2.5%	1.04	3.2%	1.39
Kuu	1.15	0.1%	1.15	5.3%	1.34
Muu	1.07	0.0%	1.06	2.3%	1.11

	PaToH		onmetisHP		
name	cutsize	%LI	cutsize	%LI	speedup
bcsstk38	1.14	3.6%	1.14	3.8%	1.31
aft01	1.07	0.2%	1.06	4.8%	1.21
fv1	1.04	0.9%	1.04	0.0%	1.51
fv3	1.05	0.2%	1.04	2.3%	1.49
fv2	1.04	0.4%	1.04	2.3%	1.50
bundle1	1.37	0.0%	1.60	34.6%	0.15
ted_B	1.01	0.0%	1.01	0.3%	0.79
ted_B_unscaled	1.01	0.0%	1.01	0.3%	0.79
msc10848	1.26	0.0%	1.22	5.1%	1.74
bcsstk17	1.09	2.3%	1.09	4.1%	1.53
t2dah_e	1.06	0.0%	1.05	0.8%	1.23
bcsstk18	1.08	4.9%	1.09	5.4%	1.02
cbuckle	1.10	1.5%	1.10	4.8%	1.53
crystm02	1.06	2.6%	1.06	2.3%	1.26
Pres_Poisson	1.09	1.2%	1.08	2.2%	1.68
bcsstm25	1.00	0.0%	1.00	0.0%	2.80
bcsstk25	1.07	2.7%	1.07	2.9%	1.08
Dubcova1	1.06	0.0%	1.05	2.0%	1.22
olafu	1.09	2.2%	1.08	3.4%	1.76
gyro_m	1.01	2.6%	1.01	5.1%	0.99
gyro	1.05	1.8%	1.05	5.0%	1.39
bodyy4	1.03	0.0%	1.03	0.7%	1.40
bodyy5	1.03	0.0%	1.03	0.4%	1.40
bodyy6	1.03	0.0%	1.03	0.8%	1.40
raefsky4	1.11	1.9%	1.13	3.6%	1.54
LFAT5000	1.00	0.0%	1.00	0.0%	1.17
LF10000	1.00	0.0%	1.00	0.0%	1.14
t3dl_e	1.00	0.0%	1.00	0.0%	2.86
msc23052	1.09	1.6%	1.09	4.7%	1.77
bcsstk36	1.09	2.5%	1.09	4.1%	1.68
crystm03	1.04	1.7%	1.04	1.1%	1.28
smt	1.21	0.3%	1.19	8.9%	1.76
thread	1.30	0.1%	1.29	2.3%	1.54
wathen100	1.04	0.0%	1.03	1.7%	1.09
ship_001	1.09	3.1%	1.08	2.9%	2.21
nd12k	1.66	2.7%	1.65	4.9%	1.08
wathen120	1.03	0.0%	1.03	1.3%	1.12
obstclae	1.02	0.0%	1.02	0.0%	1.34
jnlbrng1	1.02	0.0%	1.02	0.0%	1.34
minsurfo	1.02	0.0%	1.02	0.0%	1.35
bcsstm39	1.00	0.0%	1.00	0.0%	3.03
vanbody	1.04	3.6%	1.04	5.7%	1.73
gridgena	1.02	1.1%	1.02	1.4%	1.17
cvxbqp1	1.03	0.0%	1.03	0.2%	1.52
ct20stif	1.09	3.3%	1.08	6.2%	1.58
crankseg_1	1.11	2.7%	1.09	6.0%	2.23
nasasrb	1.03	2.3%	1.03	1.0%	1.80
Andrews	1.16	7.1%	1.22	10.7%	1.12
crankseg_2	1.11	2.4%	1.10	2.0%	2.23
Dubcova2	1.03	0.0%	1.02	1.4%	1.20
qa8fm	1.09	1.1%	1.08	3.0%	1.26
cfd1	1.05	1.8%	1.06	4.1%	1.25
nd24k	1.50	2.3%	1.49	4.2%	1.32
oilpan	1.04	2.1%	1.04	2.4%	1.75
finan512	1.00	0.0%	1.00	0.1%	0.87
apache1	1.04	0.0%	1.04	0.0%	1.45
shallow_water1	1.02	0.0%	1.02	0.0%	1.36
shallow_water2	1.02	0.0%	1.02	0.0%	1.36

Table 5.17 – continued from previous page

Table 5.17 – continued from previous page					
	PaToH		*onmetisHP*		
name	cutsize	%LI	cutsize	%LI	speedup
thermal1	1.01	1.6%	1.01	1.6%	1.35
denormal	1.03	0.0%	1.03	0.0%	1.23
s3dkt3m2	1.04	0.0%	1.04	0.1%	1.64
s3dkq4m2	1.04	0.0%	1.03	3.0%	1.96
m_t1	1.07	4.2%	1.06	3.7%	2.42
2cubes_sphere	1.11	5.0%	1.12	1.2%	1.13
thermomech_TK	1.01	2.0%	1.01	2.4%	1.56
thermomech_TC	1.01	1.4%	1.01	2.2%	1.58
x104	1.06	1.6%	1.05	1.6%	2.31
shipsec8	1.07	1.1%	1.07	1.6%	1.79
ship_003	1.07	2.6%	1.07	4.5%	1.78
cfd2	1.05	2.2%	1.05	3.9%	1.22
boneS01	1.08	2.2%	1.07	1.8%	1.63
shipsec1	1.05	0.8%	1.04	2.4%	1.95
bmw7st_1	1.03	2.9%	1.03	3.0%	1.89
Dubcova3	1.03	0.0%	1.02	1.1%	1.21
bmwcra_1	1.02	7.5%	1.04	3.5%	1.73
G2_circuit	1.01	0.0%	1.01	2.7%	1.42
shipsec5	1.05	5.2%	1.05	2.7%	1.90
thermomech_dM	1.00	1.1%	1.00	0.9%	1.76
pwtk	1.01	0.6%	1.01	0.9%	2.03
hood	1.02	0.9%	1.02	1.5%	1.87
BenElechi1	1.02	0.0%	1.01	2.2%	2.04
offshore	1.04	2.9%	1.05	2.8%	1.29
F1	1.02	2.3%	1.02	2.6%	1.46
msdoor	1.01	1.2%	1.01	1.4%	1.93
af_2_k101	1.01	0.0%	1.01	0.0%	1.59
af_5_k101	1.01	0.0%	1.01	0.0%	1.58
af_1_k101	1.01	0.0%	1.01	0.0%	1.58
af_4_k101	1.01	0.0%	1.01	0.0%	1.60
af_3_k101	1.01	0.0%	1.01	0.0%	1.58
af_0_k101	1.01	0.0%	1.01	0.0%	1.58
inline_1	1.02	2.6%	1.02	4.1%	1.58
af_shell8	1.01	0.0%	1.01	0.0%	1.58
af_shell3	1.01	0.0%	1.01	0.0%	1.59
af_shell4	1.01	0.0%	1.01	0.0%	1.60
af_shell7	1.01	0.0%	1.01	0.0%	1.61
parabolic_fem	1.01	0.0%	1.01	0.0%	1.82
apache2	1.01	0.0%	1.01	0.0%	1.48
tmt_sym	1.01	1.8%	1.01	1.0%	1.31
boneS10	1.01	2.7%	1.01	1.9%	1.87
ldoor	1.01	2.5%	1.01	2.0%	1.94
ecology2	1.00	0.0%	1.00	0.0%	1.33
thermal2	1.00	2.4%	1.00	1.0%	1.45
G3_circuit	1.00	0.0%	1.00	0.0%	1.45

Table 5.18: 8-way partitioning performance of the PD matrix collection for connectivity metric with node balancing.

name	PaToH		onmetisHP		speedup
	cutsize	%LI	cutsize	%LI	
msc01050	1.80	5.3%	1.84	27.8%	0.76
bcsstm08	1.00	0.6%	1.00	0.6%	2.94
bcsstm09	1.00	0.5%	1.00	0.5%	2.93
bcsstk09	1.49	2.3%	1.48	5.0%	1.57
bcsstk10	1.23	4.2%	1.22	9.9%	1.85
1138_bus	1.08	2.0%	1.08	4.6%	1.99
bcsstk27	1.46	4.2%	1.41	9.7%	1.87
mhd1280b	1.06	2.7%	1.05	3.9%	1.79
plbuckle	1.34	3.3%	1.33	6.1%	1.65
msc01440	1.49	2.5%	1.47	7.8%	1.52
bcsstk11	1.31	3.4%	1.31	4.8%	1.69
bcsstm11	1.00	0.5%	1.00	0.5%	2.93
bcsstm12	1.24	2.0%	1.24	3.6%	1.81
bcsstk12	1.31	3.3%	1.31	4.9%	1.69
ex33	1.16	4.6%	1.13	10.2%	1.79
bcsstk14	1.50	1.7%	1.49	6.1%	1.43
ex3	1.42	0.7%	1.41	9.3%	1.36
nasa1824	1.46	2.7%	1.47	10.9%	1.30
plat1919	1.27	2.5%	1.27	7.5%	1.65
bcsstm26	1.00	0.3%	1.00	0.3%	2.93
bcsstk26	1.28	1.7%	1.28	7.4%	1.43
bcsstk13	2.01	5.4%	2.01	25.1%	0.86
nasa2146	1.37	2.0%	1.36	5.5%	1.63
ex10	1.20	1.1%	1.18	12.0%	1.43
Chem97ZtZ	1.00	0.1%	1.00	2.5%	0.60
ex10hs	1.18	2.3%	1.16	6.0%	1.49
ex13	1.31	0.8%	1.29	5.1%	1.42
nasa2910	1.64	0.1%	1.60	12.0%	1.15
bcsstk23	1.67	1.7%	1.70	4.8%	1.12
bcsstm23	1.00	0.1%	1.00	0.1%	2.95
mhd3200b	1.01	0.2%	1.01	4.5%	1.60
bibd_81_2	1.00	0.0%	1.00	0.0%	3.02
ex9	1.26	1.1%	1.25	4.3%	1.44
bcsstm24	1.00	0.2%	1.00	0.2%	3.03
bcsstk24	1.35	1.4%	1.37	3.9%	1.69
bcsstk21	1.16	0.2%	1.16	0.3%	1.57
bcsstm21	1.00	0.0%	1.00	0.0%	2.99
bcsstk15	1.47	3.0%	1.47	5.9%	1.23
sts4098	1.37	5.6%	1.47	26.5%	0.48
t2dal_e	1.00	0.2%	1.00	0.2%	3.01
bcsstk28	1.29	3.0%	1.28	8.4%	1.90
msc04515	1.18	4.0%	1.18	7.3%	1.52
nasa4704	1.29	3.3%	1.28	6.8%	1.43
mhd4800b	1.01	0.2%	1.00	4.5%	1.50
crystm01	1.19	4.3%	1.19	5.9%	1.44
bcsstk16	1.35	5.4%	1.34	6.1%	1.70
s3rmt3m3	1.25	0.7%	1.25	1.0%	1.76
s3rmt3m1	1.26	0.3%	1.27	1.4%	1.73
s2rmq4m1	1.29	2.3%	1.29	5.2%	1.95
s1rmt3m1	1.27	0.4%	1.27	1.1%	1.74
s1rmq4m1	1.29	2.5%	1.29	5.3%	1.95
s2rmt3m1	1.27	0.4%	1.27	1.2%	1.74
s3rmq4m1	1.29	1.9%	1.29	4.5%	1.95
ex15	1.08	1.7%	1.08	3.6%	1.59
Kuu	1.30	0.2%	1.29	8.5%	1.40
Muu	1.15	0.4%	1.15	5.6%	1.22
Continued on next page					

Table 5.18 – continued from previous page

name	PaToH		onmetisHP		speedup
	cutsize	%LI	cutsize	%LI	
bcsstk38	1.28	3.7%	1.29	11.5%	1.34
aft01	1.12	0.1%	1.11	5.4%	1.32
fv1	1.09	2.1%	1.08	1.5%	1.71
fv3	1.08	2.2%	1.08	2.6%	1.70
fv2	1.08	2.4%	1.08	2.7%	1.71
bundle1	1.82	3.7%	2.19	57.8%	0.16
ted_B	1.02	0.3%	1.02	0.7%	0.93
ted_B_unscaled	1.02	0.3%	1.02	0.5%	0.92
msc10848	1.43	0.1%	1.39	7.1%	1.82
bcsstk17	1.17	2.5%	1.16	6.6%	1.70
t2dah_e	1.10	0.1%	1.10	2.6%	1.36
bcsstk18	1.14	3.3%	1.15	9.2%	1.11
cbuckle	1.18	3.0%	1.18	6.3%	1.73
crystm02	1.14	3.2%	1.13	5.5%	1.38
Pres_Poisson	1.17	2.6%	1.16	4.7%	1.86
bcsstm25	1.00	0.0%	1.00	0.0%	2.97
bcsstk25	1.15	1.6%	1.15	3.2%	1.17
Dubcova1	1.11	0.0%	1.10	2.9%	1.31
olafu	1.17	2.5%	1.16	4.8%	1.94
gyro_m	1.03	2.4%	1.03	6.5%	1.09
gyro	1.13	2.0%	1.10	12.8%	1.41
bodyy4	1.05	0.6%	1.06	0.8%	1.57
bodyy5	1.05	0.1%	1.05	0.5%	1.57
bodyy6	1.05	0.0%	1.05	0.2%	1.56
raefsky4	1.22	2.6%	1.22	5.8%	1.70
LFAT5000	1.00	0.0%	1.00	0.0%	1.26
LF10000	1.00	0.0%	1.00	0.0%	1.25
t3dl_e	1.00	0.0%	1.00	0.0%	3.03
msc23052	1.16	2.8%	1.15	6.5%	1.98
bcsstk36	1.17	2.8%	1.16	7.3%	1.84
crystm03	1.10	2.9%	1.10	4.6%	1.37
smt	1.41	1.2%	1.38	8.4%	1.77
thread	1.61	0.2%	1.55	4.5%	1.52
wathen100	1.07	0.0%	1.07	2.6%	1.21
ship_001	1.21	2.0%	1.20	4.6%	2.27
nd12k	2.14	2.6%	2.12	8.8%	1.03
wathen120	1.07	0.0%	1.06	2.1%	1.21
obstclae	1.04	0.0%	1.03	0.4%	1.47
jnlbrng1	1.04	0.0%	1.04	0.1%	1.46
minsurfo	1.04	0.0%	1.04	0.0%	1.46
bcsstm39	1.00	0.0%	1.00	0.0%	3.19
vanbody	1.08	3.8%	1.07	8.4%	1.94
gridgena	1.04	1.9%	1.04	4.2%	1.26
cvxbqp1	1.05	0.0%	1.06	0.4%	1.61
ct20stif	1.15	2.9%	1.14	8.8%	1.72
crankseg_1	1.38	1.7%	1.31	8.6%	2.03
nasasrb	1.08	2.5%	1.08	2.2%	1.97
Andrews	1.28	7.7%	1.37	16.5%	1.11
crankseg_2	1.38	2.3%	1.31	4.4%	2.06
Dubcova2	1.05	0.0%	1.05	2.7%	1.29
qa8fm	1.17	1.3%	1.15	3.9%	1.29
cfd1	1.10	3.1%	1.10	5.9%	1.32
nd24k	1.85	3.0%	1.82	8.2%	1.31
oilpan	1.07	1.7%	1.07	4.6%	1.92
finan512	1.01	0.0%	1.01	0.2%	0.93
apache1	1.07	0.0%	1.07	0.0%	1.54
shallow_water1	1.03	0.0%	1.03	2.9%	1.46
shallow_water2	1.03	0.0%	1.03	0.0%	1.45

name	PaToH		onmetisHP		
	cutsize	%LI	cutsize	%LI	speedup
thermal1	1.02	2.3%	1.02	4.3%	1.42
denormal	1.05	0.0%	1.05	0.0%	1.33
s3dkt3m2	1.06	0.0%	1.06	0.4%	1.86
s3dkq4m2	1.07	0.0%	1.06	3.8%	2.17
m_t1	1.11	4.3%	1.10	6.5%	2.72
2cubes_sphere	1.20	2.9%	1.21	3.4%	1.16
thermomech_TK	1.02	1.6%	1.02	4.6%	1.67
thermomech_TC	1.02	1.2%	1.02	5.3%	1.67
x104	1.09	2.3%	1.09	5.6%	2.56
shipsec8	1.12	2.8%	1.11	4.4%	1.97
ship_003	1.13	2.9%	1.13	7.3%	1.91
cfd2	1.09	1.2%	1.08	6.3%	1.29
boneS01	1.13	2.6%	1.12	5.4%	1.76
shipsec1	1.09	1.8%	1.09	4.9%	2.14
bmw7st_1	1.06	4.0%	1.05	6.4%	2.08
Dubcova3	1.05	0.0%	1.04	2.6%	1.28
bmwcra_1	1.07	6.3%	1.09	8.4%	1.82
G2_circuit	1.02	0.0%	1.02	3.5%	1.44
shipsec5	1.09	2.5%	1.08	4.4%	2.11
thermomech_dM	1.01	1.8%	1.01	3.4%	1.82
pwtk	1.03	1.4%	1.03	2.8%	2.30
hood	1.03	2.0%	1.03	4.2%	2.09
BenElechi1	1.04	0.1%	1.03	4.2%	2.28
offshore	1.08	2.1%	1.08	4.0%	1.33
F1	1.08	2.0%	1.07	8.0%	1.50
msdoor	1.02	2.0%	1.02	4.9%	2.17
af_2_k101	1.02	0.0%	1.02	0.0%	1.74
af_5_k101	1.02	0.0%	1.02	0.0%	1.75
af_1_k101	1.02	0.0%	1.02	0.0%	1.75
af_4_k101	1.02	0.0%	1.02	0.0%	1.75
af_3_k101	1.02	0.0%	1.02	0.0%	1.75
af_0_k101	1.02	0.0%	1.02	0.0%	1.76
inline_1	1.04	1.9%	1.04	5.1%	1.73
af_shell8	1.02	0.0%	1.02	0.1%	1.75
af_shell3	1.02	0.0%	1.02	0.0%	1.76
af_shell4	1.02	0.0%	1.02	0.2%	1.77
af_shell7	1.02	0.0%	1.02	0.1%	1.75
parabolic_fem	1.01	0.0%	1.01	0.0%	1.87
apache2	1.03	0.0%	1.02	0.0%	1.50
tmt_sym	1.01	2.5%	1.01	1.7%	1.37
boneS10	1.02	3.6%	1.02	7.0%	2.08
ldoor	1.01	2.4%	1.01	4.1%	2.17
ecology2	1.01	0.0%	1.01	0.0%	1.35
thermal2	1.01	2.1%	1.01	1.7%	1.53
G3_circuit	1.01	0.0%	1.01	0.0%	1.49

Table 5.18 – continued from previous page

Table 5.19: 16-way partitioning performance of the PD matrix collection for connectivity metric with node balancing.

name	*PaToH*		*onmetisHP*		speedup
	cutsize	%LI	cutsize	%LI	
msc01050	2.31	5.0%	2.27	49.4%	0.72
bcsstm08	1.00	1.3%	1.00	1.3%	3.10
bcsstm09	1.00	0.5%	1.00	0.5%	3.08
bcsstk09	1.82	3.4%	1.83	15.7%	1.48
bcsstk10	1.52	3.8%	1.47	27.7%	1.60
1138_bus	1.13	3.3%	1.14	7.8%	1.83
bcsstk27	2.02	3.4%	2.00	25.4%	1.41
mhd1280b	1.15	3.9%	1.10	12.7%	1.76
plbuckle	1.64	4.1%	1.62	16.8%	1.58
msc01440	1.91	3.4%	1.87	24.6%	1.39
bcsstk11	1.63	3.4%	1.63	14.7%	1.56
bcsstm11	1.00	1.0%	1.00	1.0%	3.11
bcsstm12	1.41	2.3%	1.41	11.2%	1.80
bcsstk12	1.63	3.4%	1.63	14.7%	1.56
ex33	1.34	3.6%	1.31	14.2%	1.83
bcsstk14	1.84	3.0%	1.80	15.6%	1.38
ex3	1.75	0.6%	1.73	15.8%	1.28
nasa1824	1.79	3.2%	1.78	19.1%	1.22
plat1919	1.49	3.0%	1.50	12.1%	1.68
bcsstm26	1.00	0.7%	1.00	0.7%	3.09
bcsstk26	1.46	3.1%	1.46	17.0%	1.50
bcsstk13	2.67	5.3%	2.76	40.8%	0.74
nasa2146	1.66	3.4%	1.65	14.1%	1.58
ex10	1.41	1.1%	1.37	19.8%	1.40
Chem97ZtZ	1.00	0.2%	1.00	10.1%	0.66
ex10hs	1.40	1.3%	1.36	13.8%	1.43
ex13	1.57	1.4%	1.55	13.7%	1.38
nasa2910	2.14	0.4%	2.03	27.7%	0.96
bcsstk23	2.02	2.5%	2.05	10.1%	1.08
bcsstm23	1.00	0.1%	1.00	0.1%	3.10
mhd3200b	1.02	0.6%	1.02	4.8%	1.86
bibd_81_2	1.00	0.2%	1.00	0.2%	3.11
ex9	1.49	0.9%	1.48	9.3%	1.42
bcsstm24	1.00	0.2%	1.00	0.2%	3.09
bcsstk24	1.62	2.4%	1.63	9.3%	1.63
bcsstk21	1.29	0.8%	1.30	0.7%	1.66
bcsstm21	1.00	0.0%	1.00	0.0%	3.12
bcsstk15	1.74	3.6%	1.73	8.9%	1.21
sts4098	1.61	5.9%	1.71	32.8%	0.50
t2dal_e	1.00	0.4%	1.00	0.4%	3.14
bcsstk28	1.52	3.0%	1.50	15.4%	1.85
msc04515	1.30	2.7%	1.30	7.2%	1.57
nasa4704	1.45	3.0%	1.46	9.6%	1.38
mhd4800b	1.01	0.4%	1.01	4.6%	1.67
crystm01	1.37	3.6%	1.37	9.9%	1.47
bcsstk16	1.79	4.2%	1.82	16.4%	1.39
s3rmt3m3	1.41	1.1%	1.41	3.1%	1.76
s3rmt3m1	1.44	1.0%	1.44	3.1%	1.76
s2rmq4m1	1.48	2.1%	1.47	9.0%	1.94
s1rmt3m1	1.44	1.2%	1.44	3.0%	1.75
s1rmq4m1	1.49	2.4%	1.47	7.8%	1.95
s2rmt3m1	1.44	1.4%	1.44	2.7%	1.75
s3rmq4m1	1.48	2.9%	1.48	6.4%	1.94
ex15	1.17	2.5%	1.17	6.6%	1.69
Kuu	1.52	0.3%	1.49	13.3%	1.38
Muu	1.30	0.2%	1.30	11.0%	1.21
				Continued on next page	

	PaToH		onmetisHP		
name	cutsize	%LI	cutsize	%LI	speedup
bcsstk38	1.51	3.7%	1.53	21.8%	1.25
aft01	1.22	0.3%	1.20	8.1%	1.40
fv1	1.14	2.2%	1.13	3.9%	1.86
fv3	1.13	3.0%	1.13	4.0%	1.85
fv2	1.13	2.8%	1.13	4.0%	1.84
bundle1	2.72	4.0%	2.73	100.5%	0.18
ted_B	1.04	0.1%	1.04	1.0%	1.02
ted_B_unscaled	1.04	0.5%	1.04	1.0%	1.02
msc10848	1.75	0.3%	1.63	27.0%	1.63
bcsstk17	1.31	3.2%	1.30	11.0%	1.72
t2dah_e	1.18	0.5%	1.17	5.4%	1.43
bcsstk18	1.25	6.0%	1.25	13.5%	1.16
cbuckle	1.32	2.4%	1.31	8.5%	1.81
crystm02	1.25	4.1%	1.24	8.1%	1.42
Pres_Poisson	1.30	3.6%	1.29	5.9%	1.92
bcsstm25	1.00	0.0%	1.00	0.0%	3.14
bcsstk25	1.31	2.0%	1.32	3.6%	1.19
Dubcova1	1.17	0.0%	1.15	3.8%	1.40
olafu	1.29	3.2%	1.28	11.0%	1.98
gyro_m	1.08	3.1%	1.07	9.9%	1.12
gyro	1.25	1.1%	1.18	28.3%	1.37
bodyy4	1.09	1.1%	1.09	4.7%	1.73
bodyy5	1.09	1.0%	1.09	3.4%	1.70
bodyy6	1.09	0.9%	1.09	3.6%	1.71
raefsky4	1.40	3.4%	1.40	8.3%	1.70
LFAT5000	1.00	0.1%	1.00	0.1%	1.35
LF10000	1.00	0.0%	1.00	0.0%	1.35
t3dl_e	1.00	0.0%	1.00	0.0%	3.18
msc23052	1.27	3.1%	1.25	10.5%	2.05
bcsstk36	1.27	3.5%	1.25	8.8%	1.93
crystm03	1.20	3.2%	1.20	9.4%	1.43
smt	1.73	0.6%	1.65	18.7%	1.65
thread	1.97	0.1%	1.88	10.0%	1.42
wathen100	1.12	0.0%	1.10	3.3%	1.30
ship_001	1.48	1.5%	1.45	7.7%	1.99
nd12k	2.84	2.9%	2.84	19.7%	0.90
wathen120	1.11	0.1%	1.09	3.0%	1.27
obstclae	1.06	0.1%	1.06	2.3%	1.57
jnlbrng1	1.06	0.2%	1.06	3.4%	1.56
minsurfo	1.06	0.1%	1.06	1.1%	1.56
bcsstm39	1.00	0.0%	1.00	0.0%	3.26
vanbody	1.14	3.9%	1.13	11.0%	2.01
gridgena	1.07	1.3%	1.07	5.8%	1.33
cvxbqp1	1.08	0.3%	1.09	3.2%	1.66
ct20stif	1.22	3.8%	1.21	12.2%	1.79
crankseg_1	1.69	0.5%	1.55	13.4%	1.85
nasasrb	1.17	3.0%	1.16	3.8%	2.05
Andrews	1.46	7.4%	1.57	25.5%	1.10
crankseg_2	1.68	1.7%	1.55	13.4%	1.77
Dubcova2	1.09	0.0%	1.07	2.2%	1.37
qa8fm	1.25	2.9%	1.23	7.2%	1.33
cfd1	1.17	3.9%	1.16	9.5%	1.34
nd24k	2.36	2.7%	2.35	19.3%	1.16
oilpan	1.13	1.7%	1.13	6.1%	2.02
finan512	1.02	0.1%	1.02	0.4%	0.95
apache1	1.12	0.0%	1.11	2.7%	1.60
shallow_water1	1.04	0.0%	1.04	4.1%	1.54
shallow_water2	1.04	0.0%	1.04	3.5%	1.54

Table 5.19 – continued from previous page

	PaToH		onmetisHP		
name	cutsize	%LI	cutsize	%LI	speedup
thermal1	1.04	2.3%	1.04	7.7%	1.51
denormal	1.08	0.0%	1.07	1.2%	1.40
s3dkt3m2	1.10	0.0%	1.10	2.0%	1.97
s3dkq4m2	1.12	0.5%	1.10	4.4%	2.33
m_t1	1.21	2.7%	1.19	6.8%	2.76
2cubes_sphere	1.29	2.7%	1.30	4.3%	1.19
thermomech_TK	1.03	1.8%	1.03	6.9%	1.72
thermomech_TC	1.03	2.2%	1.03	7.2%	1.73
x104	1.17	1.5%	1.15	8.2%	2.68
shipsec8	1.18	2.5%	1.16	6.5%	2.04
ship_003	1.23	3.3%	1.22	9.4%	1.92
cfd2	1.14	2.8%	1.13	7.7%	1.36
boneS01	1.20	2.8%	1.19	5.9%	1.83
shipsec1	1.15	2.4%	1.14	5.9%	2.21
bmw7st_1	1.09	3.5%	1.08	9.0%	2.21
Dubcova3	1.08	0.0%	1.07	3.3%	1.32
bmwcra_1	1.19	6.3%	1.18	14.2%	1.84
G2_circuit	1.04	0.1%	1.04	3.6%	1.49
shipsec5	1.12	3.5%	1.12	7.2%	2.20
thermomech_dM	1.02	1.7%	1.02	6.1%	1.87
pwtk	1.06	1.4%	1.05	4.0%	2.43
hood	1.05	2.0%	1.05	7.0%	2.20
BenElechi1	1.06	0.1%	1.06	5.5%	2.41
offshore	1.12	4.1%	1.12	8.6%	1.33
F1	1.15	1.2%	1.15	10.4%	1.46
msdoor	1.03	1.9%	1.03	6.1%	2.29
af_2_k101	1.04	0.0%	1.04	0.8%	1.83
af_5_k101	1.04	0.0%	1.04	0.5%	1.83
af_1_k101	1.04	0.0%	1.04	0.3%	1.84
af_4_k101	1.04	0.0%	1.04	0.2%	1.85
af_3_k101	1.04	0.0%	1.04	1.9%	1.85
af_0_k101	1.04	0.0%	1.04	0.5%	1.83
inline_1	1.07	2.3%	1.07	6.9%	1.78
af_shell8	1.03	0.0%	1.03	0.5%	1.84
af_shell3	1.03	0.0%	1.03	0.3%	1.85
af_shell4	1.03	0.0%	1.03	0.6%	1.84
af_shell7	1.03	0.0%	1.03	0.6%	1.84
parabolic_fem	1.02	0.0%	1.02	0.7%	1.87
apache2	1.04	0.0%	1.04	0.2%	1.53
tmt_sym	1.02	2.8%	1.02	4.1%	1.42
boneS10	1.04	3.4%	1.03	8.2%	2.20
ldoor	1.02	2.0%	1.02	6.2%	2.33
ecology2	1.01	0.0%	1.01	0.0%	1.40
thermal2	1.01	2.1%	1.01	3.7%	1.60
G3_circuit	1.01	0.0%	1.01	1.6%	1.51

Table 5.19 – continued from previous page

Table 5.20: 32-way partitioning performance of the PD matrix collection for connectivity metric with node balancing.

| | $PaToH$ | | $onmetisHP$ | | |
name	cutsize	$\%LI$	cutsize	$\%LI$	speedup
ex33	1.62	3.2%	1.57	24.2%	1.69
bcsstk14	2.43	3.2%	2.38	32.0%	1.16
ex3	2.24	1.2%	2.23	36.3%	1.09
nasa1824	2.27	3.4%	2.30	42.1%	1.08
plat1919	1.84	3.0%	1.87	22.1%	1.58
bcsstm26	1.00	1.6%	1.00	1.6%	3.18
bcsstk26	1.74	3.7%	1.70	32.1%	1.38
bcsstk13	3.64	5.1%	3.63	61.7%	0.66
nasa2146	2.11	2.6%	2.07	24.4%	1.43
ex10	1.78	1.8%	1.72	29.8%	1.24
Chem97ZtZ	1.02	2.2%	1.03	31.3%	0.67
ex10hs	1.76	1.0%	1.74	25.9%	1.29
ex13	1.99	1.2%	2.00	29.6%	1.21
nasa2910	2.93	1.2%	2.73	44.2%	0.78
bcsstm23	1.00	0.1%	1.00	0.1%	3.17
bcsstk23	2.45	2.6%	2.55	20.9%	1.03
mhd3200b	1.05	0.7%	1.04	5.0%	2.08
bibd_81_2	1.00	0.7%	1.00	0.7%	3.20
ex9	1.86	1.5%	1.85	20.2%	1.31
bcsstm24	1.00	0.6%	1.00	0.6%	3.19
bcsstk24	2.03	3.2%	1.98	23.4%	1.52
bcsstk21	1.49	1.4%	1.49	3.9%	1.76
bcsstm21	1.00	0.4%	1.00	0.4%	3.21
bcsstk15	2.14	4.0%	2.15	21.8%	1.16
sts4098	1.97	5.8%	2.17	73.4%	0.45
t2dal_e	1.00	0.7%	1.00	0.7%	3.21
bcsstk28	1.88	2.7%	1.81	35.9%	1.72
msc04515	1.51	3.4%	1.51	12.6%	1.60
nasa4704	1.72	3.2%	1.71	23.4%	1.35
mhd4800b	1.03	0.8%	1.03	5.1%	1.93
crystm01	1.65	4.3%	1.61	23.7%	1.47
bcsstk16	2.38	3.6%	2.36	40.7%	1.17
s3rmt3m3	1.67	2.1%	1.66	9.5%	1.71
s2rmq4m1	1.83	3.0%	1.80	15.9%	1.82
s1rmq4m1	1.83	3.1%	1.81	16.7%	1.83
s1rmt3m1	1.71	2.9%	1.71	9.0%	1.70
s2rmt3m1	1.71	2.5%	1.71	7.3%	1.70
s3rmq4m1	1.83	3.2%	1.80	13.7%	1.82
s3rmt3m1	1.71	2.5%	1.71	10.3%	1.70
ex15	1.27	2.4%	1.28	7.2%	1.80
Kuu	1.86	0.4%	1.83	26.0%	1.25
Muu	1.50	0.6%	1.48	16.7%	1.20
bcsstk38	1.83	3.9%	1.80	35.0%	1.18
aft01	1.35	0.8%	1.32	9.1%	1.44
fv1	1.22	2.3%	1.22	5.5%	1.94
fv3	1.22	3.1%	1.22	5.8%	1.92
fv2	1.22	2.9%	1.22	5.6%	1.92
bundle1	3.98	4.3%	3.36	152.4%	0.17
ted_B	1.09	1.2%	1.08	6.2%	1.08
ted_B_unscaled	1.09	1.4%	1.08	2.8%	1.08
msc10848	2.27	0.7%	2.07	37.9%	1.41
bcsstk17	1.54	3.4%	1.52	14.8%	1.68
t2dah_e	1.29	0.5%	1.27	5.7%	1.46
bcsstk18	1.41	4.7%	1.41	20.4%	1.15
cbuckle	1.49	3.2%	1.47	10.3%	1.80
crystm02	1.43	3.9%	1.40	14.0%	1.44
				Continued on next page	

	PaToH		onmetisHP		
name	cutsize	%LI	cutsize	%LI	speedup
Pres_Poisson	1.49	2.8%	1.48	7.5%	1.90
bcsstk25	1.52	2.1%	1.54	7.6%	1.20
bcsstm25	1.00	0.1%	1.00	0.1%	3.22
Dubcova1	1.28	0.1%	1.25	5.3%	1.45
olafu	1.50	3.6%	1.46	19.7%	1.93
gyro_m	1.16	2.3%	1.13	17.3%	1.16
gyro	1.51	1.6%	1.43	51.4%	1.17
bodyy4	1.14	1.9%	1.14	5.8%	1.84
bodyy5	1.14	1.7%	1.14	3.7%	1.83
bodyy6	1.14	0.9%	1.14	4.4%	1.84
raefsky4	1.69	4.8%	1.68	17.0%	1.59
LFAT5000	1.00	0.1%	1.00	0.1%	1.45
LF10000	1.01	0.2%	1.01	0.2%	1.44
t3dl_e	1.00	0.1%	1.00	0.1%	3.27
bcsstk36	1.43	3.9%	1.42	13.1%	1.90
msc23052	1.43	3.2%	1.41	13.0%	2.04
crystm03	1.33	3.4%	1.31	12.4%	1.46
smt	2.16	1.0%	2.06	32.4%	1.39
thread	2.45	0.6%	2.31	20.0%	1.31
wathen100	1.19	0.3%	1.17	3.6%	1.34
ship_001	1.83	1.3%	1.80	13.2%	1.79
nd12k	3.86	3.8%	3.92	42.0%	0.71
wathen120	1.17	0.4%	1.15	4.7%	1.35
obstclae	1.09	0.4%	1.08	5.6%	1.68
jnlbrng1	1.09	1.0%	1.08	6.0%	1.67
minsurfo	1.09	0.6%	1.08	4.5%	1.67
bcsstm39	1.00	0.0%	1.00	0.0%	3.36
vanbody	1.24	4.4%	1.23	15.0%	2.03
gridgena	1.11	1.4%	1.11	6.3%	1.42
cvxbqp1	1.11	1.8%	1.13	5.4%	1.73
ct20stif	1.33	4.4%	1.30	19.7%	1.80
crankseg_1	2.09	0.1%	1.88	24.0%	1.55
nasasrb	1.27	2.9%	1.26	6.2%	2.11
Andrews	1.71	7.1%	1.84	26.8%	1.12
crankseg_2	2.09	0.6%	1.85	30.7%	1.59
Dubcova2	1.14	0.1%	1.12	3.1%	1.40
qa8fm	1.39	3.8%	1.37	10.6%	1.36
cfd1	1.30	4.4%	1.29	13.0%	1.37
nd24k	3.05	3.2%	3.07	24.5%	1.03
oilpan	1.21	1.8%	1.20	9.0%	2.09
finan512	1.03	0.4%	1.03	1.0%	1.00
apache1	1.18	0.5%	1.17	8.8%	1.66
shallow_water2	1.06	0.0%	1.06	6.5%	1.63
shallow_water1	1.06	0.3%	1.06	7.0%	1.63
thermal1	1.06	2.3%	1.06	9.4%	1.58
denormal	1.12	0.8%	1.11	6.0%	1.46
s3dkt3m2	1.16	0.4%	1.16	3.7%	2.04
s3dkq4m2	1.18	1.4%	1.16	5.8%	2.40
m_t1	1.34	2.1%	1.31	10.1%	2.76
2cubes_sphere	1.41	2.7%	1.42	5.7%	1.21
thermomech_TC	1.05	2.4%	1.05	9.2%	1.77
thermomech_TK	1.05	2.0%	1.05	9.3%	1.78
x104	1.28	1.5%	1.25	10.4%	2.68
shipsec8	1.26	2.7%	1.25	10.5%	2.08
ship_003	1.35	3.4%	1.34	11.7%	1.94
cfd2	1.22	2.9%	1.21	12.1%	1.38
boneS01	1.28	2.6%	1.27	9.5%	1.86
shipsec1	1.22	2.6%	1.21	9.7%	2.24

Table 5.20 – continued from previous page

	PaToH		onmetisHP		
name	cutsize	%LI	cutsize	%LI	speedup
bmw7st_1	1.14	3.9%	1.13	12.2%	2.27
Dubcova3	1.13	0.0%	1.11	4.9%	1.35
bmwcra_1	1.32	5.5%	1.32	18.2%	1.77
G2_circuit	1.07	0.1%	1.06	5.0%	1.54
shipsec5	1.19	3.3%	1.17	9.7%	2.25
thermomech_dM	1.03	1.8%	1.03	9.3%	1.88
pwtk	1.12	1.7%	1.11	6.3%	2.48
hood	1.09	1.8%	1.09	8.4%	2.26
BenElechi1	1.10	0.3%	1.09	7.8%	2.49
offshore	1.19	4.0%	1.19	10.0%	1.32
F1	1.26	0.8%	1.26	12.8%	1.40
msdoor	1.05	2.4%	1.06	8.6%	2.37
af_4_k101	1.06	0.1%	1.06	4.3%	1.90
af_0_k101	1.06	0.0%	1.06	4.1%	1.90
af_5_k101	1.06	0.0%	1.06	4.5%	1.90
af_1_k101	1.06	0.0%	1.06	4.2%	1.90
af_2_k101	1.06	0.0%	1.06	3.8%	1.88
af_3_k101	1.06	0.1%	1.06	4.3%	1.90
inline_1	1.12	1.7%	1.12	9.0%	1.77
af_shell8	1.06	0.1%	1.06	4.9%	1.91
af_shell3	1.06	0.1%	1.06	4.3%	1.89
af_shell7	1.06	0.0%	1.06	4.9%	1.89
af_shell4	1.06	0.0%	1.06	4.3%	1.90
parabolic_fem	1.03	0.0%	1.03	2.9%	1.87
apache2	1.06	0.0%	1.06	1.3%	1.55
tmt_sym	1.02	2.2%	1.02	7.5%	1.44
boneS10	1.05	3.1%	1.05	11.4%	2.25
ldoor	1.04	2.4%	1.04	8.1%	2.39
ecology2	1.02	0.0%	1.02	0.6%	1.43
thermal2	1.02	2.5%	1.02	7.0%	1.63
G3_circuit	1.02	0.3%	1.02	4.6%	1.52

Table 5.20 – continued from previous page

Table 5.21: 64-way partitioning performance of the PD matrix collection for connectivity metric with node balancing.

name	PaToH		onmetisHP		speedup
	cutsize	%LI	cutsize	%LI	
bcsstk13	5.23	4.2%	5.01	111.7%	0.61
Chem97ZtZ	1.21	3.5%	1.22	42.1%	0.85
mhd3200b	1.10	1.1%	1.08	5.9%	2.12
bibd_81_2	1.00	0.7%	1.00	0.7%	3.28
ex9	2.41	1.8%	2.39	42.3%	1.14
bcsstm24	1.00	0.6%	1.00	0.6%	3.26
bcsstk24	2.69	3.3%	2.56	46.5%	1.31
bcsstm21	1.00	1.3%	1.00	1.3%	3.30
bcsstk21	1.75	1.9%	1.79	9.2%	1.69
bcsstk15	2.75	4.1%	2.75	35.6%	1.06
sts4098	2.54	11.3%	2.71	111.2%	0.43
t2dal_e	1.00	0.7%	1.00	0.7%	3.30
bcsstk28	2.50	3.8%	2.35	50.2%	1.48
msc04515	1.84	3.8%	1.83	23.9%	1.51
nasa4704	2.10	3.6%	2.11	38.0%	1.24
mhd4800b	1.06	1.5%	1.06	6.0%	2.04
crystm01	2.10	4.5%	2.10	33.7%	1.34
bcsstk16	3.24	4.3%	3.25	61.8%	0.95
s3rmt3m3	2.07	2.7%	2.04	31.4%	1.57
s2rmq4m1	2.37	3.2%	2.28	35.3%	1.60
s1rmt3m1	2.13	2.4%	2.10	31.4%	1.57
s1rmq4m1	2.38	3.0%	2.26	32.5%	1.62
s3rmt3m1	2.14	2.7%	2.10	34.0%	1.57
s3rmq4m1	2.38	2.9%	2.26	32.2%	1.62
s2rmt3m1	2.14	2.3%	2.11	28.7%	1.57
ex15	1.48	3.1%	1.50	15.7%	1.80
Muu	1.84	1.1%	1.82	27.0%	1.13
Kuu	2.35	1.1%	2.31	44.4%	1.08
bcsstk38	2.29	3.9%	2.26	72.5%	1.06
aft01	1.56	1.2%	1.53	12.3%	1.48
fv1	1.33	3.7%	1.33	7.6%	2.04
fv3	1.33	3.1%	1.32	8.6%	2.03
fv2	1.33	3.2%	1.33	8.6%	2.03
bundle1	6.16	7.0%	4.49	275.0%	0.17
ted_B	1.20	1.5%	1.16	30.4%	1.11
ted_B_unscaled	1.20	1.4%	1.17	32.5%	1.11
msc10848	3.05	1.2%	2.74	73.4%	1.14
bcsstk17	1.87	4.3%	1.82	27.1%	1.58
t2dah_e	1.47	0.9%	1.44	8.7%	1.48
bcsstk18	1.64	5.1%	1.66	34.8%	1.14
cbuckle	1.79	3.2%	1.76	15.5%	1.73
crystm02	1.72	4.6%	1.70	17.3%	1.41
Pres_Poisson	1.80	3.2%	1.77	16.3%	1.82
bcsstk25	1.77	2.6%	1.79	13.0%	1.17
bcsstm25	1.00	0.3%	1.00	0.3%	3.26
Dubcova1	1.42	0.4%	1.37	7.7%	1.48
olafu	1.86	3.5%	1.79	29.0%	1.75
gyro	1.91	1.8%	1.82	75.3%	1.00
gyro_m	1.34	2.7%	1.30	30.4%	1.10
bodyy4	1.22	1.9%	1.22	6.2%	1.92
bodyy5	1.22	1.6%	1.22	6.2%	1.93
bodyy6	1.22	1.5%	1.22	7.1%	1.91
raefsky4	2.16	4.5%	2.11	29.9%	1.43
LFAT5000	1.01	0.2%	1.01	0.3%	1.60
LF10000	1.01	0.5%	1.01	0.5%	1.57
t3dl_e	1.00	0.3%	1.00	0.3%	3.33
				Continued on next page	

Table 5.21 – continued from previous page

| name | PaToH | | onmetisHP | | |
	cutsize	%LI	cutsize	%LI	speedup
bcsstk36	1.65	3.8%	1.63	18.8%	1.85
msc23052	1.65	3.9%	1.63	16.9%	1.95
crystm03	1.55	4.1%	1.54	16.3%	1.45
smt	2.86	1.0%	2.67	57.8%	1.11
thread	3.09	1.0%	2.90	40.7%	1.14
wathen100	1.29	0.8%	1.25	4.9%	1.37
ship_001	2.30	1.3%	2.23	31.8%	1.51
nd12k	5.33	4.2%	5.69	64.5%	0.57
wathen120	1.26	0.8%	1.23	4.8%	1.40
obstclae	1.13	1.6%	1.12	6.9%	1.79
jnlbrng1	1.13	1.8%	1.12	5.9%	1.78
minsurfo	1.13	1.7%	1.12	6.4%	1.78
bcsstm39	1.00	0.0%	1.00	0.0%	3.40
vanbody	1.40	3.8%	1.38	22.3%	1.96
gridgena	1.18	1.8%	1.17	9.2%	1.50
cvxbqp1	1.16	2.2%	1.18	8.7%	1.77
ct20stif	1.48	4.0%	1.45	22.5%	1.80
crankseg_1	2.70	0.2%	2.45	39.5%	1.10
nasasrb	1.39	2.8%	1.38	8.3%	2.10
Andrews	2.06	6.8%	2.24	30.7%	1.11
crankseg_2	2.65	0.1%	2.39	51.6%	1.14
Dubcova2	1.21	0.2%	1.17	4.7%	1.46
qa8fm	1.56	3.6%	1.54	13.9%	1.38
cfd1	1.50	4.7%	1.50	17.6%	1.38
nd24k	4.08	3.7%	4.16	52.2%	0.80
oilpan	1.32	2.0%	1.32	10.3%	2.11
finan512	1.18	1.5%	1.13	4.3%	1.05
apache1	1.26	1.7%	1.25	10.3%	1.73
shallow_water2	1.08	0.9%	1.08	8.9%	1.74
shallow_water1	1.08	0.7%	1.08	8.3%	1.74
thermal1	1.10	2.2%	1.09	10.4%	1.68
denormal	1.18	1.5%	1.17	7.7%	1.53
s3dkt3m2	1.24	0.6%	1.25	4.5%	2.07
s3dkq4m2	1.28	1.5%	1.25	9.5%	2.44
m_t1	1.52	1.5%	1.46	12.0%	2.73
2cubes_sphere	1.55	2.3%	1.57	8.4%	1.22
thermomech_TK	1.08	2.3%	1.08	11.1%	1.83
thermomech_TC	1.08	2.0%	1.08	11.9%	1.83
x104	1.43	1.0%	1.39	12.1%	2.63
shipsec8	1.38	3.1%	1.36	13.4%	2.06
ship_003	1.51	3.1%	1.48	16.3%	1.90
cfd2	1.34	3.4%	1.32	14.8%	1.40
boneS01	1.40	3.0%	1.37	13.9%	1.85
shipsec1	1.31	2.5%	1.30	12.5%	2.26
bmw7st_1	1.22	3.7%	1.20	15.5%	2.28
Dubcova3	1.19	0.1%	1.15	4.1%	1.37
bmwcra_1	1.48	5.5%	1.49	22.3%	1.73
G2_circuit	1.10	1.3%	1.10	8.4%	1.60
shipsec5	1.28	3.5%	1.27	13.8%	2.26
thermomech_dM	1.06	2.0%	1.05	11.2%	1.90
pwtk	1.19	2.0%	1.18	9.9%	2.53
hood	1.15	1.8%	1.15	10.8%	2.28
BenElechi1	1.16	1.2%	1.14	9.9%	2.55
offshore	1.28	4.1%	1.28	11.5%	1.32
F1	1.40	0.7%	1.40	14.6%	1.33
msdoor	1.08	2.2%	1.09	12.9%	2.39
af_2_k101	1.09	0.3%	1.09	5.7%	1.92
af_3_k101	1.09	0.4%	1.09	5.8%	1.92

name	PaToH cutsize	PaToH %LI	onmetisHP cutsize	onmetisHP %LI	speedup
Table 5.21 – continued from previous page					
af_5_k101	1.09	0.6%	1.09	5.4%	1.94
af_0_k101	1.09	0.6%	1.09	6.4%	1.92
af_1_k101	1.09	0.3%	1.09	6.4%	1.93
af_4_k101	1.09	0.3%	1.09	6.1%	1.92
inline_1	1.19	1.2%	1.18	11.0%	1.73
af_shell4	1.09	0.3%	1.09	6.2%	1.94
af_shell7	1.09	0.3%	1.09	5.9%	1.93
af_shell8	1.09	0.2%	1.09	6.2%	1.93
af_shell3	1.09	0.6%	1.09	5.6%	1.93
parabolic_fem	1.04	0.1%	1.04	6.9%	1.87
apache2	1.09	0.3%	1.09	7.8%	1.58
tmt_sym	1.03	2.3%	1.03	8.6%	1.46
boneS10	1.09	3.7%	1.08	15.0%	2.28
ldoor	1.06	2.2%	1.06	11.7%	2.43
ecology2	1.03	0.0%	1.03	5.1%	1.44
thermal2	1.03	2.3%	1.02	8.9%	1.65
G3_circuit	1.03	0.3%	1.03	6.2%	1.53

Table 5.22: 128-way partitioning performance of the PD matrix collection for connectivity metric with node balancing.

	PaToH		onmetisHP		
name	cutsize	%LI	cutsize	%LI	speedup
bcsstk13	7.65	7.7%	6.92	151.5%	0.55
Chem97ZtZ	1.52	75.6%	1.53	230.4%	0.75
sts4098	3.41	38.7%	3.45	141.8%	0.43
ex15	1.79	3.1%	1.77	30.1%	1.70
Muu	2.32	1.4%	2.30	43.6%	1.01
Kuu	3.21	1.4%	3.06	75.0%	0.91
bcsstk38	2.99	3.7%	2.88	94.4%	0.94
aft01	1.86	1.3%	1.83	25.2%	1.41
fv1	1.52	2.8%	1.54	9.7%	2.00
fv2	1.51	3.0%	1.53	10.3%	1.99
fv3	1.51	3.0%	1.53	11.0%	1.99
bundle1	10.02	16.5%	5.71	484.2%	0.15
ted_B_unscaled	1.42	1.9%	1.34	42.1%	1.03
ted_B	1.42	2.6%	1.34	48.2%	1.03
msc10848	4.33	1.3%	3.80	133.1%	0.92
bcsstk17	2.37	3.9%	2.32	47.9%	1.39
t2dah_e	1.71	1.2%	1.68	17.7%	1.47
bcsstk18	1.97	4.7%	2.02	40.3%	1.13
cbuckle	2.23	3.6%	2.16	35.2%	1.60
crystm02	2.19	4.6%	2.20	32.0%	1.33
Pres_Poisson	2.29	3.2%	2.24	31.5%	1.65
bcsstm25	1.00	0.3%	1.00	0.3%	3.28
bcsstk25	2.11	2.9%	2.15	23.6%	1.16
Dubcova1	1.64	1.0%	1.61	15.5%	1.49
olafu	2.38	3.6%	2.30	56.5%	1.48
gyro_m	1.63	2.4%	1.62	51.3%	1.04
gyro	2.52	1.5%	2.47	105.0%	0.82
bodyy4	1.33	2.2%	1.34	7.9%	2.04
bodyy5	1.33	1.8%	1.33	8.8%	2.02
bodyy6	1.32	1.6%	1.33	6.9%	2.02
raefsky4	2.82	4.7%	2.81	39.6%	1.22
LFAT5000	1.02	0.8%	1.02	1.1%	1.85
LF10000	1.03	1.1%	1.03	1.6%	1.81
t3dl_e	1.00	0.6%	1.00	0.6%	3.35
bcsstk36	1.98	4.0%	1.92	35.5%	1.74
msc23052	1.97	3.7%	1.93	34.7%	1.84
crystm03	1.89	4.2%	1.88	21.8%	1.41
smt	3.86	1.2%	3.62	67.4%	0.91
thread	4.05	1.3%	3.82	62.3%	0.93
wathen100	1.43	1.2%	1.41	6.6%	1.38
ship_001	3.02	1.4%	2.95	60.4%	1.21
nd12k	7.60	4.1%	8.38	106.1%	0.47
wathen120	1.39	1.3%	1.36	6.4%	1.40
obstclae	1.18	1.6%	1.18	9.6%	1.87
jnlbrng1	1.19	2.2%	1.18	8.7%	1.86
minsurfo	1.19	1.8%	1.18	7.7%	1.86
bcsstm39	1.00	0.2%	1.00	0.2%	3.45
vanbody	1.64	4.3%	1.60	26.3%	1.88
gridgena	1.27	1.9%	1.27	9.4%	1.57
cvxbqp1	1.23	1.9%	1.26	12.2%	1.81
ct20stif	1.71	3.8%	1.66	31.8%	1.73
crankseg_1	3.65	0.7%	3.39	73.3%	0.82
nasasrb	1.60	3.2%	1.57	10.2%	2.04
Andrews	2.50	5.9%	2.76	43.8%	1.05
crankseg_2	3.59	0.6%	3.28	93.7%	0.84
Dubcova2	1.31	0.7%	1.28	5.9%	1.48
				Continued on next page	

Table 5.22 – continued from previous page				
	PaToH		*onmetisHP*	
name	cutsize	%LI	cutsize	%LI	speedup
qa8fm	1.79	4.3%	1.75	17.2%	1.37
cfd1	1.74	5.1%	1.73	20.5%	1.38
nd24k	5.60	4.7%	5.95	80.5%	0.64
oilpan	1.48	2.0%	1.47	11.5%	2.08
finan512	1.34	2.2%	1.25	8.2%	1.06
apache1	1.38	2.1%	1.36	11.0%	1.77
shallow_water1	1.12	1.3%	1.12	9.6%	1.84
shallow_water2	1.12	0.9%	1.12	9.2%	1.84
thermal1	1.14	2.1%	1.14	13.2%	1.76
denormal	1.26	1.5%	1.24	9.3%	1.59
s3dkt3m2	1.37	1.3%	1.37	6.2%	2.09
s3dkq4m2	1.42	1.9%	1.38	9.0%	2.42
m_t1	1.77	1.4%	1.70	26.1%	2.53
2cubes_sphere	1.74	2.3%	1.76	9.6%	1.23
thermomech_TK	1.13	2.2%	1.12	13.7%	1.90
thermomech_TC	1.13	2.4%	1.12	14.5%	1.89
x104	1.65	1.0%	1.60	22.6%	2.48
shipsec8	1.55	3.3%	1.53	18.3%	2.02
ship_003	1.72	3.3%	1.71	20.9%	1.82
cfd2	1.50	4.0%	1.47	20.8%	1.42
boneS01	1.55	2.6%	1.51	18.5%	1.82
shipsec1	1.44	2.8%	1.43	17.4%	2.25
bmw7st_1	1.34	3.8%	1.32	19.4%	2.25
Dubcova3	1.28	0.5%	1.24	7.5%	1.38
bmwcra_1	1.71	5.0%	1.71	30.0%	1.65
G2_circuit	1.15	1.4%	1.14	8.8%	1.66
shipsec5	1.42	3.7%	1.41	16.0%	2.22
thermomech_dM	1.08	2.3%	1.08	13.3%	1.94
pwtk	1.28	2.5%	1.26	9.9%	2.54
hood	1.23	1.7%	1.23	14.2%	2.28
BenElechi1	1.24	1.5%	1.22	12.6%	2.58
offshore	1.40	3.9%	1.40	16.2%	1.31
F1	1.61	0.7%	1.60	22.4%	1.25
msdoor	1.13	2.7%	1.13	16.1%	2.42
af_3_k101	1.14	0.5%	1.14	7.1%	1.96
af_1_k101	1.14	0.8%	1.14	7.7%	1.96
af_2_k101	1.14	0.7%	1.14	7.0%	1.96
af_4_k101	1.14	0.5%	1.14	6.8%	1.96
af_0_k101	1.14	0.6%	1.14	8.2%	1.96
af_5_k101	1.14	0.7%	1.14	8.3%	1.96
inline_1	1.30	1.0%	1.29	13.8%	1.68
af_shell7	1.13	0.7%	1.13	7.7%	1.95
af_shell3	1.13	0.7%	1.13	8.4%	1.97
af_shell4	1.13	1.0%	1.13	7.5%	1.95
af_shell8	1.13	0.9%	1.13	7.6%	1.96
parabolic_fem	1.06	0.5%	1.06	9.9%	1.88
apache2	1.13	1.0%	1.12	10.9%	1.61
tmt_sym	1.05	2.5%	1.05	11.1%	1.50
boneS10	1.14	3.6%	1.12	17.3%	2.27
ldoor	1.10	2.4%	1.10	14.3%	2.45
ecology2	1.04	0.2%	1.04	8.6%	1.47
thermal2	1.04	2.2%	1.04	11.3%	1.66
G3_circuit	1.04	0.6%	1.04	6.3%	1.55